Theses and Dissertations | 1. Thesis and Dissertation Collection, all items

2005-06

Baroclinicity, forcing mechanism and prediction of chemical propagation of San Diego Bay and their effects on naval applications

Kyriakidis, Kleanthis

Monterey, California. Naval Postgraduate School

http://hdl.handle.net/10945/1943

NAVAL POSTGRADUATE SCHOOL

THESIS

BAROCLINICITY, FORCING MECHANISM AND PREDICTION OF CHEMICAL PROPAGATION OF SAN DIEGO BAY AND THEIR EFFECTS ON NAVAL APPLICATIONS

by

Kleanthis Kyriakidis

June 2005

Thesis Advisor: Peter Chu
Second Reader: Steven Haeger

Approved for public release; distribution is unlimited

THIS PAGE INTENTIONALLY LEFT BLANK

REPORT DOCUMENTATION PAGE			*Form Approved OMB No. 0704-0188*
Public reporting burden for this collection of information is estimated to average 1 hour per response, including the time for reviewing instruction, searching existing data sources, gathering and maintaining the data needed, and completing and reviewing the collection of information. Send comments regarding this burden estimate or any other aspect of this collection of information, including suggestions for reducing this burden, to Washington headquarters Services, Directorate for Information Operations and Reports, 1215 Jefferson Davis Highway, Suite 1204, Arlington, VA 22202-4302, and to the Office of Management and Budget, Paperwork Reduction Project (0704-0188) Washington DC 20503.			
1. AGENCY USE ONLY (*Leave blank*)	**2. REPORT DATE** June 2005	**3. REPORT TYPE AND DATES COVERED** Master's Thesis	
4. TITLE AND SUBTITLE: Baroclinicity, Forcing Mechanism and Prediction of Chemical Propagation of San Diego Bay and Their Effects on Naval Applications			**5. FUNDING NUMBERS**
6. AUTHOR(S) Kleanthis Kyriakidis			
7. PERFORMING ORGANIZATION NAME(S) AND ADDRESS(ES) Naval Postgraduate School Monterey, CA 93943-5000			**8. PERFORMING ORGANIZATION REPORT NUMBER**
9. SPONSORING /MONITORING AGENCY NAME(S) AND ADDRESS(ES) N/A			**10. SPONSORING/MONITORING AGENCY REPORT NUMBER**
11. SUPPLEMENTARY NOTES The views expressed in this thesis are those of the author and do not reflect the official policy or position of the Department of Defense or the U.S. Government.			
12a. DISTRIBUTION / AVAILABILITY STATEMENT Approved for public release; distribution is unlimited			**12b. DISTRIBUTION CODE**
13. ABSTRACT (maximum 200 words) Both instantaneous current and chemical propagation predictions are of utmost importance for all littoral naval operations, including diving, amphibious and mine warfare ones. Undoubtedly, the operating limits and environmental thresholds are crucial and highly reliant on the accuracy and precision of the predictions. San Diego Bay is important because it hosts a large part of the U.S. fleet and has special ecological significance.\n\nA hydrodynamic model, "Water Quality Management and Analysis Package" (WQMAP), is used to predict the instantaneous currents with various forcing functions (tides, winds, and lateral boundary fluxes) and a hydrochemical model, "Chemical Management and Analysis Package", (CHEMMAP) to predict the water contamination and to simulate chemical attacks/accidents in San Diego Bay, which raise considerations regarding public health, economy, ecology or even national security.\n\nThe study shows the barotropic nature of San Diego Bay, the slight significance of wind and the vulnerability of a semi-enclosed tidal basin in a possible chemical attack or accident. Simultaneously, it evaluates and uses two models used by NAVOCEANO.			

14. SUBJECT TERMS Baroclinicity, Forcing, WQMAP, CHEMMAP, Prediction, San Diego Bay, Chemical Propagation, Model Evaluation			**15. NUMBER OF PAGES** 115
			16. PRICE CODE

17. SECURITY CLASSIFICATION OF REPORT Unclassified	**18. SECURITY CLASSIFICATION OF THIS PAGE** Unclassified	**19. SECURITY CLASSIFICATION OF ABSTRACT** Unclassified	**20. LIMITATION OF ABSTRACT** UL

THIS PAGE INTENTIONALLY LEFT BLANK

Approved for public release; distribution is unlimited

BAROCLINICITY, FORCING MECHANISM AND PREDICTION OF CHEMICAL PROPAGATION OF SAN DIEGO BAY AND THEIR EFFECTS ON NAVAL APPLICATIONS

Kleanthis Kyriakidis
Lieutenant Commander, Hellenic Navy
B.S., Hellenic Naval Academy, 1991

Submitted in partial fulfillment of the
requirements for the degree of

MASTER OF SCIENCE IN PHYSICAL OCEANOGRAPHY

from the

NAVAL POSTGRADUATE SCHOOL
June 2005

Author: Kleanthis Kyriakidis

Approved by: Peter C. Chu
               Thesis Advisor

               Steven D. Haeger
               Second Reader

               Mary Bateen
               Chairman, Department of Oceanography

iii

THIS PAGE INTENTIONALLY LEFT BLANK

ABSTRACT

Both instantaneous current and chemical propagation predictions are of utmost importance for all littoral naval operations, including diving, amphibious and mine warfare ones. Undoubtedly, the operating limits and environmental thresholds are crucial and highly reliant on the accuracy and precision of the predictions. San Diego Bay is important because it hosts a large part of the U.S. fleet and has special ecological significance.

A hydrodynamic model, "Water Quality Management and Analysis Package" (WQMAP), is used to predict the instantaneous currents with various forcing functions (tides, winds, and lateral boundary fluxes) and a hydrochemical model, "Chemical Management and Analysis Package", (CHEMMAP) to predict the water contamination and to simulate chemical attacks/accidents in San Diego Bay, which raise considerations regarding public health, economy, ecology or even national security.

The study shows the barotropic nature of San Diego Bay, the slight significance of wind and the vulnerability of a semi-enclosed tidal basin in a possible chemical attack or accident. Simultaneously, it evaluates and uses two models used by NAVOCEANO.

THIS PAGE INTENTIONALLY LEFT BLANK

TABLE OF CONTENTS

viii

LIST OF FIGURES

THIS PAGE INTENTIONALLY LEFT BLANK

LIST OF TABLES

THIS PAGE INTENTIONALLY LEFT BLANK

ACKNOWLEDGMENTS

THIS PAGE INTENTIONALLY LEFT BLANK

I.   INTRODUCTION

The United States military has undergone numerous changes since the end of the Cold War. Specifically, the U.S. Navy experienced a shift in the area of engagement from the "blue water" (water depth greater than 100 m) Soviet threat, to littoral regions of the world. It is important to predict instantaneous currents and tides in littoral zones such as the continental shelf, estuary, and rivers. The Naval Oceanographic Office (NAVOCEANO) implements and runs several types of two-dimensional (2D) and three-dimensional (3D) circulation models for many geographical domains around the world. Most of these are run in an operational mode that generates daily products for the Fleet. These products support a wide variety of applications ranging from Special Operations, Mine Warfare, Expeditionary Warfare, Object Drift, Search and Rescue, Chemical and Oil Spill.

Complexity of coastal bay physics as well as the forcing functions at the seaward boundary to the open coast often warrants the use of high resolution, three dimensional (3D), baroclinic models, which are nested to offshore, data assimilating circulation models. The purpose of this study is to determine how well 2D depth-integrated models will satisfy certain Navy applications in coastal bays. In regions dominated by tides and local wind forcing, this assumption is reasonable for time scales ranging from "instantaneous" (what a diver will feel in the water) to days (the drift of floating objects). The effort to implement, tune, and validate these types of models for limited, specific applications, is a fraction of the time than for baroclinic, nested models.

This thesis provides guidance for identifying the baroclinicity and determining which forcing function should be ignored or included in modeling the littoral area of interest. The San Diego Bay is selected for the study because of the plethora of data available, its unique pure tidal forcing and its significance for the U.S. Navy. The hydrodynamic model "Water Quality Management and Analysis Package" (WQMAP) is used to predict the instantaneous currents with various forcing functions (tides, winds, and lateral boundary fluxes) and the hydrochemical model "Chemical Management and Analysis Package" (CHEMMAP) is used to predict the water contamination and simulate

chemical attacks/accidents in San Diego Bay, which raise considerations regarding public health, the economy, ecology or even national security. Both models were purchased by U.S. NAVOCEANO. Finally, the study shows the barotropic nature of San Diego Bay, the slight significance of wind and the vulnerability of a semi-enclosed tidal basin in a possible chemical attack or accident.

The rest of the thesis is organized as follows. Chapter II examines the geography, the topography and the forcing in San Diego Bay in a detailed study of the site. Water exchange and water quality monitoring will also be addressed. Chapter III investigates the baroclinicity of the San Diego Bay using available data and shows how and where this barotropic nature cannot be assumed or applied. Chapter IV describes the WQMAP model, its physics, possibilities, assumptions and shortcomings. Chapter V evaluates the WQMAP model. The evaluation will be done through statistical analysis of u and v components of current speed based on verified data (ADCP measurements) but also through harmonic analysis and decomposition of the tides produced by the model and comparison with verified data. Chapter VI briefly describes the CHEMMAP model and presents the chemical elements used in the study, explains the selections of chemicals, and possible outcomes. Chapter VII presents the results of the six threat scenarios and their combinations to obtain general conclusions but also some distinct differences. Chapter VIII presents the overall conclusions and suggests further research and applications for future studies.

II.   SAN DIEGO BAY OCEANOGRAPHY

A.   GEOGRAPHY AND BOTTOM TOPOGRAPHY

San Diego Bay (Figure 1) is located near the west coast of southern California. It is a relatively small basin[1] (43-57 km^2) nearly 25 km long and 1-4 km wide. It shapes a flipped "Γ" and extends to the north to the city of San Diego and to the south to Coronado Island and Silver Strand, with a northwest to southeast orientation. It is a natural harbor sheltered by overlapping peninsulas (in west Point Loma and in east Coronado). San Diego, being the last southwest major city neighboring Mexico, is a very important port, especially for the U.S. Navy, since it hosts the headquarters of the 11th U.S. Naval District and a large portion of the American Fleet.
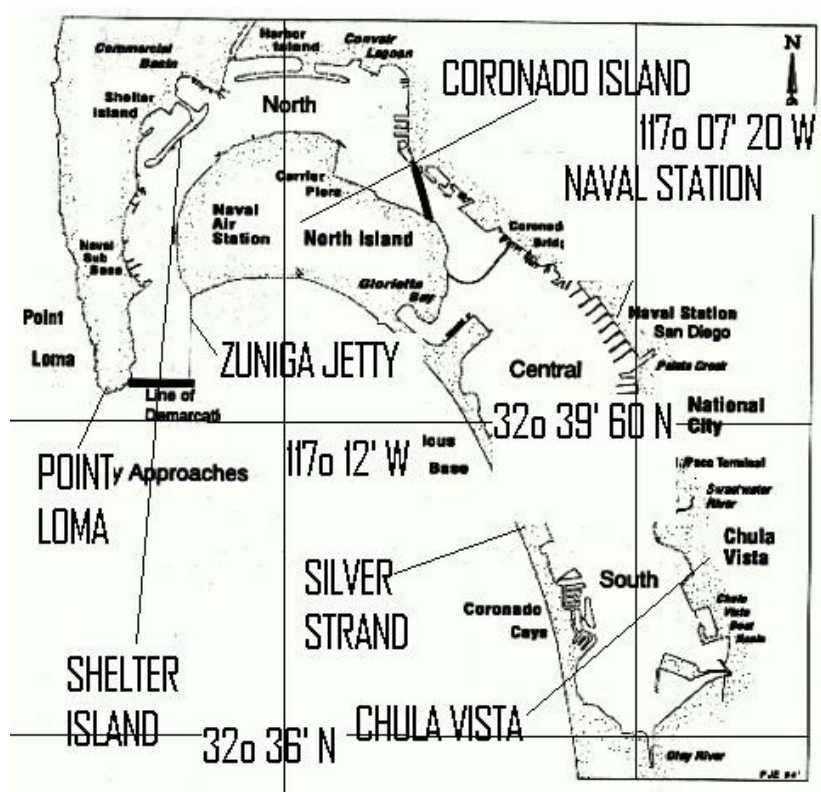
Figure 1.   Main geographical locations in San Diego Bay I (From: http://sdbay.sdsc.edu/html, last accessed on May 25, 2005).

---

[1] The area, 43km^2, is measured at mean lower low water (MLLW).
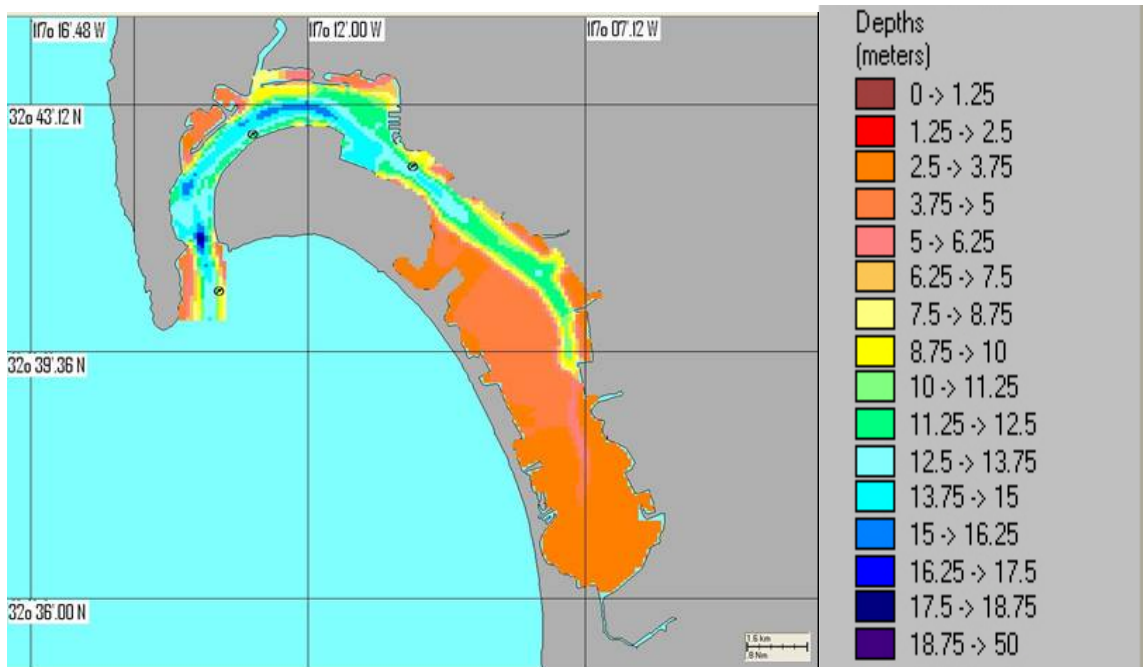
Figure 2.   San Diego Bay Bathymetry (From: WQMAP).

The topography is not homogeneous (Figure 2), and the average depth is of 6.5 m (measured from the mean sea level). The northern/outer part of the bay is narrower (1-2 km wide) and deeper (reaching depth of 15 m) and the southern/inner part is wider (2-4 km wide) and shallower (depth less than 5 m).

Since San Diego is a semi-closed bay, it exchanges with the Pacific Ocean only through a single channel at the mouth. Near the mouth of the bay, the north-south channel is about 1.2 km wide, bounded by Point Loma to the west and Zuniga jetty to the east with depths between 7 and 15 m (Chadwick – Largier, 1999a). The western side of the channel is shallower than the east side.

B.   TIDES AND TIDAL CURRENTS

San Diego Bay is a perfect example of a tidal basin connected to the ocean by an inlet with an artificial jetty (Zuniga) built to control beach erosion. The Zuniga jetty extends almost one mile offshore Zuniga Point and most of it is not clearly visible at high water (Figure 3). Obviously, the bay has been intensively engineered to accommodate shipping activities. Ninety percent of all available marsh lands and fifty percent of all

available inter-tidal lands have been reclaimed and dredging activities within the bay have been equally extensive (Peeling, 1975; Wang et al., 1998). Kelp forests extend approximately 2 km south of Point Loma (Figure 4) and along its western side. They are quite thick and they create seasonal dumping of currents to about one-third their values outside (Jackson and Winant, 1983).

Currents in San Diego Bay are predominately produced by tides (Wang et al., 1998). This tidal exchange between the ocean and the bay is a result of a phenomenon called "tidal pumping" (Fischer et al, 1979). The "pumping" of water is caused due to the flow difference between the ebb and the flood flows.

Being located at mid-latitude, tides and currents within the San Diego Bay are dominated by a mixed diurnal-semidiurnal component[2] (Peeling, 1975). The tidal range from mean lower-level water (MLLW) to mean higher-high water (MHHW) is 1.7 m with extreme tidal ranges close to 3 m (Chadwick and Largier, 1999a). Typical tidal current speeds range between 0.3-0.5 m/s near the inlet and 0.1-0.2 m/s in the southern region of the bay (Wang et al., 1998). The phase propagation suggests that the tides behave almost as standing waves with typical lags between the mouth and the back portion of the bay of 10 min and a slight increase in tidal amplitude in the inner bay compared to the outer bay. The overall tidal prism for the bay is 5.5×10^7 m^3 and the tidal excursion is larger than the mouth with a value of 4.4 km (Chadwick and Largier, 1999b). Offshore of the bay, the average current speed is 0.1 m/s. The currents are equatorward in all seasons and ninety percent of their measurements range between 1 and 0.25 m/s (Jackson and Winant, 1983).

The form ratio (ratio between diurnal -K1+O1- and semidiurnal -M2+S2-) shows that the tidal constituents are mixed (Table 1). Although there are 21 harmonic tidal constituents, it is possible to approach the solution by using four or five (including N2).

---

[2] Hence, time series data collection should cover at least two weeks, preferably 32 days to account for spring-neap variations (Wang et al., 1998)
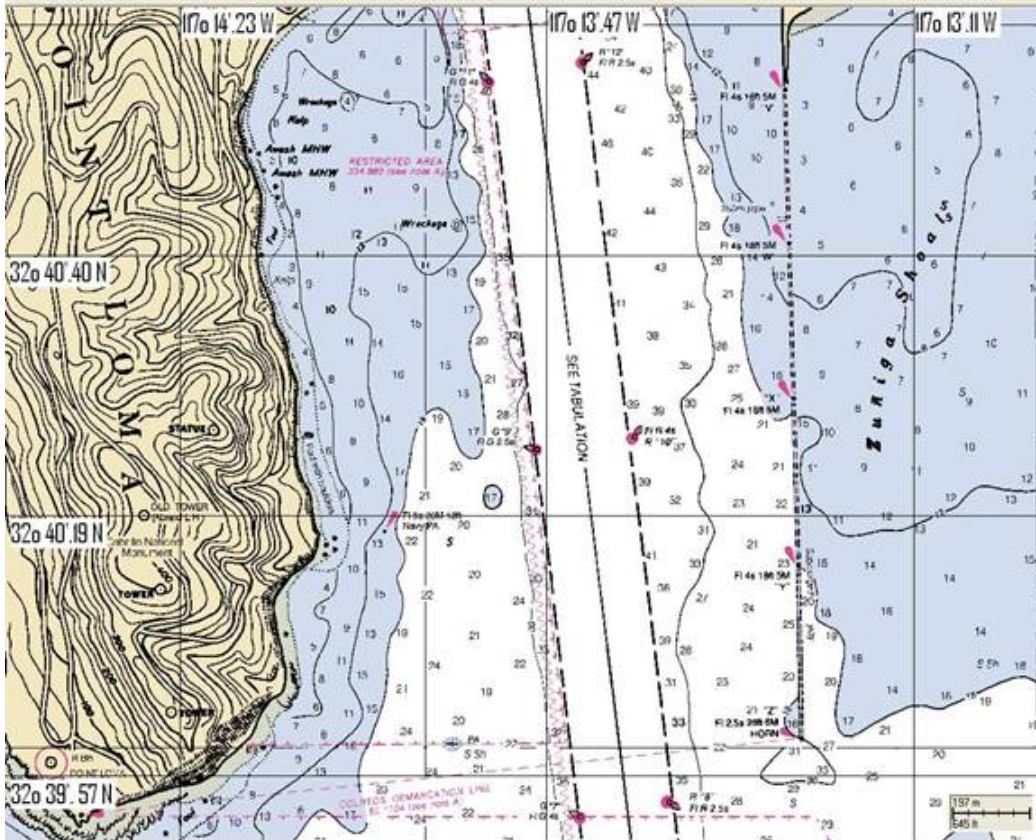
Figure 3.   Zuniga point and jetty in the entrance of San Diego Bay.
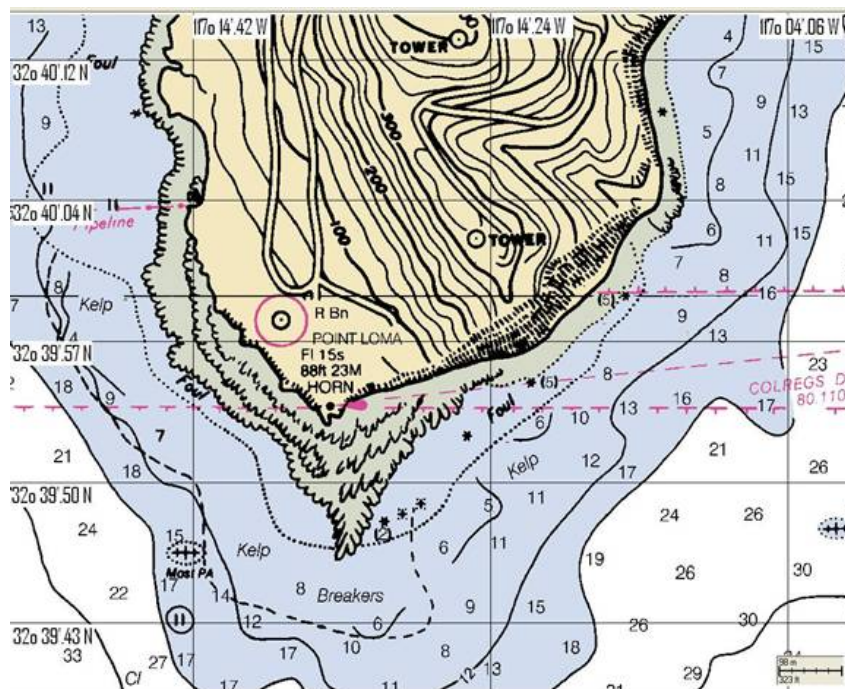
Figure 4.   Point Loma in the western entrance of San Diego Bay.

	Name	Amplitude (m)	Epoch (degrees)
1	M2	0.576	148.9
2	S2	0.233	145.9
3	N2	0.136	128.7
4	K1	0.352	210.5
5	O1	0223	195.6
6	NU2	0.027	134.3
7	MU2	0.010	109.7
8	2N2	0.018	108.7
9	OO1	0.010	225.4
10	LAM2	0.004	147.5
11	M1	0.011	194.2
12	J1	0.018	217.9
13	SSA	0.017	272.7
14	SA	0.063	182.0
15	RHO	0.008	189.2
16	Q1	0.041	188.7
17	T2	0.014	145.9
18	2Q1	0.006	180.7
19	P1	0.109	208.8
20	L2	0.013	121.7
21	K2	0.065	139.3

Table 1.   The mixed diurnal-semidiurnal nature of San Diego Bay tides. (From: National Ocean Service (NOS) accepted harmonic constants for station number 9410170 in San Diego, CA Latitude: 32° 42.8' N Longitude: 117°10.4' W).

C.   WATER EXCHANGE

Since San Diego Bay has a relatively narrow mouth and a large portion of shallow water, the percentage of total bay water exchanged during a tidal cycle can be quite significant. At mean low low water, the bay has a surface area of 4.3×10^7 m^2 and a volume of 2.795×10^8 m^3. At the mouth of the bay, the tidal prism, or volumetric flux passing a cross-section during a single flooding cycle, can reach 40% of the mean volume of the bay during a strong flood. For an average tidal cycle, the tidal prism at the mouth is about 13% of the mean total bay volume. During a single tidal cycle, water from the front portion of the bay mixes with open ocean water and exchanges with the bay water that existed on the previous cycle. This open ocean water exchanges further into the bay on successive cycles (Figure 5).

Time for exchange of 50% of total bay volume with the ocean water
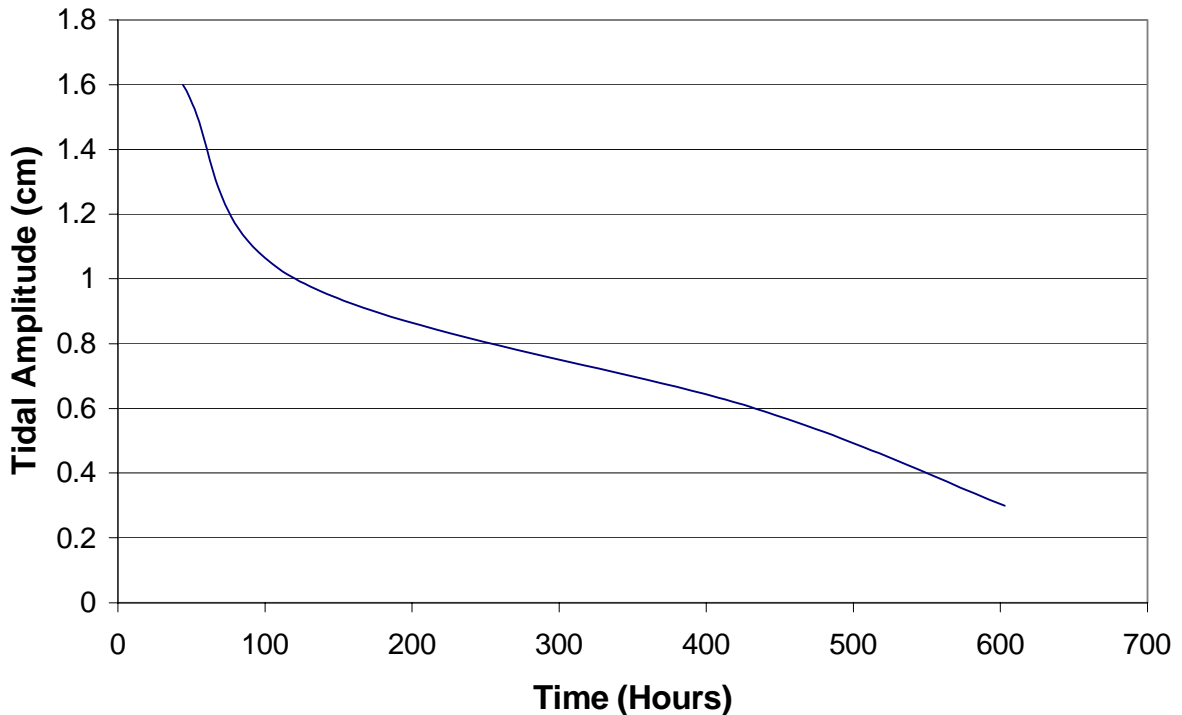
Figure 5.   Time for exchange of 50% of total bay volume with the ocean water.
(From: http://sdbay.sdsc.edu/html/modeling2.html, last accessed on May 25,
2005).

D.   HYDROGRAPHIC CONDITIONS

Freshwater inflow to the bay is minimal, comes less from the Otay River and mainly from the Sweetwater River located to the southern part of the Bay and occurs only during winter storms. Both rivers are regulated by storage reservoirs. The San Diego River has been diverted by the U. S. Army Corps of Engineers since 1875 and no longer empties into San Diego Bay.

San Diego Bay can be regarded as a vertically well-mixed estuary (Wang et al., 1998). In the south bay, the currents are much smaller than in the north and the model performance cannot be well documented. The average water temperature in San Diego Bay is 21°C and ranging between 14°C and 26°C. The average temperature during the summer (late June to late August) is 23°C. The temporal variations of temperature can be

8

seen in Figure 6. Using data from five different stations of the Bay Wide Water Quality Monitoring Program of the Port of San Diego, the conclusion was that there is zonal separation as regards the water temperature.
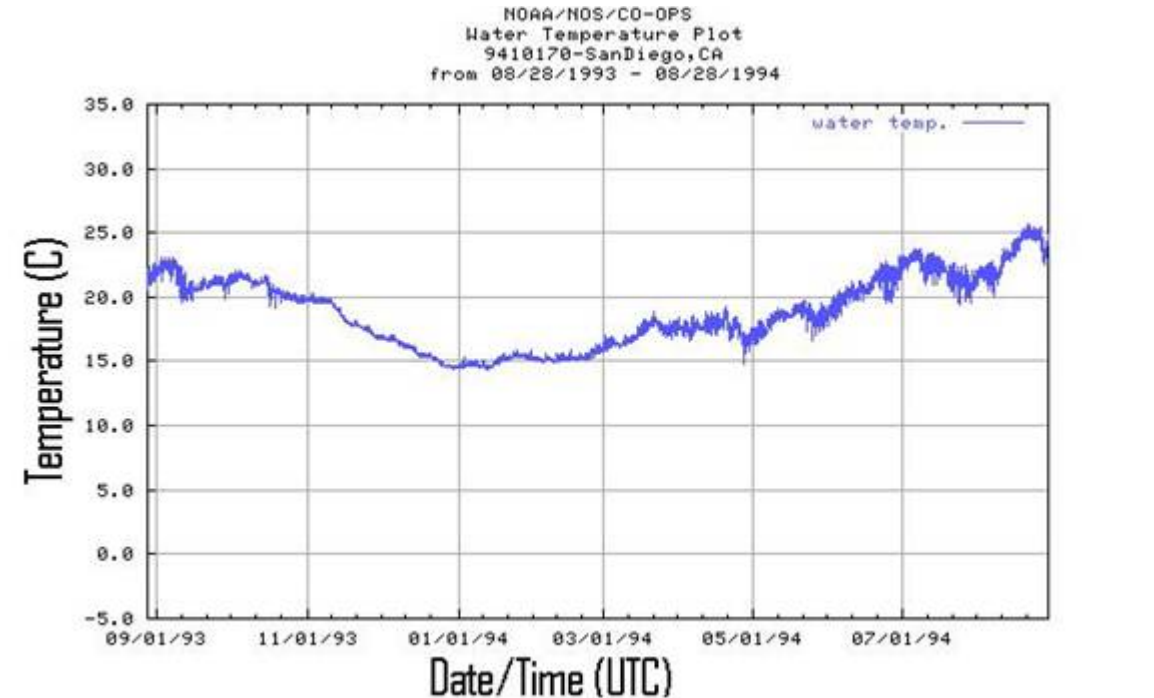
Figure 6.　　Water temperature variation in San Diego Bay from 8/28/93 to 8/28/94 (From: http://www.co-ops.nos.noaa.gov, last accessed on May 25, 2005).

In the northern part (off the Shelter Island – SI/1, number 1 in Figure 7), the range is between 14°C and 19.5^{o}C during the year and 17.5^{o}C to 19.5^{o}C during the summer. At the Laurel Street Anchorage (LSA/2, number 2 in Figure 7), it reaches 21°C, with a range of 14°C to 21°C during the year but only 19°C to 21°C during the summer. Further south at the Bay Bridge Anchorage (BBA/3, number 3 in Figure 7) the range is from 15°C to 22°C and again in the summer is from 20°C to 22°C. At the Sweet Water Channel (SWC/4, number 4 in Figure 7) the range is from 14°C to 25°C with 22°C to 25°C in the summer. In Chula Vista Marina (CVM/5, number 5 in Figure 7), it reaches a maximum of 26°C and a minimum of 23°C in the summer. As expected, the north part of the bay is colder than the south and in the summer the water is much warmer than in the winter. For this study, a standard water temperature of 23°C is used since the data were gathered in the summer.

9

The salinity varies from 32.5 to 37.5 ppt and the average is 35 ppt. The zonal separation is similar to the temperature. In LSA and SI, the range is from 33 to 35.5 ppt. In BBA, it reaches 36 ppt. In SWC, the range is from 32 to 37 ppt. In CVM, it is from 34 to 37.5 ppt. Again, detailed analysis shows that in the summer, salinity increases with an average of 1 ppt because of the zero precipitation. Therefore, 36 ppt is used as the standard salinity during the summertime.

E.   ATMOSPHERIC FORCING

The winds have a very small effect on the currents because of their intensity and the geography of the bay. Both mean westerly winds in the afternoon and mean easterly winds in the morning and evening are less than 5 m/s (10 knots).[3] NOAA's weather description for San Diego during June, July and August points out that, during these months, there are practically no storms. Wind forcing is always less significant than tidal forcing. The shallow waters make instrument deployment problematic. With small currents, the angular momentum of the instruments induces direction errors. Hence, the model is more difficult to validate in these areas.

Annual precipitation is about 0.26 m (Woodward and Clyde, 1996) and occurs mostly in winter. Therefore, in terms of estuarine classification, San Diego Bay is generally positive, i.e., drainage inflow exceeds evaporation (Pritchard, 1952). However, during the summer, the evaporation rate, about 0.16 m, exceeds precipitation[4] (Peeling, 1975) and a "reversed estuary" phenomenon is observed (Defant, 1961). In general, the low inflow of fresh water provokes very small buoyancy forcing; hence the density-driven circulation is driven by seasonal heating and evaporation. Note that for precipitation, in June, the rainfall is negligible averaging only 0.17 cm, in July 0.5 cm and in August 0.25 cm.[5] Therefore, small surface water mass flux (mostly in winter) and wind forcing for the San Diego Bay are ignored. This study area is a small basin with circulation driven by tidal flow (Fagherazzi et al., 2003).

---

[3] In accordance with the Golden Date Weather Services archive, the average speed is between 6.4 and 7.8 knots. See http://ggweather.com, last accessed on May 25, 2005.

[4] The precipitation during the summer is usually zero.

[5] NOAA. See http://www.wrh.noaa.gov/sgx/climate/san-san-month.htm, last accessed on May 25, 2005.

The Californian Current has a significant influence on the regional oceanography of the Californian coast. Under certain conditions, the alongshore flow can influence the shelf circulation in southern California, which in turn, drives flow around Point Loma. This can lead to either a re-circulating eddy in the lee of the headland or northward currents inshore.

F.   WATER QUALITY MONITORING

In 1960, an earthquake with a Richter scale of 9 in Chile caused the biggest sudden rise in sea level ever recorded in the San Diego area of 1.07 m at the Scripps pier. There is a natural protection due to the 160 km wide continental shelf of San Diego. There is a fault off San Diego Bay, but it is inactive. These are the reasons why from the 15 locally generated tsunamis in California since 1812, only two have occurred in Southern California, and only one in San Diego, dating back to 1862.
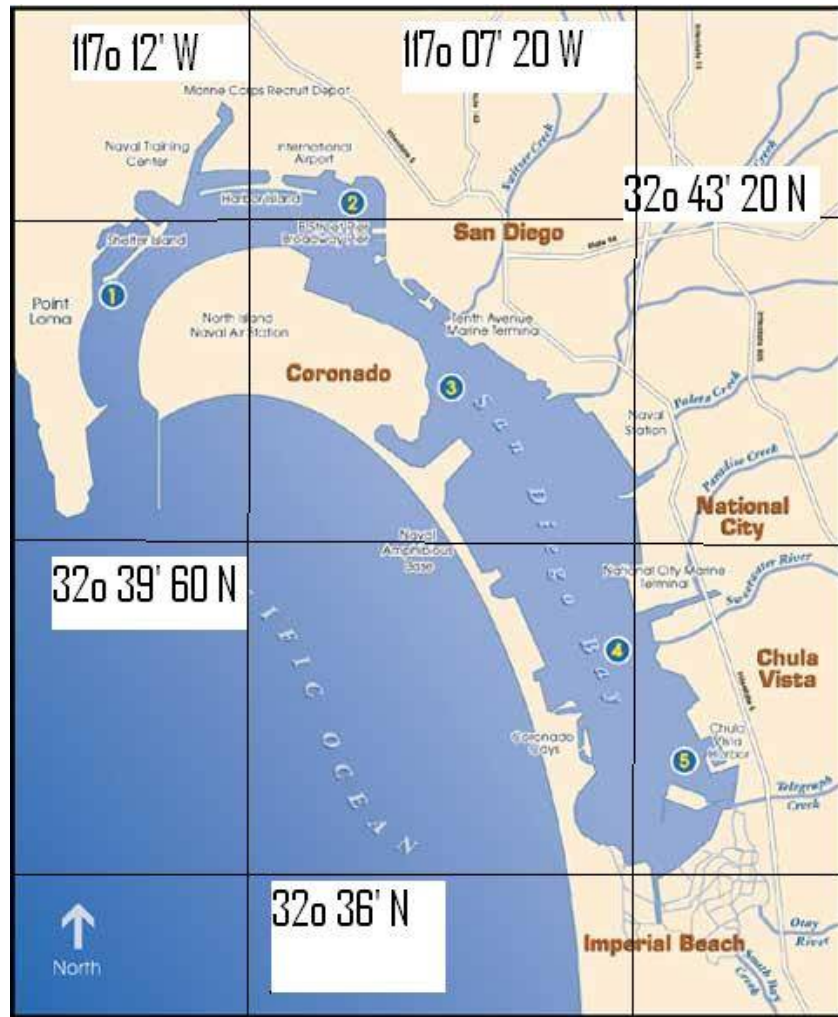
Figure 7.   Bay Wide Water Quality Monitoring Program Stations (From:
http://www.portofsandiego.org/sandiego_environment/bay_water_sampling.asp),
last accessed on May 25, 2005.

Several mineral resource extraction activities are now occurring or have occurred
in the recent past in San Diego Bay. Among them, the most important are the production
of sodium chloride (salt), bromine and other chemicals from sea water, magnesium,
magnesium compounds and brine. There is widespread toxicity in San Diego Bay
sediments attributable to copper, zinc, mercury, polycyclic aromatic hydrocarbons,
polychlorinated biphenyls (PCBs) and chlordane.

No single chemical or chemical group has a dominant role in contributing to the
identified toxicity. Contributions of trace metals from vessel activities have long been

suspected as a potentially large source to San Diego Bay. Shelter Island Yacht Basin, a semi-enclosed boat harbor, has been added to the State's list of impaired water bodies (the 303d list). These contributions arise from specially formulated paints, impregnated with biocides, and applied to boat hulls to retard the growth of fouling organisms such as barnacles. Levels of potentially toxic trace metals, especially copper and zinc (Figure 8) exceed regulatory water quality objectives and gradients of toxicity to mussels increase as one enters the Shelter Island (Figure 1).
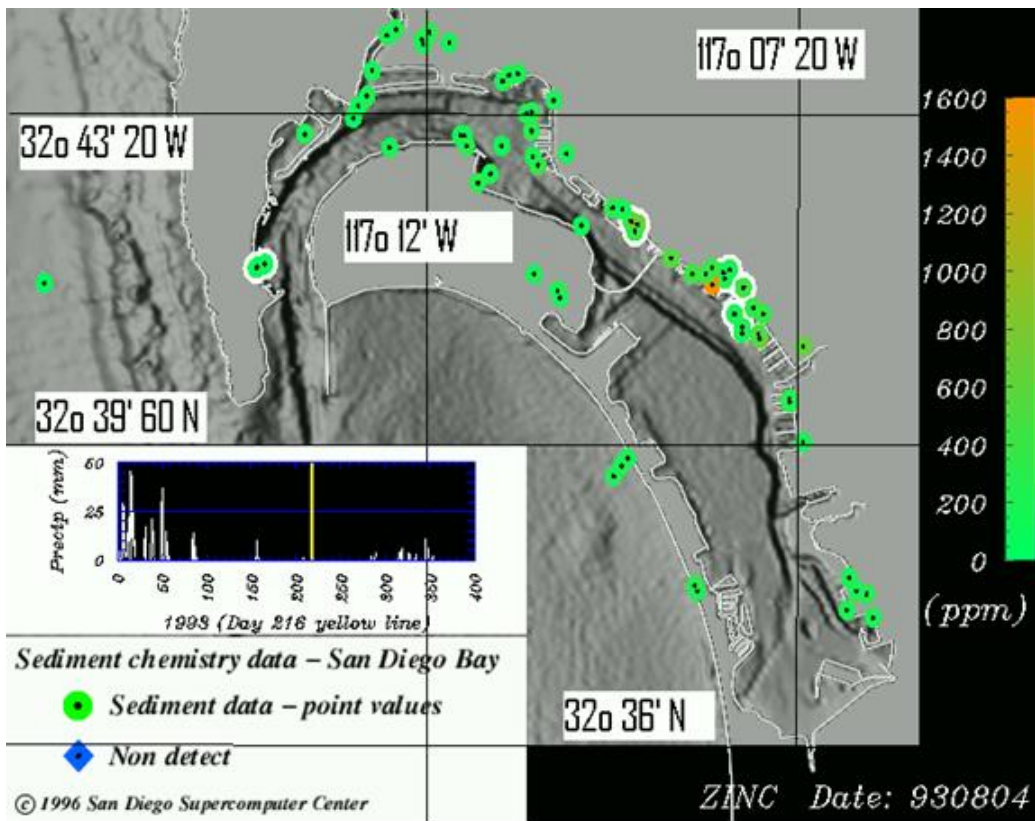
Figure 8.   Zinc concentration in San Diego Bay on July 4, 1993 (From: http://sdbay.sdsc.edu/html, last accessed on May 25, 2005).

13

THIS PAGE INTENTIONALLY LEFT BLANK

III. BAROTROPIC AND BAROCLINIC CURRENTS

Three Acoustic Doppler Current Profilers (ADCPs) (Figure 9) were deployed by SPAWAR in 1993 and their measurements will be used in this study. The first was a broad band one (bb) and was deployed in position ($32^o42'25.8"$N, $117^o13'30.6"$ W) from June 22 until July 23, 1993. The second was a narrowband one (nb1) and was deployed in position ($32^o42'43.98"$N, $117^o12'55.68"$W) from June 22 until August 26, 1993. The last was a narrowband one (nb2) and was deployed in position (32° 42' 17.22"N, $117^o10'$ 8.88"W) from June 23 until August 27, 1993.
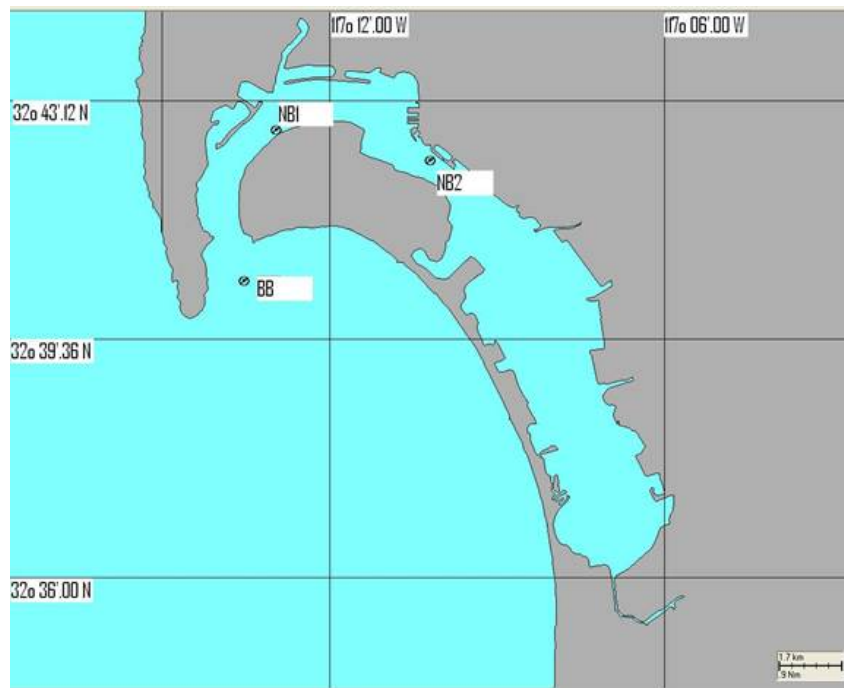
Figure 9.   Positions of the ADCPs deployed in 1993 (From: WQMAP).

By checking the ADCP data inside the bay (nb1, nb2), San Diego Bay was concluded to be vertically well mixed. The u and v components are plotted in three different depths for the ADCP measurements to prove the aforementioned statement (Figures 10-15).

U in water column for NB1
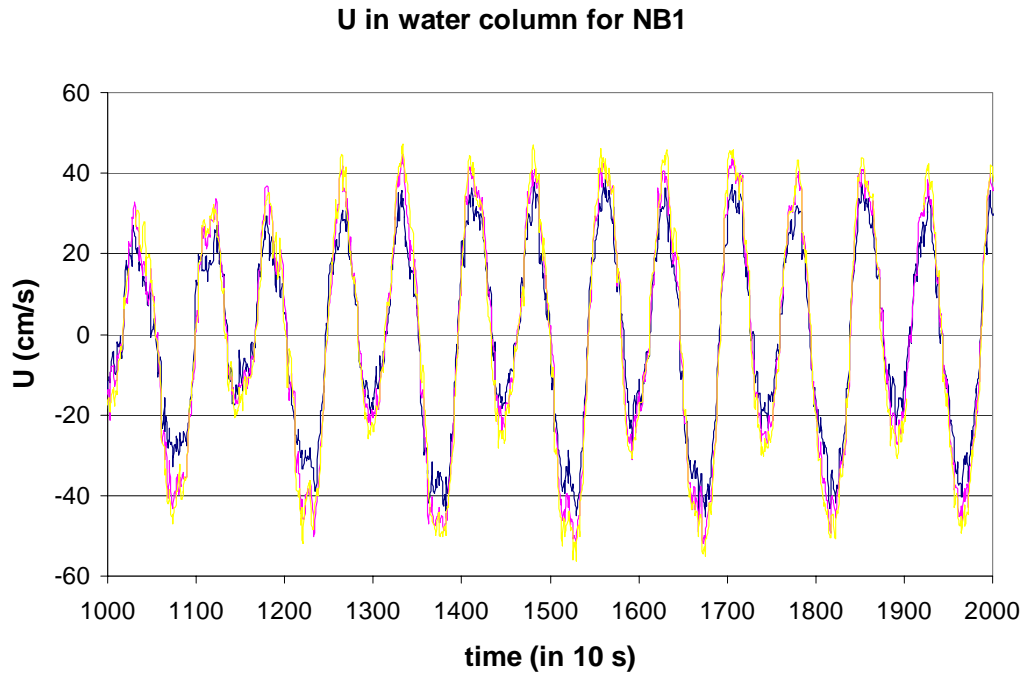
Figure 10.   U component from ADCP data (nb1) for surface (yellow), middle depth (purple) and bottom (blue).

V in water column for NB1
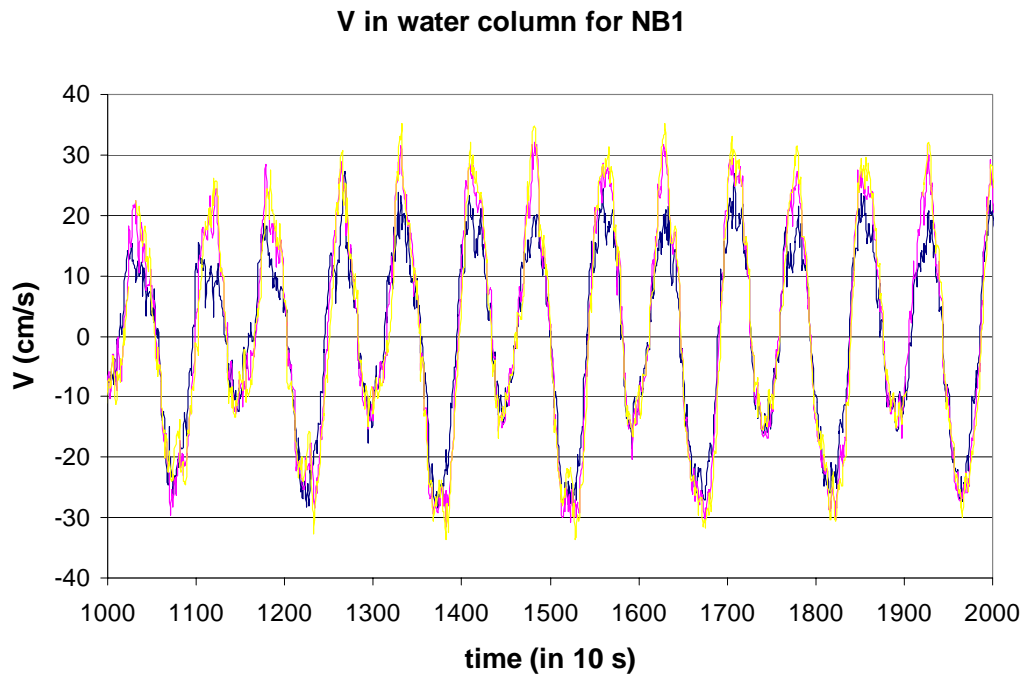
Figure 11.   V component from ADCP data (nb1) for surface (yellow), middle depth (purple) and bottom (blue).

16

U in water column for NB2
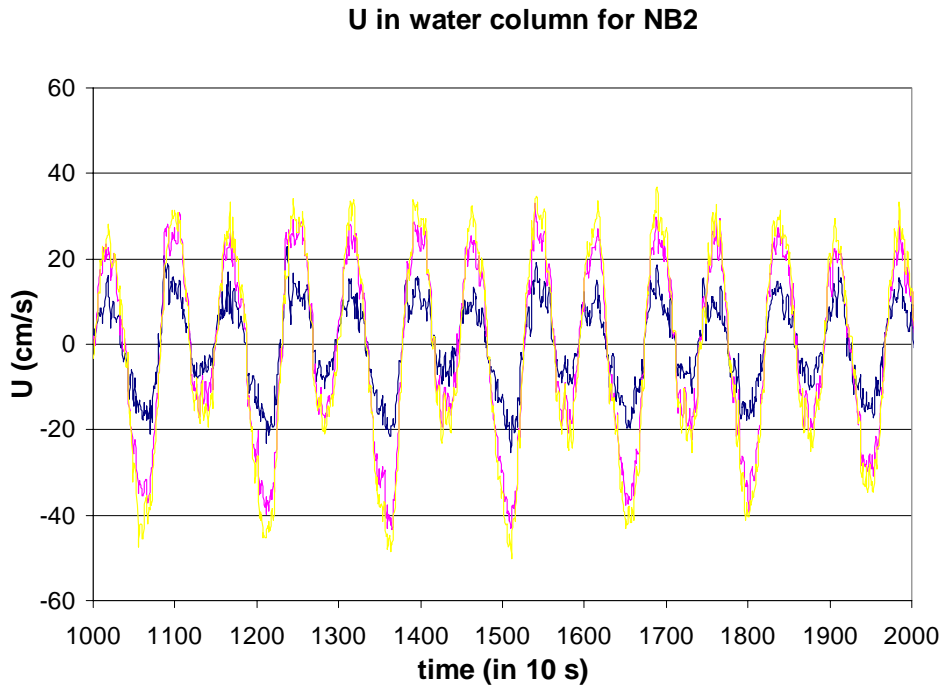
Figure 12.   U component from ADCP data (nb2) for surface (yellow), middle depth (purple) and bottom (blue).

V in water column for NB2
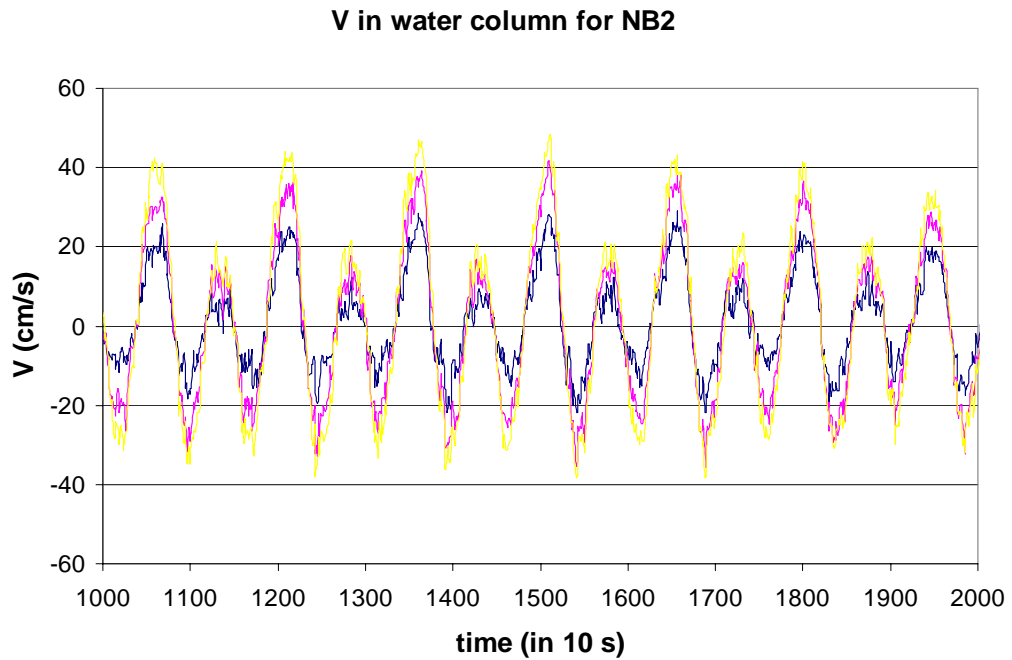
Figure 13.   V component from ADCP data (nb2) for surface (yellow), middle depth (purple) and bottom (blue).

17

V in water column for BB
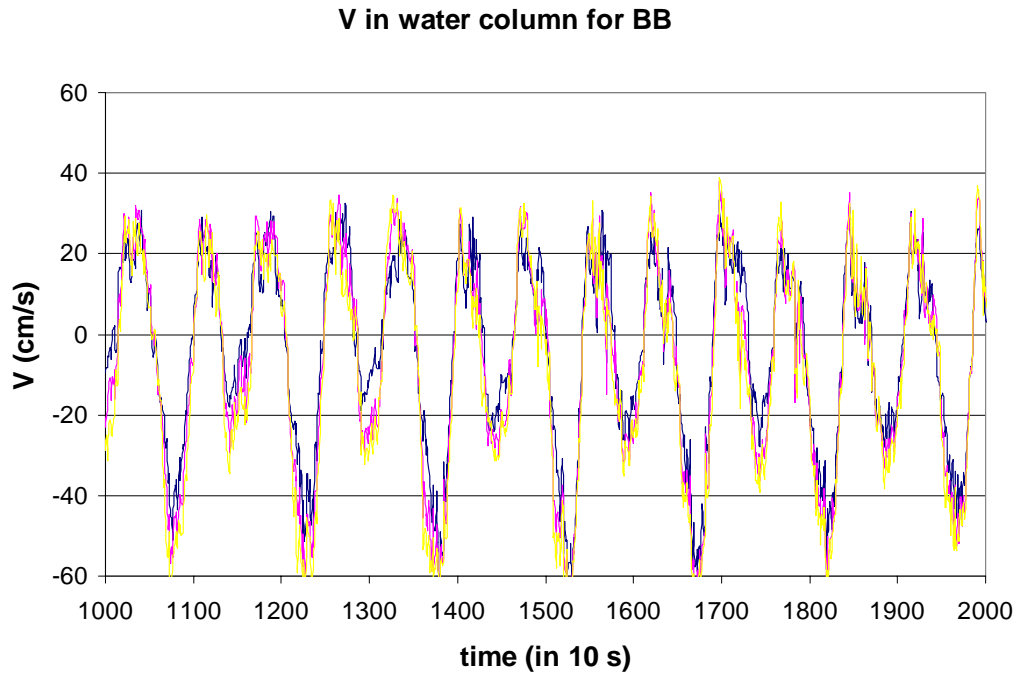
Figure 14.   V component from ADCP data (bb) for surface (yellow), middle depth
(purple) and bottom (blue).

U in water column for BB
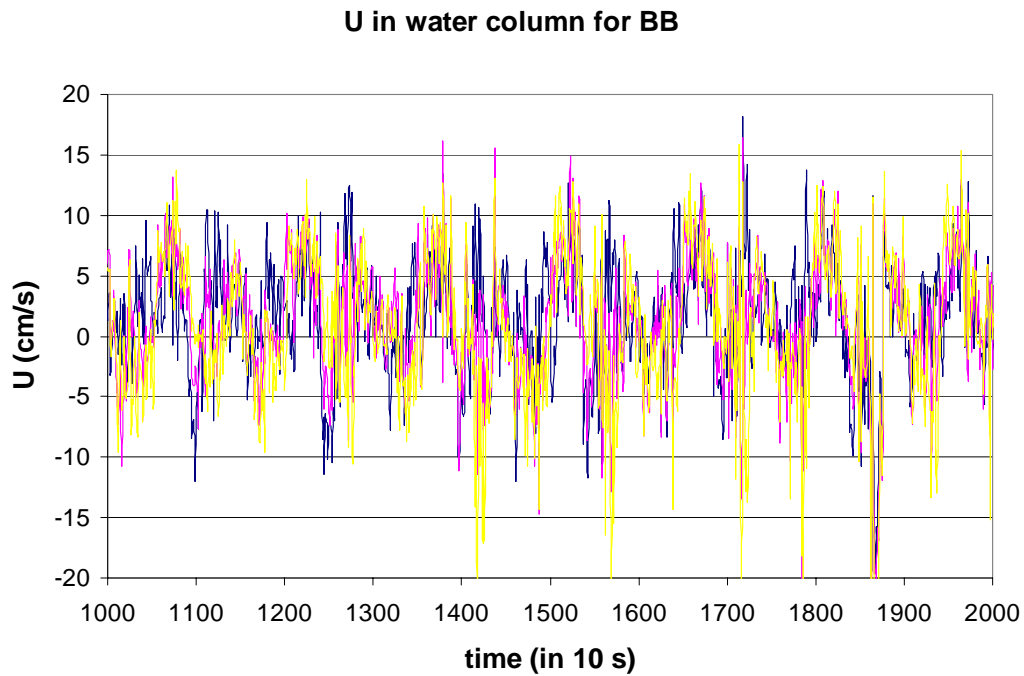
Figure 15.   U component from ADCP data (nb2) for surface (yellow), middle depth
(purple) and bottom (blue).

For nb1, the correlation coefficient between the surface and bottom is 97.16% for the u-component and 97.16% for the v-component 96.32%. For nb2, the correlation coefficient between the surface and bottom is 91.89% for the u-component and 94.71% for the v-component 96.32%. Between the surface and bottom, the phase matches very well and so does the trend in the respective amplitudes. In terms of actual amplitude matching, it is possible to optically verify the good match. The differences observed cannot contradict that San Diego Bay is well mixed.

The bb is a more interesting case because it is not in the main bay, since it is further south from Coronado Island to the east of Point Loma. In that case, an excellent correlation still exists for the v component but not for the u. The correlation coefficient between the surface and bottom is 92.94% for the v-component and 35.19% for the u-component. By checking the correlation between the u component in the surface and in middle depth, the coefficient improves and becomes 78.44% and by comparing the v component of the bottom and the middle depth it becomes 61.65%. In order to understand the reasons for this, the power spectrum diagram (PSD) of u component at bb is calculated for both the surface and the bottom (Figures 16-17).
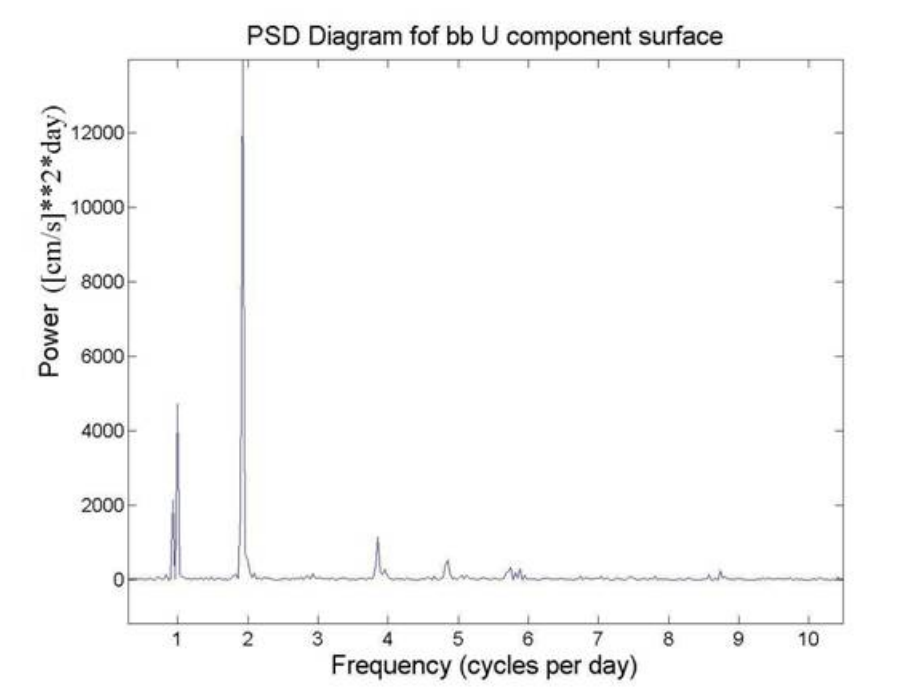
Figure 16.   Power spectrum diagram (PSD) for bb u component in the surface.

19
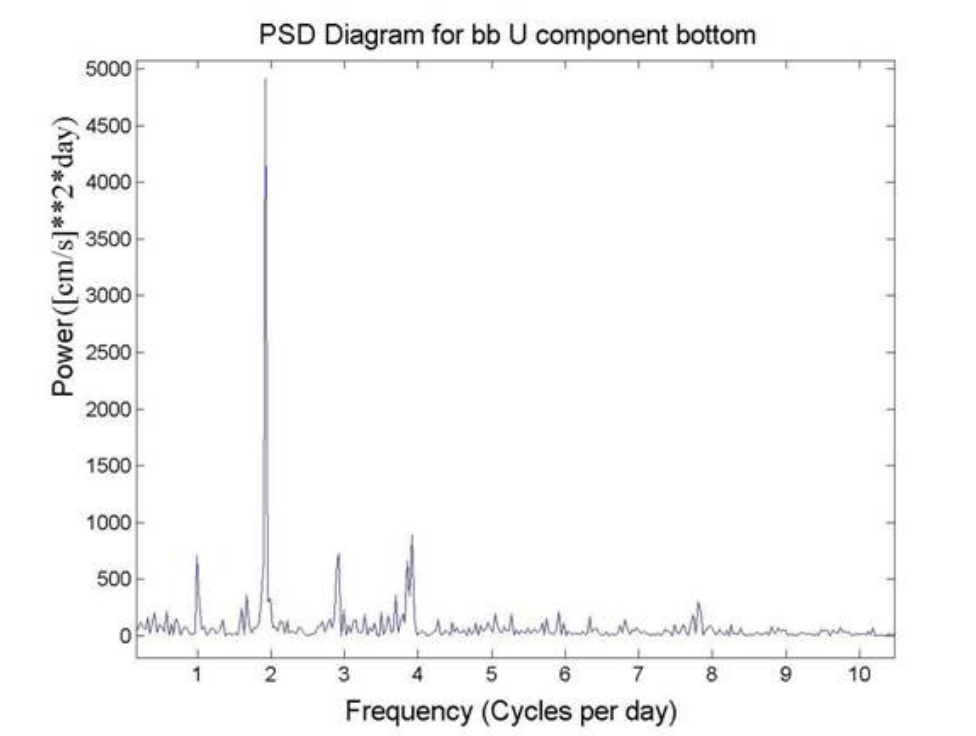
Figure 17.   Power spectrum diagram (PSD) for bb u component at the bottom.

Distinction of the power spectra of u at bb between the surface and bottom clearly indicate that waters cannot be treated as well-mixed. Obviously, the spikes both at low and high frequencies (lower than 1 cycle per day and higher than 2 – especially at 3 and 4 cycles per day) are very significant. Since it is not in a more "open ocean" environment, it is very normal that both the California Current System and the wind play a significant role. However, it is not only the long term or short term forcing that is responsible for this difference. Even when filtering the data to keep only the part that results from the tidal influence, the correlation was not satisfactory. A band-pass butterworth filter was used to filter out all frequencies either smaller than 0.5 cycles per day or greater than 2.5 cycles per day. For v, an absolutely perfect correlation (100%) was achieved, but for u, a correlation coefficient of only 49.53% was achieved.

Since the correlation of the v component is perfect, something obviously influences the u component. It is possible to easily conclude the proximity of the ADCP data to the Zuniga jetty (which has a North-South direction) influences the u component due to reflections. Hence, suffice it to say that there are well mixed waters inside San

20

Diego Bay and without ruling out the well-mixed nature of the waters in the mouth of the Bay, it is possible to conclude that the waters are less well-mixed. Hence, the application of a 3-D, if not necessary, will produce better results. However, firstly, it was concluded that the influence of other factors (such as the wind driven circulation) cannot be entirely ignored outside the bay, and secondly, that there are well mixed waters only inside San Diego Bay.

ADCP site	Velocity component	Correlation coefficient	Remarks
Nb1	u	97.16%	unfiltered
Nb1	v	96.32%	unfiltered
Nb2	u	91.89%	unfiltered
Nb2	v	94.71%	unfiltered
bb	u	35.19%	unfiltered
bb	v	92.94%	unfiltered
bb	u	49.53%	Filtered 0.5 – 2.5 cycles per day
bb	v	100.00%	Filtered 0.5 – 2.5 cycles per day

Table 2.   Correlation between surface and bottom measurements in all ADCP sites – proof of barotropic nature of San Diego Bay.

THIS PAGE INTENTIONALLY LEFT BLANK

IV.   HYDRODYNAMIC MODEL

A.   MODEL DESCRIPTION

The hydrodynamic model used in this study is the "Water Quality Management and Analysis Package" (WQMAP) developed by the Applied Science Associates, Inc. in Narragansett, Rhode Island. It consists of a boundary conforming grid generation model, a three-dimensional[6] time dependent primitive equation model, and a suite of pollutant transport and fate models. These models are executed on a boundary fitted grid system. However, they can be operated on any orthogonal curvilinear grid or a rectangular grid, which are special cases of the boundary fitted grid. The model is configured to run in a vertically averaged (barotropic) mode or in a fully three-dimensional mode. Several approximations are made in the model formulation, including the hydrostatic and Boussinesq approximations (Chu et al., 2004). As happens in all vertically-averaged models, it is implicitly assumed that the water density and velocity are nearly depth-independent over the water column.[7] It is also assumed that the water depth is sufficiently shallow so as to neglect the Ekman layer (Cheng et al., 1983).

WQMAP embeds the Geographic Information System (GIS) with maps for any region in the world and environmental data management tools. The GIS can be used to provide input data to the models, as well as to present model predictions better. The model solves the three dimensional conservation of mass, momentum, and energy equations on a spherical, non-orthogonal, boundary conforming grid system and can be applied to both estuarine and littoral regions. The eddy viscosities are either specified by the user or based on a one-equation turbulent kinetic energy (TKE) model. Output of the TKE model can be used in conjunction with a prescribed mixing length to determine the vertical eddy viscosities. The model predicts time varying fields of surface elevations and velocities. Environmental forcing inputs include tides, river inflows, surface elevations,

---

[6] WQMAP can also run in a two-dimensional mode, which is a better simplifying choice for San Diego Bay.

[7] Normally, the horizontal density gradients are treated explicitly in the momentum equations; however, due to the predominantly tidal current production in San Diego Bay, the horizontal density gradient can be neglected in short-time prediction.

and wind fields. A sigma stretching system is incorporated to diagram the free surface and bottom to resolve bathymetric variations (Armstrong, 2004). Calculations are achieved on a space-staggered grid system in the horizontal and a non-staggered system in the vertical.

The three-dimensional hydrodynamic equations contain fast moving external gravity waves and slow moving internal gravity waves. The equations of motion are split into vertically averaged equations (exterior mode) and vertical structure equations (interior mode). This technique allows the calculation of the free surface elevation from the exterior mode and the three dimensional currents and thermodynamic properties from the interior mode. The external mode equations are obtained by integrating the three dimensional equations of continuity and conservation of momentum from $\sigma = 0$ to $\sigma = 1$ (WQMAP Technical Manual, 2003). In the exterior mode, the Helmholtz equation, given in terms of the sea surface elevation, is solved to ease the time step restrictions normally imposed by the aforementioned gravity wave propagation. In the interior mode, the flow is predicted by an explicit finite difference method, except that the vertical diffusion term is treated implicitly (Madala and Piaczek, 1977). The time step generally remains the same for both exterior and interior modes (Spaulding et al., 1999). Hence, the user can specify the variable (currents, temperature, surface elevation and salinity) over a certain simulation period and then the results/ predictions are presented in either color contours or vectors.

B. MOMENTUM AND CONTINUITY EQUATIONS FOR BAROTROPIC MODE

If U is the vertically averaged component in ξ-direction, V the vertically averaged component in η-direction, A_h the horizontal eddy viscosity, τ^w the wind stress, and τ^b the bottom stress, then the two-dimensional vertically averaged conservation of momentum equations are as follows:

$$\frac{\partial UD}{\partial t}+\frac{1}{\sqrt{g_{11}g_{22}}}\left[\partial\frac{\left(U^2D\sqrt{g_{22}}\right)}{\partial\xi}+\partial\frac{\left(UVD\sqrt{g_{11}}\right)}{\partial\eta}+UVD\frac{\partial\left(\sqrt{g_{11}}\right)}{\partial\eta}-V^2\frac{\partial\left(\sqrt{g_{22}}\right)}{\partial\xi}\right]$$

$$-fDV=-\frac{gD}{R\sqrt{g_{11}}}\left[\frac{\partial\zeta}{\partial\xi}+\frac{D}{\rho_o}\int_{-1}^{0}\int_{\sigma}^{0}\left(\frac{\partial\rho}{\partial\xi}-\frac{\sigma}{D}\frac{\partial D}{\partial\xi}\frac{\partial\rho}{\partial\sigma}\right)d\sigma\right]+\frac{1}{\rho_o}\left(\tau_\xi^w-\tau_\xi^b\right)+A_hD\nabla^2U \tag{1}$$

$$\frac{\partial VD}{\partial t}+\frac{1}{\sqrt{g_{11}g_{22}}}\left[\partial\frac{\left(UVD\sqrt{g_{22}}\right)}{\partial\xi}+\partial\frac{\left(V^2D\sqrt{g_{11}}\right)}{\partial\eta}+UVD\frac{\partial\left(\sqrt{g_{22}}\right)}{\partial\xi}-U^2\frac{\partial\left(\sqrt{g_{11}}\right)}{\partial\eta}\right]$$

$$+fDV=-\frac{gD}{R\sqrt{g_{22}}}\left[\frac{\partial\zeta}{\partial\eta}+\frac{D}{\rho_o}\int_{-1}^{0}\int_{\sigma}^{0}\left(\frac{\partial\rho}{\partial\eta}-\frac{\sigma}{D}\frac{\partial D}{\partial\eta}\frac{\partial\rho}{\partial\sigma}\right)d\sigma\right]+\frac{1}{\rho_o}\left(\tau_\eta^w-\tau_\eta^b\right)+A_hD\nabla^2V \tag{2}$$

The continuity equation is given by

$$R\sqrt{g_{11}g_{22}}\frac{\partial\zeta}{\partial t}+\frac{\partial\left(UD\sqrt{g_{22}}\right)}{\partial\xi}+\frac{\partial\left(VD\sqrt{g_{11}}\right)}{\partial\eta}=0 \tag{3}$$

Here, ρ_o is the characteristic water density (1,025 kg/m³), f is the Coriolis parameter ($f=2\Omega\sin\varphi$), R is the earth radius, and

$$\sigma=\frac{z+H}{\zeta+H} \tag{4}$$

where H is the water depth, $D=H+\zeta$, is the total water depth (bathymetry and surface elevation), $\sigma=1$ represents the ocean surface, and $\sigma=0$ represents the ocean bottom. Finally, the transport equation for ψ (temperature, salt or any substance) is as follows,

$$\frac{\partial\psi}{\partial t}+\frac{u}{R\sqrt{g_{11}}}\frac{\partial\psi}{\partial\xi}+\frac{v}{R\sqrt{g_{22}}}\frac{\partial\psi}{\partial\eta}+w\frac{\partial\psi}{\partial\sigma}=$$

$$\frac{1}{R^2g_{11}}\left(D_h\frac{\partial^2\psi}{\partial\xi^2}\right)+\frac{1}{R^2g_{22}}\left(D_h\frac{\partial^2\psi}{\partial\eta^2}\right)+\frac{1}{D^2}\frac{\partial}{\partial\sigma}\left(D_v\frac{\partial\psi}{\partial\sigma}\right) \tag{5}$$

C.   COORDINATE SYSTEM AND BOUNDARY CONDITIONS

An important feature of WQMAP is its hybrid orthogonal curvilinear-terrain following coordinate system. Let (φ,θ) be the latitude and longitude and (ξ,η) be the coordinates on a generalized orthogonal curvilinear coordinate system. Let ζ be the

25

surface elevation and σ the vertical σ-coordinate. The two metric tensors connecting (φ, θ) to (ξ, η) are defined and the coefficient g_{11} is the metric tensor in ξ-direction and the coefficient g_{22} metric tensor in η-direction. These tensors permit the model to transform the boundary fitted grid to a numerical grid employed for spatial discretization utilized in an Arakawa *C* Grid (Chu et al., 2004)

$$g_{11} = \left(\frac{\partial \varphi}{\partial \xi}\right)^2 \cos^2 \theta + \left(\frac{\partial \theta}{\partial \xi}\right)^2, \quad g_{12} = \left(\frac{\partial \varphi}{\partial \eta}\right)^2 \cos^2 \theta + \left(\frac{\partial \theta}{\partial \eta}\right)^2 \tag{6}$$

which are the metric tensors in ξ and η directions. Furthermore, at the surface,

$$\frac{A_v}{D}\left(\frac{\partial u}{\partial \sigma}, \frac{\partial v}{\partial \sigma}\right) = C_d \rho_a \left(\sqrt{W_\xi^2 + W_\eta^2}\right)\left(W_\xi, W_\eta\right), \tag{7}$$

and at the bottom,

$$\frac{A_v}{D}\left(\frac{\partial u}{\partial \sigma}, \frac{\partial v}{\partial \sigma}\right) = C_d \rho_o \left(\sqrt{u^2 + v^2}\right)\left(u, v\right). \tag{8}$$

The land boundaries are assumed impermeable. Therefore, the normal component of the velocity is set to zero. Sea surface elevation or tidal harmonic constituents can be specified as a function of time along the open boundaries. At the closed boundaries, the transport of substance (i.e., salinity) is zero. At the open boundaries, the concentration is specified during the inflow, using the characteristic values for San Diego Bay (for temperature, 23° for summer months is used and for salinity 36 ppt is used). On outflow, the substance is advected out of the model domain according to the following equations:

$$\frac{\partial \psi}{\partial t} + \frac{u}{R\sqrt{g_{11}}}\frac{\partial \psi}{\partial \xi} = 0, \quad \frac{\partial \psi}{\partial t} + \frac{v}{R\sqrt{g_{22}}}\frac{\partial \psi}{\partial \eta} = 0. \tag{9}$$

D.   RECTANGULAR GRID

The scenario used for this research uses both the two-dimensional and three-dimensional hydrodynamic model, taking into account the minimal wind considerations for San Diego Bay, as analyzed in Chapter I. WQMAP is supplied with maps of the area. A small spatial extent ASA file (.bdm), containing high resolution characteristics, is used. The grid used (Figure 18) was created with a detailed resolution (I_{max} and J_{max}) 150 by

200 (30,000 nodes) grid. For this grid, the average horizontal resolution is 40m. The rectangular grid used improves the previously created boundary-fitted ones (Armstrong, 2004) having a better resolution and realistically takes into consideration the Zuniga jetty (Figure 19), not included in previous studies.
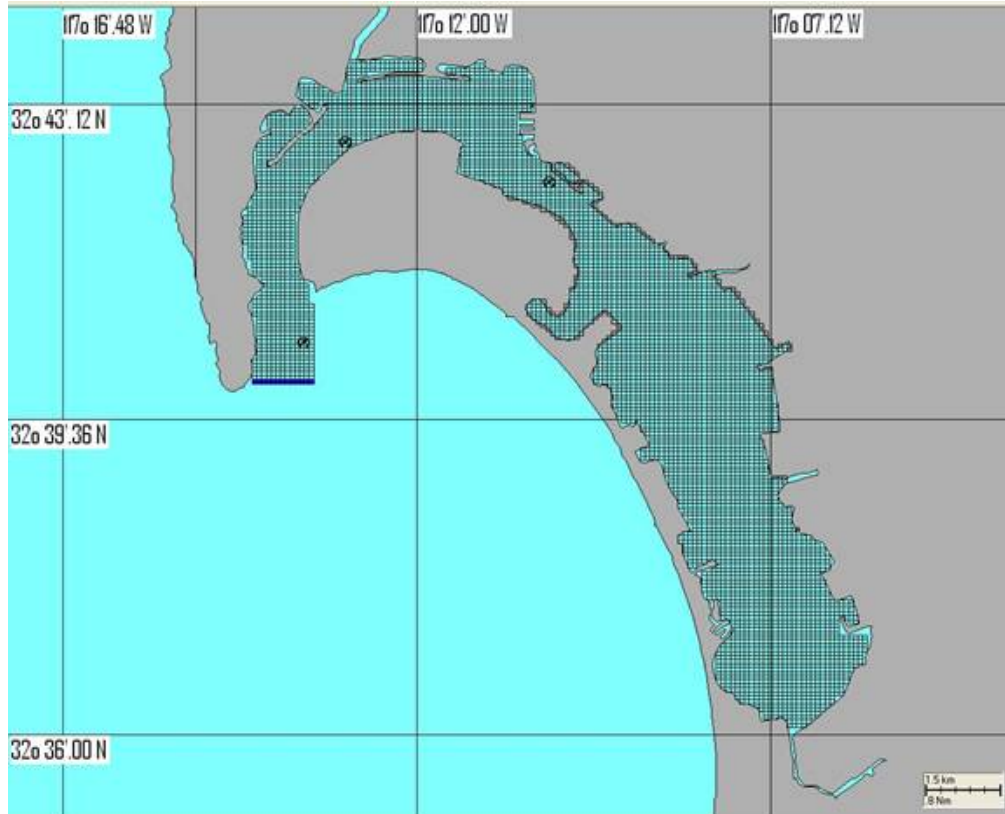
Figure 18.   High Resolution Grid of San Diego Bay (From: WQMAP).
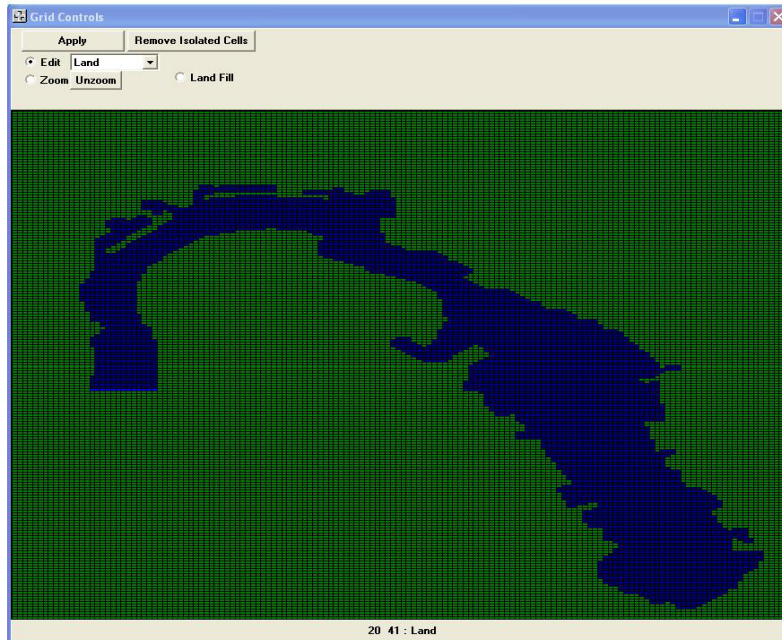
Figure 19.   Grid representation taking into account the Zuniga jetty (From: WQMAP).

The bathymetry is from the NOAA 3-second data base supported by the National Ocean Service (NOS) soundings database (i.e., Hydrographic Survey Data, version 3.2) averaged within each cell. Hence, it is adequate for model resolution; however, it should be applied with caution near the coastline because the resolution of the data base does not conform to small details in the coastline. As seen in Chapter V, this is a factor to be taken into account since the current meters are located very close to the shore. It should also be mentioned that the model requests a minimum depth (set at 2 m in our study). There is also a smoothing of the bathymetry, which is essential for the model function, but might cause significant errors in very shallow areas.

V. MODEL EVALUATION

The tidal forcing in the entrance of the bay is reproduced with time series from Wxtide32 model database based on verified data from the NOOA/NOS CO-OPS. All measurements (hourly height water level) had as a reference the MLLW and were conducted between June 22, 1993 and August 27, 1993. Figure 20 shows the water elevation, in accordance with NOAA San Diego Station number 9410170, located at $(32^o42'48''N, 117^o10'24''W)..$

The aforementioned tidal forcing (Table 3) was chosen to verify the model with actual data available for the certain period of time.

The positions of the ADCPs deployed will be repeated: (1) the broad band ADCP (at bb) at $(32^o42'25.8''N, 117^o13'30.6'' W)$ from June 22 until July 23, 1993, (2) narrowband ADCP (at nb1) at $(32^o42'43.98''N, 117^o12'55.68''W)$ from June 22 until August 26, 1993, and (3) the narrowband ADCP (at nb2) at $(32^o42' 17.22''N, 117^o10' 8.88''W)$ from June 23 until August 27, 1993. An initial comparison of unfiltered data and original model run is conducted to see if they are correlated. Therefore, the average U and V components of the ACDP data and the initial model results are plotted (Figures 21-24).

MM	0.0015122	0.0056	0.009	243.30	129.84	0.4
MSF	0.0028219	0.0036	0.010	249.32	178.00	0.14
ALP1	0.0343966	0.013	0.0024	330.95	231.81	0.034
2Q1	0.0357064	0.0027	0.012	202.55	233.41	0.055
*Q1	0.0372185	0.0345	0.016	67.28	29.68	4.8
*O1	0.0387307	0.1961	0.017	307.64	4.76	1.3e+002
NO1	0.0402686	0.0058	0.012	311.47	145.23	0.23
*K1	0.0417807	0.3282	0.015	251.01	3.03	4.5e+002
J1	0.0432929	0.0114	0.016	107.05	88.46	0.52
OO1	0.0448308	0.0047	0.013	347.02	171.41	0.14
UPS1	0.0463430	0.0044	0.011	142.41	172.82	0.15
EPS2	0.0761773	0.0014	0.008	224.64	229.71	0.029
*MU2	0.0776895	0.0184	0.011	156.62	37.23	2.9
*N2	0.0789992	0.1202	0.011	34.25	5.76	1.3e+002
*M2	0.0805114	0.5393	0.012	282.81	1.00	1.9e+003
*L2	0.0820236	0.0169	0.011	327.03	35.59	2.3
*S2	0.0833333	0.2207	0.011	306.62	2.92	3.9e+002
ETA2	0.0850736	0.0008	0.007	143.15	239.26	0.013
*MO3	0.1192421	0.0011	0.000	145.71	18.86	11
M3	0.1207671	0.0005	0.000	243.70	42.87	1.9
*MK3	0.1222921	0.0019	0.000	90.76	8.88	28
SK3	0.1251141	0.0004	0.000	158.31	49.29	1.8
*MN4	0.1595106	0.0014	0.001	230.16	20.69	7.6
*M4	0.1610228	0.0044	0.001	113.75	7.48	67
SN4	0.1623326	0.0006	0.001	214.31	50.35	1.5
*MS4	0.1638447	0.0032	0.000	144.46	10.24	41
S4	0.1666667	0.0004	0.000	200.58	87.45	0.85
*2MK5	0.2028035	0.0006	0.000	311.82	30.51	5.3
2SK5	0.2084474	0.0002	0.000	270.56	76.50	0.68
*2MN6	0.2400221	0.0002	0.000	80.78	25.22	6
M6	0.2415342	0.0001	0.000	9.97	75.96	0.84
*2MS6	0.2443561	0.0001	0.000	300.71	37.62	2.9
*2SM6	0.2471781	0.0001	0.000	288.67	33.45	2.8
*3MK7	0.2833149	0.0002	0.000	319.58	26.45	5.2
M8	0.3220456	0.0001	0.000	5.05	57.00	1.4

Table 3.   Harmonic decomposition of initial forcing.
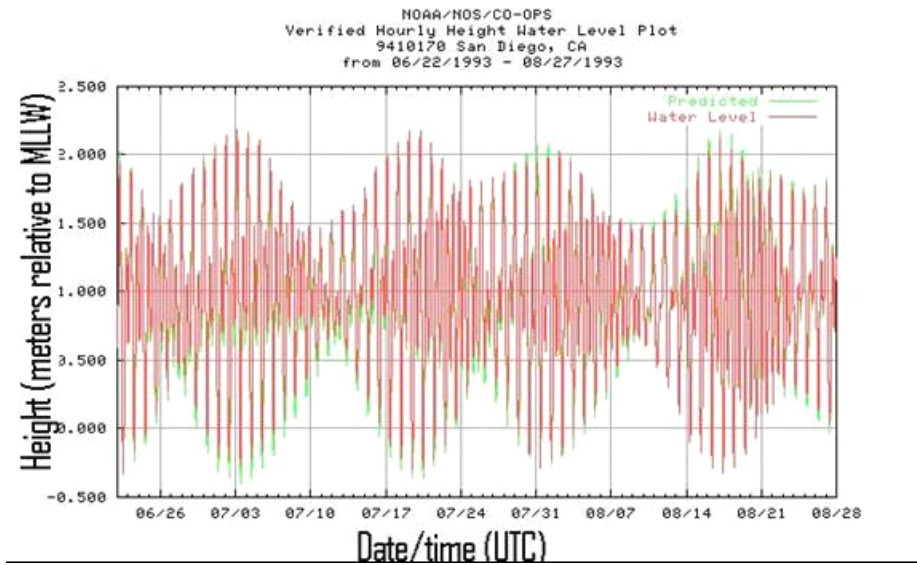
Figure 20.   Tidal forcing used for the verification of the model (From: http://www.co-ops.nos.noaa.gov, last accessed on May 25, 2005).

U for nb1
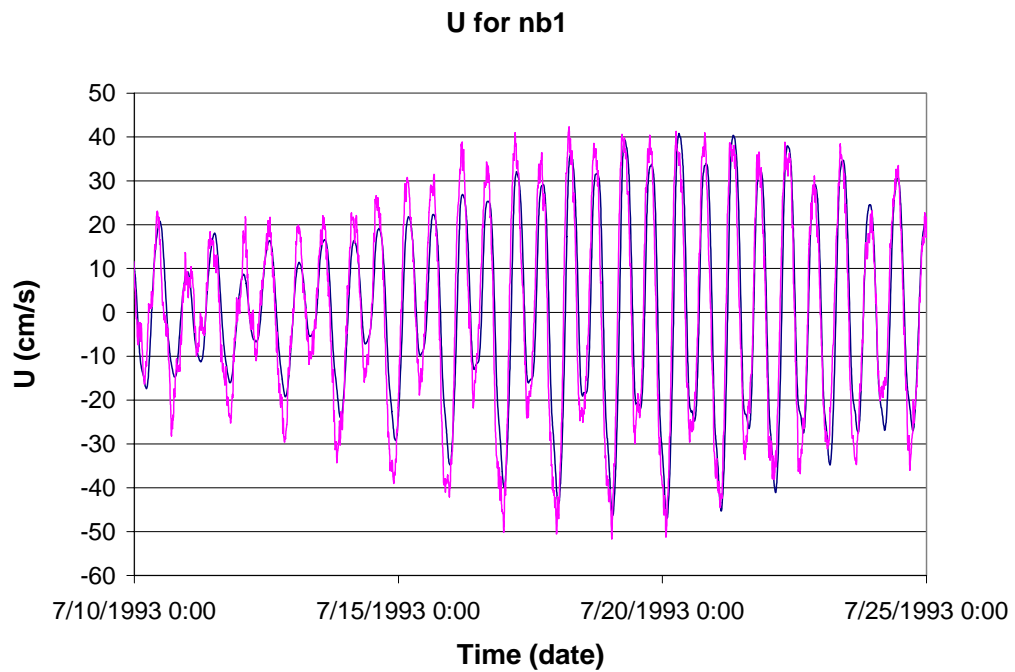
Figure 21.   Average U component from ADCP (nb1) data (purple line) compared to initial model results (blue line).

V for nb1
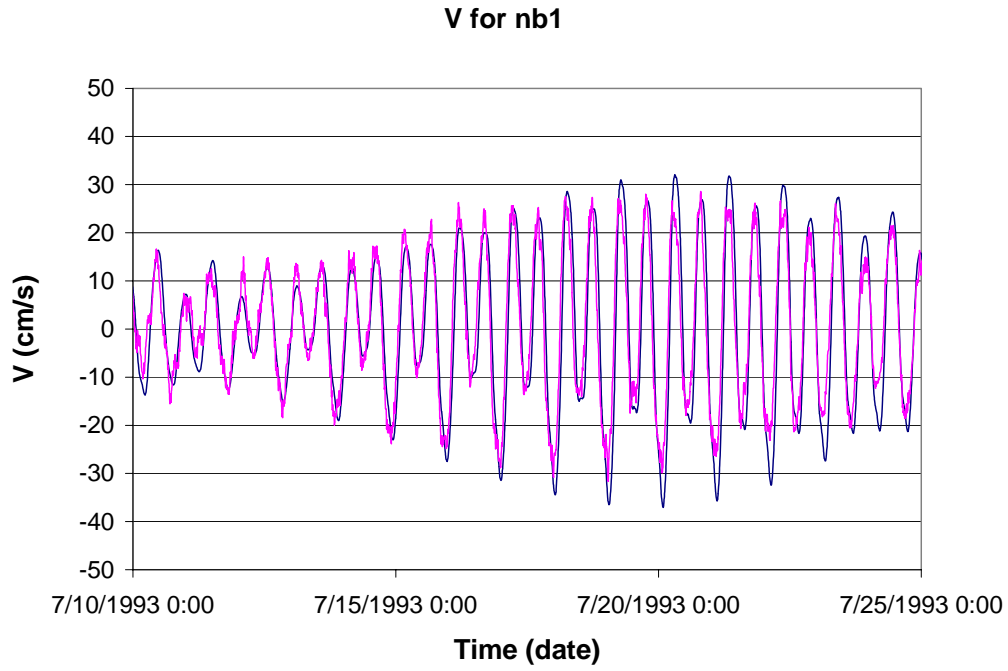
Figure 22.   Average V component from ADCP (nb1) data (purple line) compared to
initial model results (blue line).

U for nb2
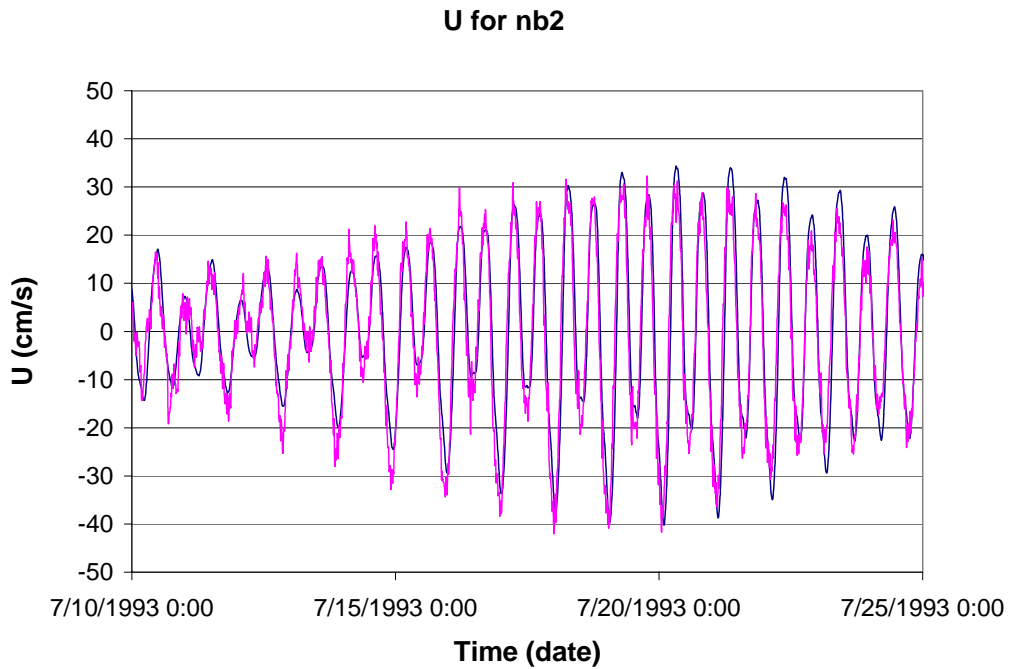
Figure 23.   Average U component from ADCP (nb2) data (purple line) compared to
initial model results (blue line).

32

V for nb2
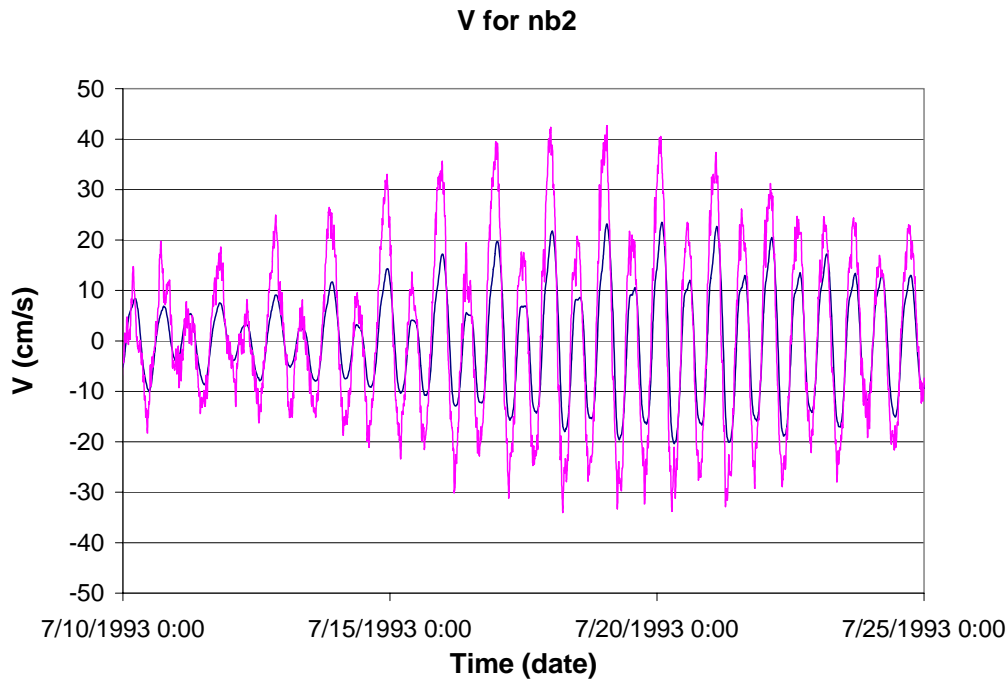
Figure 24.   Average V component from ADCP (nb2) data (purple line) compared to initial model results (blue line).

Statistical analysis shows that a good correlation exists between most of the compared signals in both phase and amplitude (correlation coefficient above 90% in all cases). For nb1, the u speed between the data and the model has a correlation coefficient of 91.87% and can be verified optically. The observational u-velocity ranges between -51.8 and 44.5 cm/s and the modeled u-velocity changes between -46.9 and 40.8 cm/s. The difference between the observational and modeled mean u-velocity is 0.49 cm/s. Furthermore, the root mean square error (between model and observation) is 9.02 cm/s. For nb1, the v speed between the data and the model has a correlation coefficient of 91.66% and can be verified optically. The observational v-velocity ranges between -31.6 and 29.6 cm/s and the modeled v-velocity changes between -37.0 and 32.0 cm/s. The difference between the observational and modeled mean v-velocity is -0.65 cm/s. The root mean square error of v-velocity is 6.83 cm/s.

For nb2, the u speed between data and model has a correlation coefficient of 92.60% and can be verified optically. The observational u-velocity ranges between -42.8 and 32.8 cm/s and the modeled u-velocity changes between -40.2 and 34.3 cm/s. The

difference between the observational and modeled mean u-velocity is 1.0862 cm/s. Furthermore, the root mean square error (between model and observation) is 6.7356 cm/s. For nb1, the v speed between the data and the model has a correlation coefficient of 92.60 % and can be verified optically. The observational v-velocity ranges between -34 and 42.7 cm/s and the modeled v-velocity changes between -20.4 and 23.5 cm/s. The difference between the observational and modeled mean v-velocity is -1.2971. The root mean square error of v-velocity is 8.5035. In order to verify the minimal significance of the wind driven circulation, the power spectra diagrams (PSD) of u and v for nb1 and nb2 are presented (Figures 25 – 28).
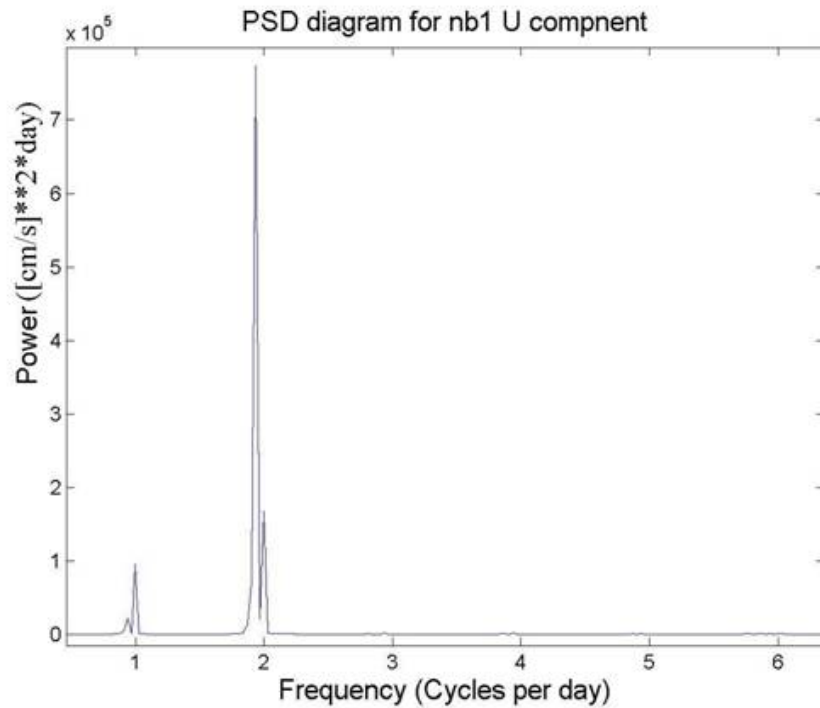
Figure 25.   Power Spectrum Diagram for nb1 u component.
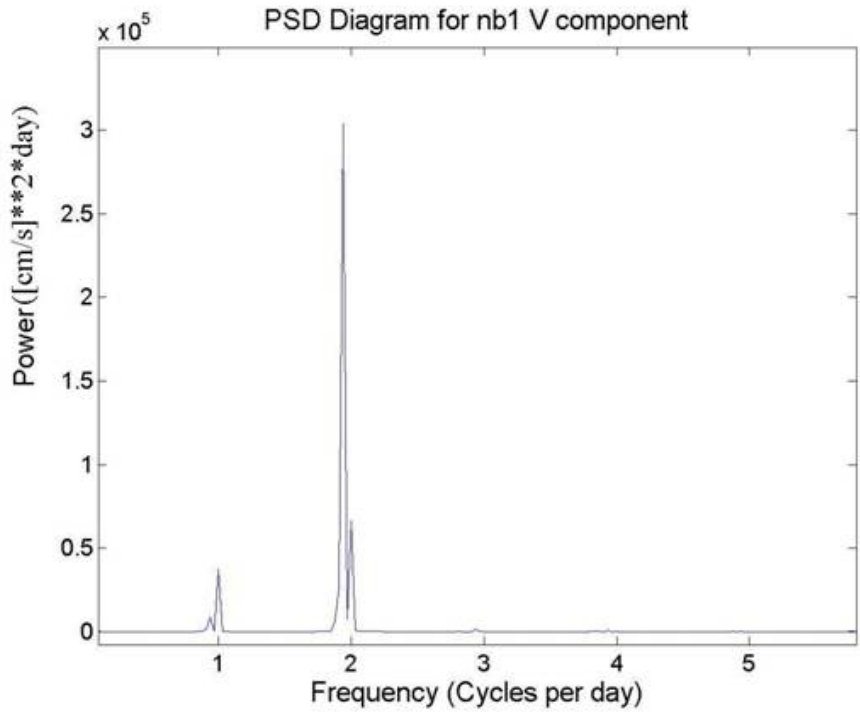
Figure 26.   Power Spectrum Diagram for nb1 v component.
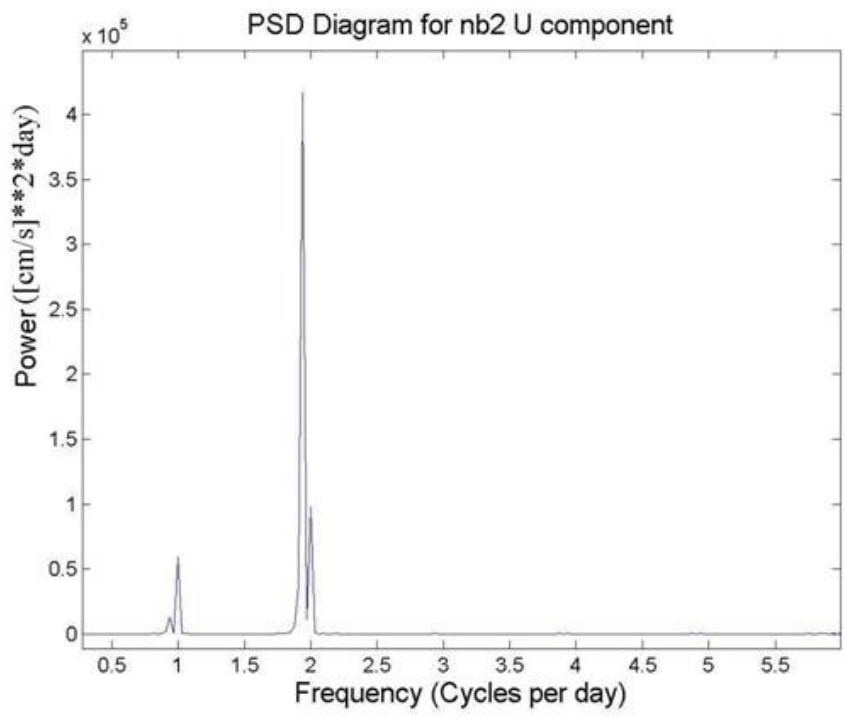
Figure 27.   Power Spectrum Diagram for nb2 u component.
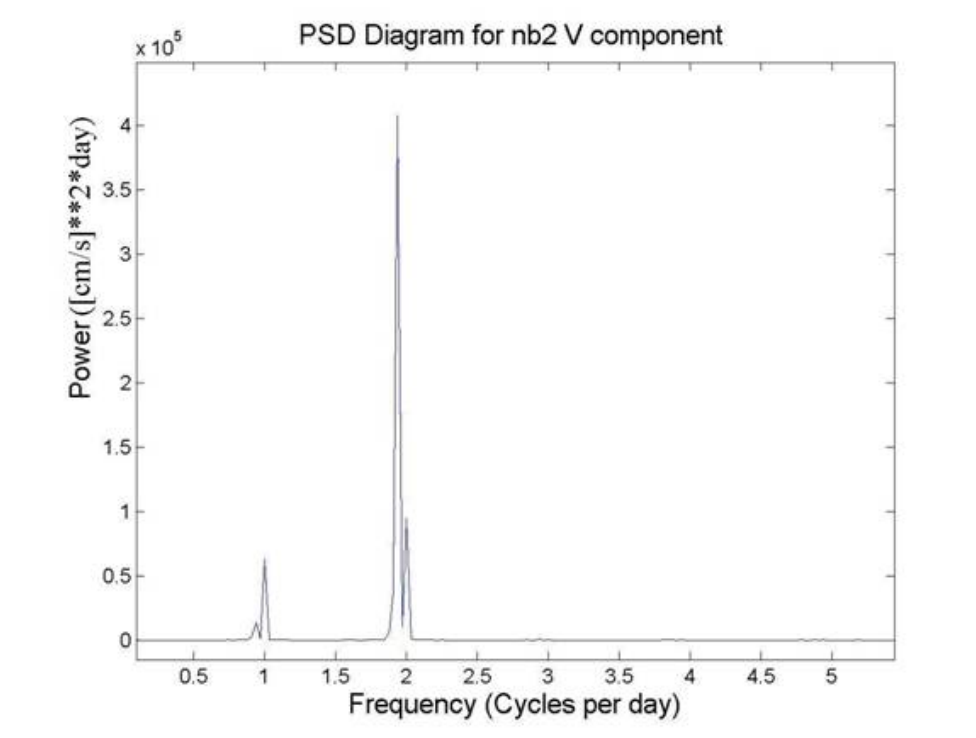
Figure 28. Power Spectrum Diagram for nb2 v component.

It is obvious that the long-term wind driven effect is minimal and can be neglected. The circulation is due mainly to the semi-diurnal and diurnal tides, as expected. Figures 29 through 32 are identical during the integration period for both nb1 and nb2 with peaks at 1 cycle (diurnal tides) and 2 cycles per day (semi-diurnal tides). Long term effects (less than 1 cycle per day) or short term ones (more than half a cycle per day) cannot be identified since there is very low energy in any other frequency.

However, it will be statistically proven that wind is insignificant. For this reason, three separate model runs will be used. The first will be with tidal forcing and an average westerly wind of 5m/s; the second with only tidal forcing; and the third only with wind. The comparisons between the runs, which include the tidal forcing, are practically identical irrespective of the wind influence. For this reason, it is not necessary to present all the results. Note that for nb1 u component the same maximum and minimum value exists in both cases. The correlation coefficient is 100%, the difference of the mean values is -0.0037 cm/s and the difference between the standard deviations is -0.0025. The root mean square error is as low as 0.0649 cm/s.

36

The comparison as regards the run that takes into account the wind without tidal forcing with the one that includes tidal forcing is very clear. Again if we take as an example the nb1 u component, the maximum value with all forcing is 40.8 cm/s and only with wind is 0.7 cm/s and the minimum -46.9 cm/s and -0.1 m/s respectively. There is no correlation at all (correlation coefficient 0). The contribution of the wind to the current speed can be plotted. Actually, in Figure 29, the u component is plotted for ADCP nb1 in the run with wind only and in the run with total forcing. Hence, we can verify again that wind is insignificant in San Diego Bay forcing and therefore by neglecting it, our results are entirely valid. Tables 4-9 provide detailed statistical analysis on model performance.
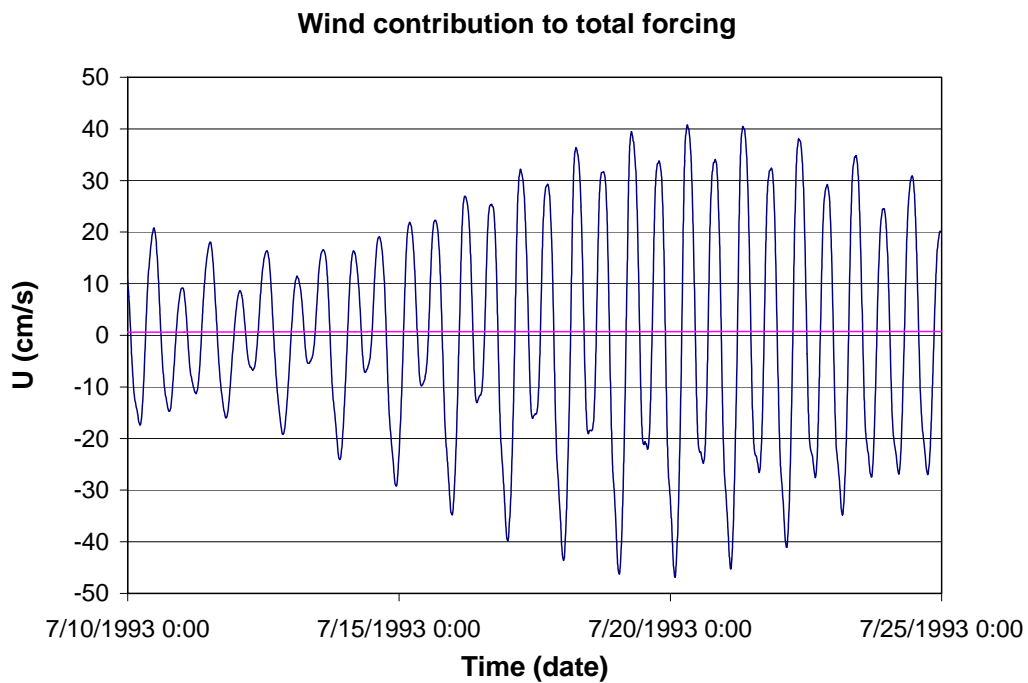
Figure 29.   Average u component from ADCP (nb1) only with wind forcing (purple line) compared to model results in a total forcing run (blue line).

	DATA	MODEL	DIFFERENCE	COMPARISON
max	44.5	40.8	-3.7	
min	-51.8	-46.9	4.9	
mean	-0.5384	-0.0483	0.4901	
std	22.7892	21.3238	-1.4654	
rme				-0.9103
rmse				9.0238
ecv				-16.7615
corrl				91.87%

Table 4.   Comparison of u component for nb1.

	DATA	MODEL	DIFFERENCE	COMPARISON
max	29.60	32.00	2.40	
min	-31.60	-37.00	-5.40	
mean	0.6190	-0.0315	-0.6505	
std	14.2799	16.7878	2.5079	
rme				1.0509
rmse				6.8315
ecv				11.0361
corrl				91.66%

Table 5.   Comparison of v component for nb1.

	DATA	MODEL	DIFFERENCE	COMPARISON
max	60.51	59.74	-0.77	
min	0.10	0.00	-0.10	
mean	23.1499	23.4548	0.3049	
std	13.7075	13.6486	-0.0589	
rme				0.0132
rmse				9.7512
ecv				0.4212
corrl				74.61%

Table 6.   Comparison of speed for nb1.

	DATA	MODEL	DIFFERENCE	COMPARISON
max	32.80	34.30	1.50	
min	-42.80	-40.20	2.60	
mean	-0.9540	0.1322	1.0862	
std	17.0167	17.4624	0.4457	
rme				-1.1386
rmse				6.7356
ecv				-7.0605
corrl				92.60%

Table 7.   Comparison of u component for nb2.

	DATA	MODEL	DIFFERENCE	COMPARISON
max	42.70	23.50	-19.20	
min	-34.00	-20.40	13.60	
mean	1.2354	-0.0617	-1.2971	
std	16.9599	10.2599	-6.70	
rme				1.05
rmse				8.5035
ecv				6.8833
corrl				92.60%

Table 8.   Comparison of v component for nb2.

	DATA	MODEL	DIFFERENCE	COMPARISON
max	60.32	46.56	-13.76	
min	0.10	0.00	-0.10	
mean	20.2309	17.4891	-2.7418	
std	12.7761	10.5454	-2.2307	
rme				0.1355
rmse				8.0369
ecv				0.3973
corrl				80.66%

Table 9.   Comparison of speed for nb2.

Comparison of the current speed between observation and the model is acceptable. As regards the point south of Coronado Island (bb), when filtering the data to keep only the part that results from the tidal influence, an improved correlation between the model and observation occur. Again, a band-pass butterworth filter is first applied to filter out all frequencies either smaller than 0.5 cycles per day or greater than 2.5 cycles per day. The correlation coefficient is 85.09% for u-velocity and 78.49% for v-velocity. Optically, the amplitude difference between the model and observation improves as well. Thus, it is possible to conclude that by filtering the results of the non-tidal influence, a 2-D model can be used in the entrance of San Diego Bay with relatively better results.

The middle and upper levels contribute much more to the vertical average u component of bb than the lower (to bottom) depths and indicate its behavior much better. Actually the correlation coefficient of the average u component and the surface u is

91.63% and between the average u component and the middle depth u is even higher (92.14%). Moreover, the middle depth represents the u component better since it has also a smaller, relative mean error (RME)

$$RME = \frac{\sum_{i=1}^{n}(X_i^{mod} - X_i^{obs})^2}{\sum_{i=1}^{n}|X_i^{mod}|^2},$$

root mean square error (RMSE)

$$RMSE = \sqrt{\frac{\sum_{i=1}^{n}(X_i^{mod} - X_i^{obs})^2}{n}},$$

and the error coefficient of variation (ecv),

$$ECV = \frac{RMSE}{\sqrt{\frac{1}{n}\sum_{i}|X_i^{mod}|^2}},$$

where $\left(X_i^{mod}, X_i^{obs}\right)$ are the modeled and observational data.

The bottom u component and the average u have a correlation coefficient of only 62.22%. For the v component, the correlation between the average and the v component in all depths is high: For bottom, the correlation coefficient is 96.24%, for surface 99.26%, and again for middle depth, it is the best with a coefficient of 99.43% and better rme, rmse and ecv than the other cases. In order to evaluate the model further, the water elevation in position nb2 is calculated and despite the fact that exact verified data is not available, an attempt will be made to compare it in two different ways. First, Table 10 describes all results after harmonic decomposition.

To compare the model results with a previous study (Wang et al., 1998), the four main tidal constituents (K1, O1, S2, M2) at downtown (further north and deeper than the nb2 position) are used. Amplitude difference (model minus observation) is 3.83 cm for M_2 (but only 1.08 cm, if compared to that of south San Diego), 3.73 cm for K_1, -2.19 cm

for O_1, and 1.1 cm for S_2. Phase difference is 1.71^o for M_2, 25.94^o for K_1, 45.33^o for O_1, and 5.41^o for S_2. Differences in bathymetry and analysis can justify such small discrepancies, especially since there is no certainty about the position for which the data was collected.

TIDE	FREQ	AMPL	AMP.ERR	PHASE	PH ERR	SNR
MSF	0.0028219	0.0061	0.014	266.81	160.24	0.2
*2Q1	0.0357064	0.0067	0.003	337.90	21.94	6.8
*Q1	0.0372185	0.0364	0.002	76.81	4.66	2.4e+002
*O1	0.0387307	0.1952	0.003	125.14	0.86	5e+003
*NO1	0.0402686	0.0096	0.003	19.17	16.04	13
*K1	0.0417807	0.3773	0.002	60.54	0.44	2.5e+004
J1	0.0432929	0.0026	0.002	97.99	69.16	1.2
*OO1	0.0448308	0.0157	0.002	129.23	9.23	40
*UPS1	0.0463430	0.0047	0.003	289.53	32.85	2.7
*N2	0.0789992	0.1226	0.014	203.96	7.74	75
*M2	0.0805114	0.5804	0.015	270.27	1.36	1.6e+003
*S2	0.0833333	0.2144	0.013	267.04	3.93	2.6e+002
ETA2	0.0850736	0.0077	0.011	7.45	98.73	0.48
*MO3	0.1192421	0.0042	0.001	258.54	22.76	8.5
*M3	0.1207671	0.0021	0.001	172.85	40.42	2.4
*MK3	0.1222921	0.0085	0.001	219.46	10.21	33
*SK3	0.1251141	0.0026	0.001	208.56	32.29	3.7
*MN4	0.1595106	0.0039	0.002	15.82	21.09	6.1
*M4	0.1610228	0.0107	0.001	75.84	8.11	71
*MS4	0.1638447	0.0074	0.002	71.22	11.13	23
S4	0.1666667	0.0014	0.001	66.29	51.91	1.2
*2MK5	0.2028035	0.0037	0.001	185.30	24.66	6.6
2SK5	0.2084474	0.0003	0.001	258.37	225.54	0.057
2MN6	0.2400221	0.0029	0.002	355.66	52.92	1.5
*M6	0.2415342	0.0059	0.002	52.23	22.32	6.5
*2MS6	0.2443561	0.0080	0.003	72.33	18.29	10
2SM6	0.2471781	0.0019	0.002	83.37	75.50	0.65
*3MK7	0.2833149	0.0042	0.002	108.25	31.28	3.4
*M8	0.3220456	0.0007	0.000	295.35	30.49	3.3

Table 10.   Harmonic decomposition of modeled results.

The best choice for a valid comparison is to compare the model results at nb2 with the NOAA San Diego station at the pier. The data is gathered too close to land, and therefore, cannot be exactly compared. However, it can be compared with a point very

near the actual San Diego Station position. Amplitude difference (model minus observation) is 2.51 cm for M_2, 0.94 cm for K_1, 0.84 cm for O_1, and 0.71 cm for S_2. Phase difference is 0.75^o for M_2, 26.08^o for K_1, 29.58^o for O_1, and 48.96^o for S_2. Again, it can be stated that differences in bathymetry and analysis can justify such small discrepancies, especially since there is no precision about the position for which the data was compared. The results from this more accurate comparison are even better than the previous one.

Overall, the model results are reasonably good, especially taking into account that the comparison between data and model is not at exactly the same position and the proximity of the ADCPs to the shore. If finer grid and more accurate bathymetry are used, the model results may be further improved.

	NOAA DATA (more precise)	SPAWAR DATA
M2 (amplitude difference)	+ 2.51 cm	+ 3.83 cm
K1 (amplitude difference)	- 0.94 cm	+ 3.73 cm
O1 (amplitude difference)	- 0.84 cm	- 2.19 cm
S2 (amplitude difference)	+ 0.71 cm	- 1.1 cm

Table 11.   Comparison of model elevation amplitude with NOAA and SPAWAR results.

	NOAA DATA (more precise)	SPAWAR DATA
M2 (phase difference in degrees)	+ 0.75	-1.71
K1 (phase difference in degrees)	- 26.08	- 25.94
O1 (phase difference in degrees)	+29.58	- 45.33
S2 (phase difference in degrees)	- 48.96	+ 5.41

Table 12.   Comparison of model elevation phase with NOAA and SPAWAR results.

VI. HYDROCHEMICAL MODEL

A. MODEL DESCRIPTION

CHEMMAP is a chemical spill model, which predicts the trajectory and fate of floating, sinking, evaporating, soluble and insoluble chemicals and product mixtures. It can estimate the distribution of chemical elements (as mass and concentrations) on the surface, in the water column and in the sediments. The model is 3D, separately tracking surface slicks, entrained droplets or particles of pure chemical, chemical adsorbed to suspended particulates, and dissolved chemical (McCay and Isaji, 2002). The CHEMMAP model is used in this chapter to predict the propagation of chemicals.

CHEMMAP can be either run as a certain scenario with specific tidal forcing, wind and spill site and in stochastic mode to estimate the probable distribution and concentrations resulting from hypothetical spills. The next chapter used six different scenarios including two locations each to cover all possible threats and different chemicals in San Diego Bay.

The model, which is very similar but not the same as WQMAP, incorporates a number of model components including simulation of the initial release for surface and subsurface spills, slick spreading, transport of floating, dissolved and particulate materials, evaporation and volatilization, dissolution and adsorption, sedimentation and degradation.

It uses physical and chemical properties such as density, viscosity, vapor pressure, surface tension, water solubility, environmental degradation rates, and adsorbed/dissolved partitioning coefficients. CHEMMAP relies on Stoke's Law in order to calculate vertical velocities. Furthermore, its approach towards propagation is Langrangian.

The outputs of the model include the trajectories, and concentrations. More specifically, it is possible to see the swept area by a floating chemical, as well as the total, absorbed, dissolved and particulate concentration in both the water column and the

sediments. The most important is that it is then possible to determine the range of distances and directions of the contamination caused from the spill at a particular location.

The choice of the chemicals used in this thesis will be based on chemical/physical properties and toxicity data and are contained in a database compiled from published literature sources, mainly French et al. (1996) and Mackay et al., (1992 a,b,c,d). Since several properties vary with temperature, the chemical data are for an initial temperature of 25°C. The model corrects these parameters to the ambient temperature for the spill incident. The algorithms for changing viscosity and vapor pressure to ambient temperature are taken from French et al. (1996), who developed regression using the data in Gambill (1959). For pure chemical processes, the increase per 10°C is assumed to be a factor of 2. For biological processes (e.g., degradation rates), the increase in rate per increase of 10°C is assumed to be a factor of 3 (McCay and Isaji, 2002).

The model is initialized for the spilled mass at the location and depth of the release. The state and solubility are the primary determining factors for the initialization algorithm. If the chemical is highly soluble in water and is either a pure chemical (e.g., the benzene scenario) or dissolved in water (e.g., the methanol scenario), the chemical mass is initialized in the water column in the dissolved state and in a user-defined initial volume. For insoluble or semi-soluble gases released underwater (e.g., the naphthalene gas scenario), the spilled mass is initialized in the water column at the release depth in a user-defined plume volume, as bubbles. The median particle size is characterized by a user-defined diameter (McCay and Isaji, 2002).

For the state where the chemical of interest is both adsorbed to particles and dissolved in the water phase of the bulk liquid (e.g. our ammonia liquefied gas scenario), dissolved mass is also initialized in the initial plume volume. The mass of chemical spilled is corrected from the bulk spill volume using the appropriate density and concentration data from the database (McCay and Isaji, 2002).

Chemical mass is transported in three-dimensional space and time, by surface wind drift, other currents, and vertical movement in accordance with buoyancy and

dispersion. The model simulates adsorption onto suspended sediment, resulting in sedimentation of material. Stoke's Law is used to compute the vertical velocity of pure chemical particles or suspended sediment with adsorbed chemical. If rise or settling velocity overcomes turbulent mixing, the particles are assumed to float or settle to the bottom. Settled particles may later re-suspend (assumed to occur above 20 cm/s current speed). Wind-driven current (drift) in the surface water layer (down to 5m) is calculated within the fates model, based on hourly wind speed and direction data. Surface wind drift of oil has been observed in the field to be 1-6% of wind speed in the direction of 0-30 degrees to the right (in the northern hemisphere) of the down-wind direction (Youssef and Spaulding, 1993). The user may also specify the wind drift speed and angle (McCay and Isaji, 2002).

CHEMMAP simulates degradation, volatilization, evaporation, dissolution, entrainment and spreading. More specifically, spreading is simulated using the Fay algorithm (Fay, 1971). Entrainment is modeled as for oil (Delvigne and Sweeney, 1988). Surface floating chemicals interaction with shorelines is simulated based on the algorithms developed for oil spills (French et al., 1999). The dissolution rate of pure chemicals is a function of solubility using a first order constant rate equation. The dissolved chemical in the water column is assumed to adsorb to particulate matter in accordance with the equilibrium partitioning theory (DiToro et al., 1991). Evaporation is modeled following the theory that the rate of mass flux to the atmosphere increases with vapor pressure, temperature, wind speed and surface area (Mackay and Matsugu, 1973). Volatilization from the water column is calculated from the chemical's vapor pressure and solubility (Lyman et al., 1982). Degradation is estimated assuming a constant rate of "decay" specific to the environment where the mass exists (i.e., atmosphere, water column or sediment).

The spilled chemical is modeled using the Lagrangian approach. At each time step, phase transfer rates (evaporation, dissolution, volatilization, and entrainment) are calculated and a proportionate percentage of the spillets are transferred to the new phase (McCay and Isaji, 2002).

B.   **ENVIRONMENTAL DATA**

The geographical database and the grid used for WQMAP are also used in CHEMMAP applications. CHEMMAP has the same tidal forcing as for WQMAP, and hourly wind data. The wind is more influential to the fate of insoluble floating chemicals than contaminants in the water column.

C.   **CHEMICAL ELEMENTS DESCRIPTION**

In the current threat environment, a chemical attack in a big city hosting a large portion of the U.S. Naval bases (such as San Diego) is anything but impossible. Since the thesis is unclassified, it is not permitted to use elements, which would be used in the case of an actual weapon with mass destruction (WMD) attack; however it is possible to simulate them and see the results by using other mainly high toxic elements. For this reason, the choices are three floating chemicals (methanol, benzene and ammonia), two sinking ones (chlorobenzene and trichloroethylene) and one dispersing in the air (naphthalene).

1.   **Floating Chemicals**

Methanol[8] (CH3OH) is a colorless fairly volatile liquid, belonging to the aliphatic alcohols chemical type. It is originally distilled from wood, but currently, it is synthetically produced from carbon oxides and hydrogen. It has a faintly sweet pungent odor like that of ethyl alcohol. It has a flash point $12.222^{o}C$ and its density is 791 kg/m^3 (at $25^{o}C$). Its vapors are slightly heavier than air and may travel some distance to a source of ignition and flash back. Any accumulation of vapors in confined spaces, such as buildings or sewers, may explode if ignited, so it is very dangerous. It is used to make chemicals, to remove water from automotive and aviation fuels, as a solvent for paints and plastics, as an alternative motor fuel and as an ingredient in a wide variety of products, so it is not easy control. The most recent inventory is estimated to be 1,125 metric tons in the U.S. alone.

Methanol reacts violently with acetyl bromide. Mixtures with concentrated sulfuric acid and concentrated hydrogen peroxide can cause explosions. It reacts with hypochlorous acid either in water solution or mixed water/carbon tetrachloride solution to

---

[8] Other synonyms include methyl alcohol, carbinol, wood alcohol, wood naptha and wood spirit.

give methyl hypochlorite, which decomposes in the cold and may explode on exposure to sunlight or heat. It gives the same product with chlorine and can react explosively with isocyanates under basic conditions. The presence of an inert solvent mitigates this reaction. A violent exothermic reaction occurred between methyl alcohol and bromine in a mixing cylinder. A flask of anhydrous lead perchlorate dissolved in methanol exploded when it was disturbed.

Hence, methanol is high flammable, is a floater, is highly volatile, is highly soluble and remains dissolved. Furthermore, is a toxic element, and therefore, very dangerous. Its immediately dangerous to life or health indicator (IDLH) is very high (6,000 ppm), its short term exposure limit (STEL) is 250 ppm and its odor threshold is 4.2 ppm. Its degradation rate is 0.097835 (%/day) in air and sediments and 0.3024 (%/day) in water.

Even though it is not "acutely" toxic, inhalation can cause cough, dizziness, headache, nausea, weakness and visual disturbance. Ingestion can be even worse causing abdominal pain, convulsions, shortness of breath, unconsciousness and vomiting. However, what is more important is its ecotoxicity. For certain fish (such as red drums), shrimps, mussels and snails, it can be lethal.

Benzene[9] (C_6H_6) is the second chemical to be used. It is also toxic, causing the same symptoms as methanol, and can be fatal to many species in the ecosystem including all the aforementioned ones as well as oysters, clams, trout, salmon, catfish and goldfish. As regards its toxicity, benzene is a confirmed carcinogen, develops and reproduces toxins, and therefore, is extremely dangerous. The water maximum contaminant level is 0.000005 kg/m^3. Its immediately dangerous to life or health indicator (IDLH) is not as high as methanol (500 ppm), its short term exposure limit (STEL) is 2.5 ppm and its odor threshold is 34 ppm for detection and 97 ppm for recognition. Its degradation rate is 0.97835 (%/day) in air, 0.097835 (%/day) in water and 0.0097835 (%/day) in sediments.

For chemical characteristics, benzene is high flammable, floater, highly volatile, highly soluble, and moderately absorbable to particles. It is a clear colorless liquid with a

---

[9] Other synonyms are benzol and cyclohexatriene.

petroleum-like odor. It is less dense than water (0.877 g/cm^3) and slightly soluble in water. Its vapors are heavier than air. Benzene reacts vigorously with alkyl chloride or other alkyl halides even at -70°C in the presence of ethyl aluminum dichloride or ethyl aluminum sesquichloride and explosions have been reported. It ignites in contact with powdered chromic anhydride. It is incompatible with oxidizing agents such as nitric acid. Mixtures with bromine trifluoride, bromine pentafluoride, iodine pentafluoride, iodine heptafluoride and other interhalogens can ignite upon heating.

The last floating chemical used is ammonia[10] (NH3) liquefied gas. It is a base. It is clear and colorless and has a strong odor. It is shipped as a liquid under its own vapor pressure. Its density in the liquid form is 12.8825 kg/m^3. Contact with the unconfined liquid can cause frostbite. Gas generally regarded as nonflammable but does burn within certain vapor concentration limits and with strong ignition. Fire hazard increases in the presence of oil or other combustible materials. Although gas is lighter than air, vapors from a leak initially hug the ground. Prolonged exposure of containers to fire or heat may cause violent rupturing and rocketing. Long-term inhalation of low concentrations of the vapors or short-term inhalation of high concentrations has adverse health effects. It is used as a fertilizer and refrigerant, and in the manufacture of other chemicals.

Ammonia is a floater, highly volatile, highly soluble and slightly absorbable to particles, and reacts exothermically with all acids. Violent reactions are possible. It also readily combines with silver oxide or mercury to form compounds that explode on contact with halogens. When in contact with chlorates, it forms explosive ammonium.

As for toxicity, its immediately dangerous to life or health indicator (IDLH) is relatively small (300 ppm), its short term exposure limit (STEL) is 35 ppm and its odor threshold is 0.019 ppm. Its degradation rate is 0.1586 in both air and water. Contact with ammonia could cause skin and eye burns and inhalation some burning sensation, cough, shortness of breath and sore throat. For the ecosystem, its slight toxicity can be lethal to shrimp, prawns, salmon, trout and catfish.

2.   **Sinking Chemicals**

---

[10] Other synonyms are nitro-sil, spirit of Hartshorn, and vaporole.

The first sinking chemical is chlorobenzene[11] (C_6H_5Cl). It is a colorless to clear, yellowish liquid with a sweet almond-like odor. It is insoluble in water and a little denser than water (1,107 kg/m^3). Its vapors are heavier than air. It is used to make pesticides, dyes, and other chemicals, chlorobenzene undergoes a sometimes explosive reaction with powdered sodium or phosphorus trichloride and sodium. It may react violently with dimethyl sulfoxide. It reacts vigorously with oxidizing agents. It attacks some forms of plastic, rubber and coatings and it forms a shock sensitive solvated salt with silver perchlorate.

Chlorobenzene is, therefore, a sinker, semi-volatile, soluble, highly flammable and moderately absorbable to particles. For toxicity, its immediately dangerous to life or health indicator (IDLH) is quite big (1,000 ppm), and its odor threshold is 1.3 ppm. Its degradation rate is 0.09784 (%/day) in air, 0.0097835 (%/day) in water and 0.00098 (%/day) in sediments. Inhalation of chlorobenzene can cause drowsiness, headache, nausea and unconsciousness. Ingestion causes abdominal pain. As regards eco-toxicity, it can be lethal to prawns, trout and goldfish.

The second sinker is trichloroethylene[12] (C_2HCl_3). It is a toxic sinker with similar results as chlorobenzene when in contact with humans. Furthermore, it is a proven carcinogen. It is a clear colorless volatile liquid having a chloroform-like odor. It is denser than water, slightly soluble in water and is non-combustible. It is used as a solvent, fumigant, in the manufacture of other chemicals, and for many other uses. It has been determined experimentally that mixtures of finely divided barium metal and a number of halogenated hydrocarbons possess an explosive capability. Specifically, impact sensitivity tests have shown that granular barium in contact with monofluorotrichloromethane, trichlorotrifluoroethane, carbon tetrachloride, trichloroethylene, or tetrachloroethylene can detonate. It has been determined experimentally that a mixture of beryllium powder with carbon tetrachloride or with trichloroethylene will flash or spark on heavy impact. A mixture of powdered magnesium

---

[11] Other synonyms are monochlorobenzene, benzene chloride and phenyl chloride.

[12] Other synonyms are TCE, acetylene trichloride, algylen, blacosolv, chlorylen, dow-tri, ethylene trichloride, fleck-flip, tri-clene and trichloroethene.

49

with trichloroethylene or with carbon tetrachloride will also flash or spark under heavy impact.

Thus, trichloroethylene is a sinker, semi-volatile, highly soluble and moderately absorbable to particles. As regards toxicity, its immediately dangerous to life or health indicator (IDLH) is the same as chlorobenzene (1,000 ppm), its short term exposure limit (STEL) is 100 ppm and its odor threshold is 82 ppm. Its degradation rate is 0.09784 (%/day) in air, 0.03024 (%/day) in water and 0.003024 (%/day) in sediments. Its dangers for the eco-system include death to toads, trout and flagfish.

3.   Gaseous Chemical

The last chemical is naphthalene[13] (gas) ($C_{10}H_8$). It is a dark liquid mixture, with much different qualities than all the previous chemicals. It is insoluble in water and denser than water. A part disperses in the atmosphere and another sinks in water. Contact with naphthalene may cause irritation to skin, eyes, and mucous membranes. It can cause confusion, headache, sweating, nausea, vomiting and jaundice when inhaled. It is toxic by ingestion and can cause abdominal pain, convulsions, diarrhea, dizziness and unconsciousness.

Its toxicity is moderate and its immediately dangerous to life or health indicator (IDLH) is 250 ppm, its short term exposure limit (STEL) is 15 ppm and its odor threshold is 0.038 ppm. It is a known carcinogen, and therefore, dangerous to humans. A mixture containing naphthalene may react vigorously with strong oxidizing agents. It can also react exothermically with bases and with diazo compounds. Naphthalene reacts violently with chromic anhydride.

Hence, naphthalene disperses in the atmosphere (but can be also a sinker), is not volatile, is semi-to non-soluble, moderately absorbable to particles, is highly flammable and does not react rapidly with either water or air. Its degradation rate is 0.97835 (%/day) in air, 0.09784 (%/day) in water and 0.00302 (%/day) in sediments. Its dangers for the eco-system include the death of toads, crabs, shrimp, cod, salmon, trout and oysters, being one of the most dangerous enemies of natural underwater life.

---

13 Other synonyms are naphthene, tar camphor and moth balls.

	Methanol	Benzene	Ammonia	Chloro-benzene	TCE	Naphthalene (gas)
Floatation	Floater	Floater	Floater	Sinker	Sinker	Sinker/ Air dispersed
Solubility	High	High	High	Normal	High	Semi
Volatility	High	High	High	Semi	Semi	None
Absorption	Dissolves	Moderate	Slight	Moderate	Moderate	Moderate
Flammability	High	High		High		High
Water/Air rapid interaction	No	No		No		No

Table 13.   Comparison of chemicals used in our CHEMMAP scenarios.

THIS PAGE INTENTIONALLY LEFT BLANK

VII. TWO REGIMES OF CHEMICAL DISPERSION

A. METHANOL

1. Pollutants Released at North San Diego Bay

Suppose a small boat drops one barrel of methanol in less than 12 minutes on midnight July 4, 1993 (Independence Day) at (32^o43'N, $117^o13.05$' W), which is located in the northern part of San Diego Bay. The release depth is 1 m and the initial plum thickness is 0.5 m. In order to make the conditions more difficult for the propagation, assume that there is no wind at all.

The model results show the following features: In three hours, the methanol is in San Diego port (Figure 30) and in 10 hours it is spread all over the North San Diego Bay (Figure 31). In 16 hours, it reaches the Naval Station. However, the south part of the Bay is contaminated much later. After two days, there are no pollutant particles south of 32^o40'N (Figure 32). After three days the Naval Station is heavily impacted but after nine days, there are still no pollutant particles south of 32^o39'N. The methanol reaches the south end of the Bay only after 20 days, but its concentration in the water column can be neglected. Figure 33 shows the final swept area after 32 days.

In such a case, it can be concluded that there is plenty of time to take protective measures for the southern part of the Bay where the results of such an incident would be minimal. However, for the port of San Diego, the effect is immediate and serious. For the Naval Station, the reaction time (19 hours to three days) is critical.
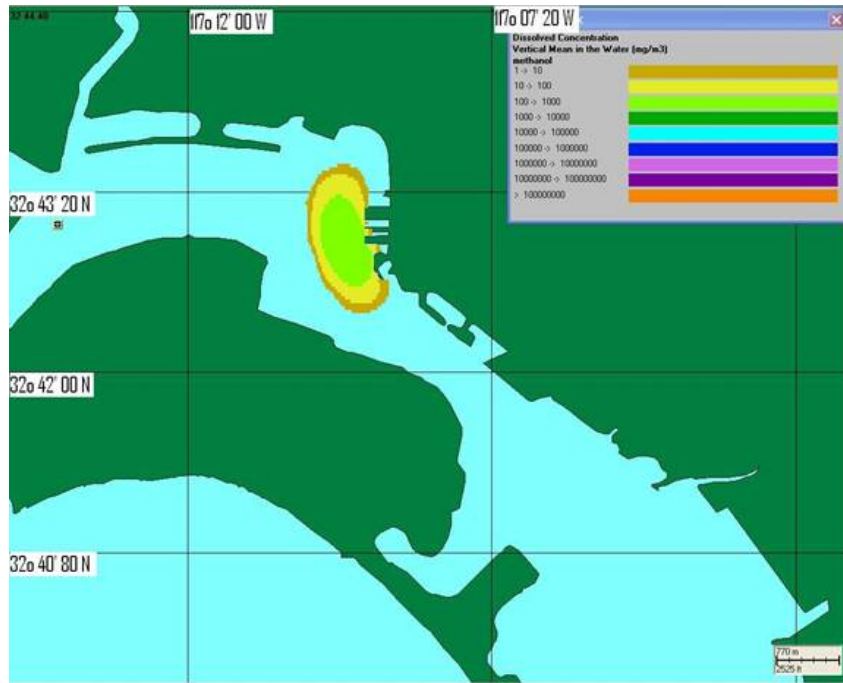
Figure 30.   Methanol dropped in North San Diego Bay, dissolved concentration in
San Diego port/city after 3 hours

Furthermore, after five entire days, one third of the methanol is still in the water column (Figure 34). Note that it takes almost 12 days for the concentration in the water column to reach 10% and 15 days for the decayed methanol to reach a level of 80%. Moreover, the end-state is the contamination not only of the San Diego Bay but also a considerable part of the sea outside the Bay. The scenario is repeated by increasing the amount of methanol, but nothing changes fundamentally. The mass balance curves and the area contaminated remain the same.
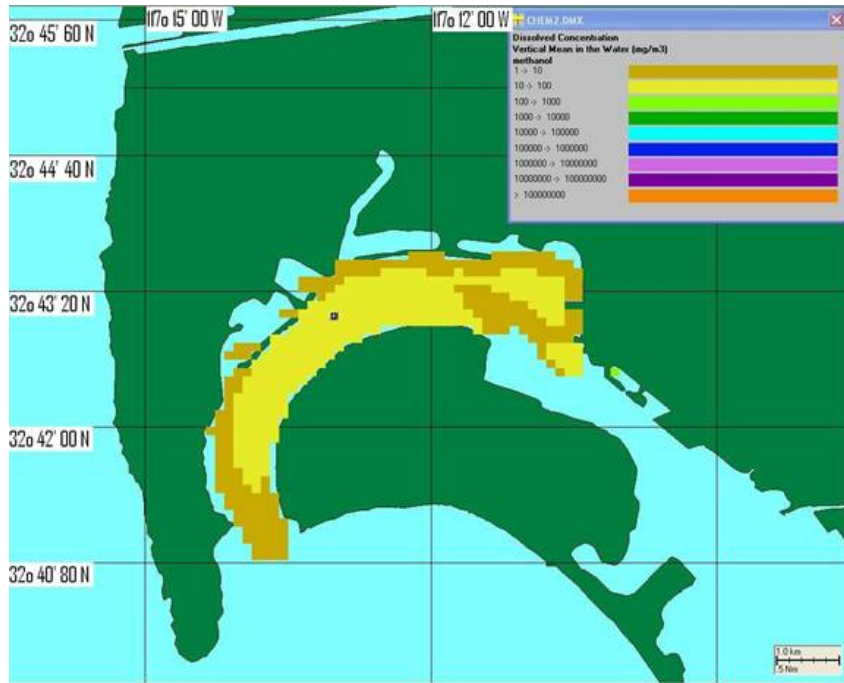
Figure 31.   Methanol dissolved concentration affecting the entire northern San Diego Bay in 10 hours.
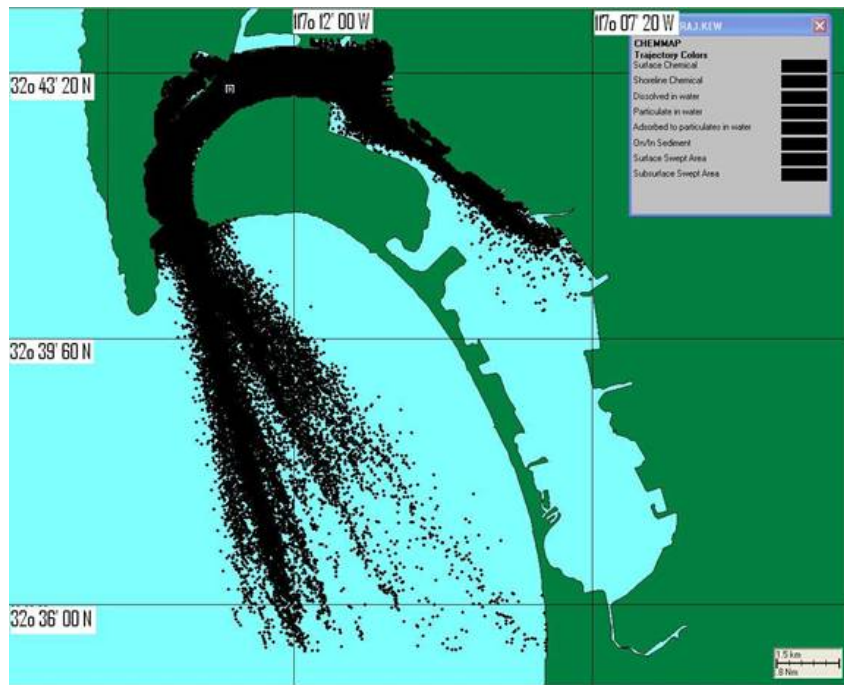
Figure 32.   Swept area after two days for methanol dropped in North San Diego Bay.
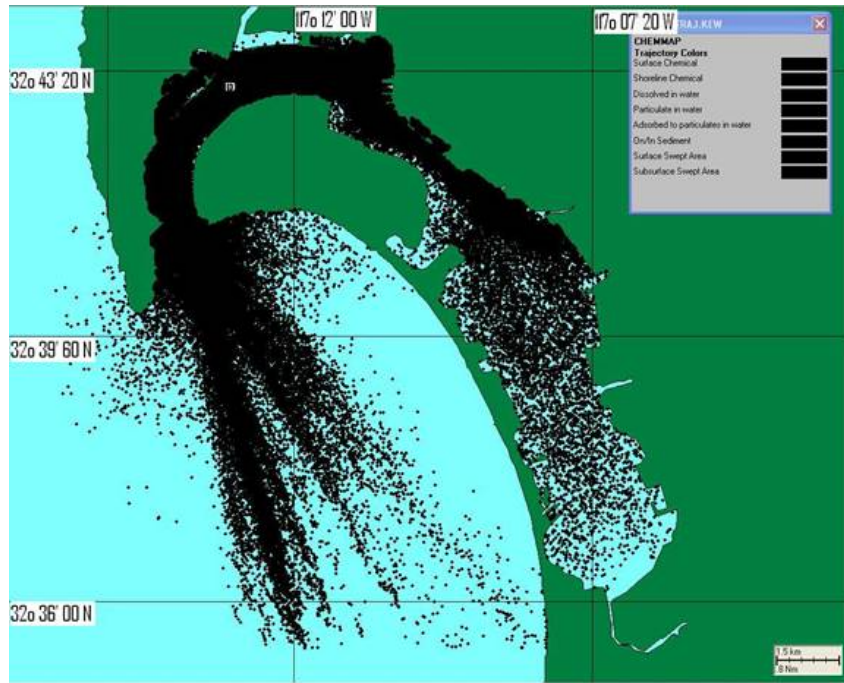
Figure 33.   Total swept area after 32 days for methanol dropped in North San Diego Bay.
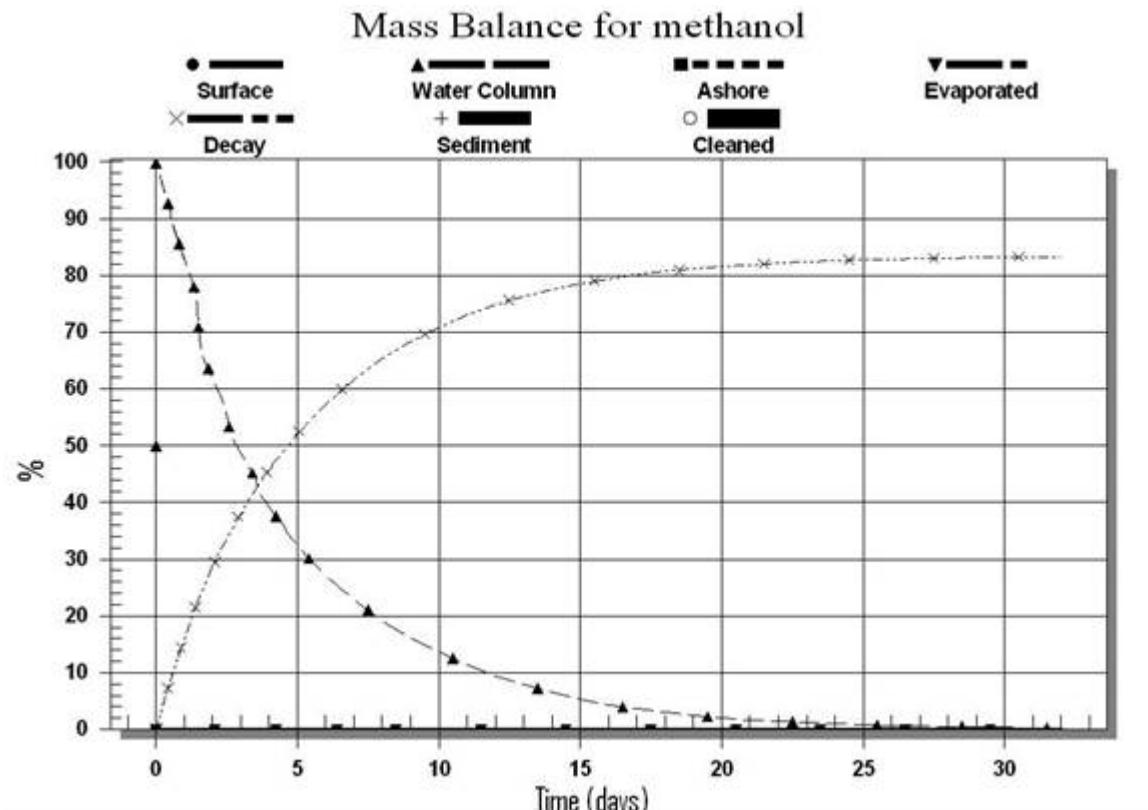
Figure 34.   Mass balance for methanol dropped in North San Diego Bay

2.   Pollutants Released at South San Diego Bay

Suppose a small boat drops one barrel of methanol in less than 12 minutes on midnight July 4, 1993 (Independence Day) at (32°39'N, 117°07.92' W), which is located in the southern part of San Diego Bay. The release depth is 1 m and the initial plum thickness is 0.5 m. In order to make the conditions more difficult for the propagation, assume that there is no wind at all.

The model results show the following features. First of all, very few pollutants reach 32°41'N parallel and in no case does methanol reach San Diego port (Figure 35). However, in 13 hours, it has reached the Naval Station (Figure 36) with a heavy impact in less than two days. In any case, since the northern part, which is contaminated, is the Naval Station, it is safe to conclude that the northern San Diego Bay is more important as a potential target. It is crucial for protective measures to highlight this fact because a chemical attack in the South San Diego Bay will have minimal effects, or at least much less considerable than an attack (or accident) in the north part of the bay. Figure 37 shows a similar but different result as regards the mass balance curves.
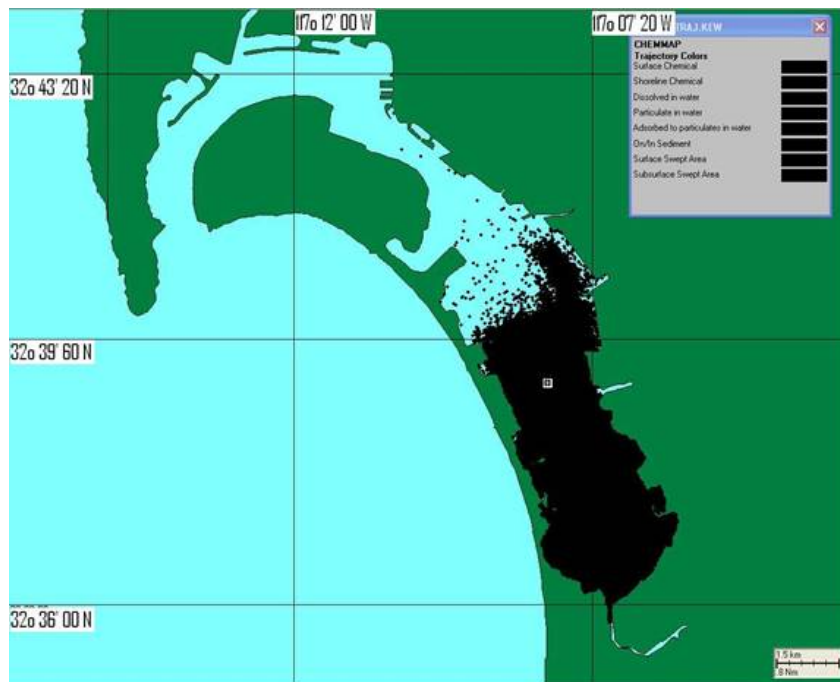
Figure 35.   Total swept area after 32 days for methanol dropped in South San Diego Bay.
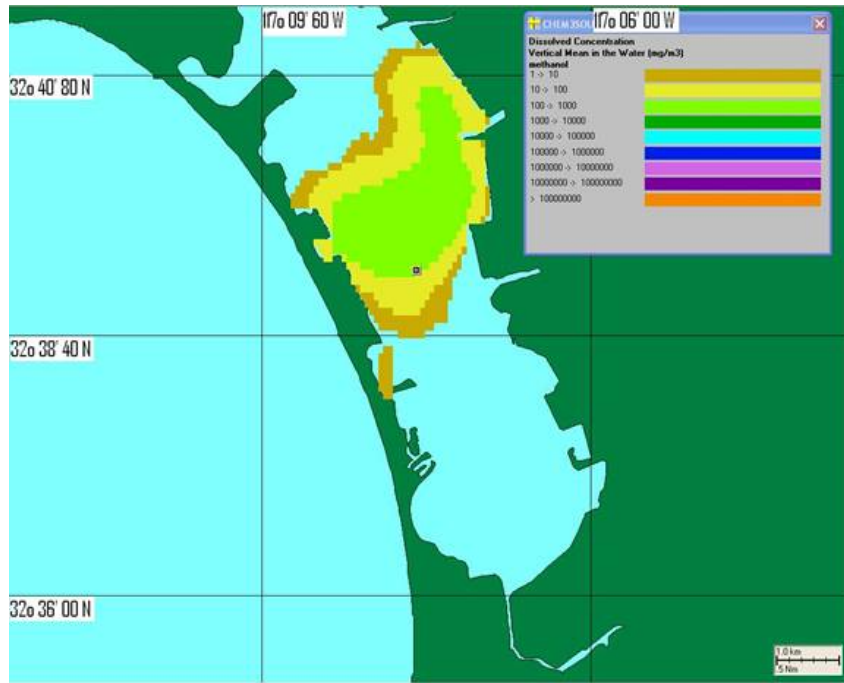
Figure 36.   Methanol dissolved concentration affecting the San Diego Naval Station after 13 hours.
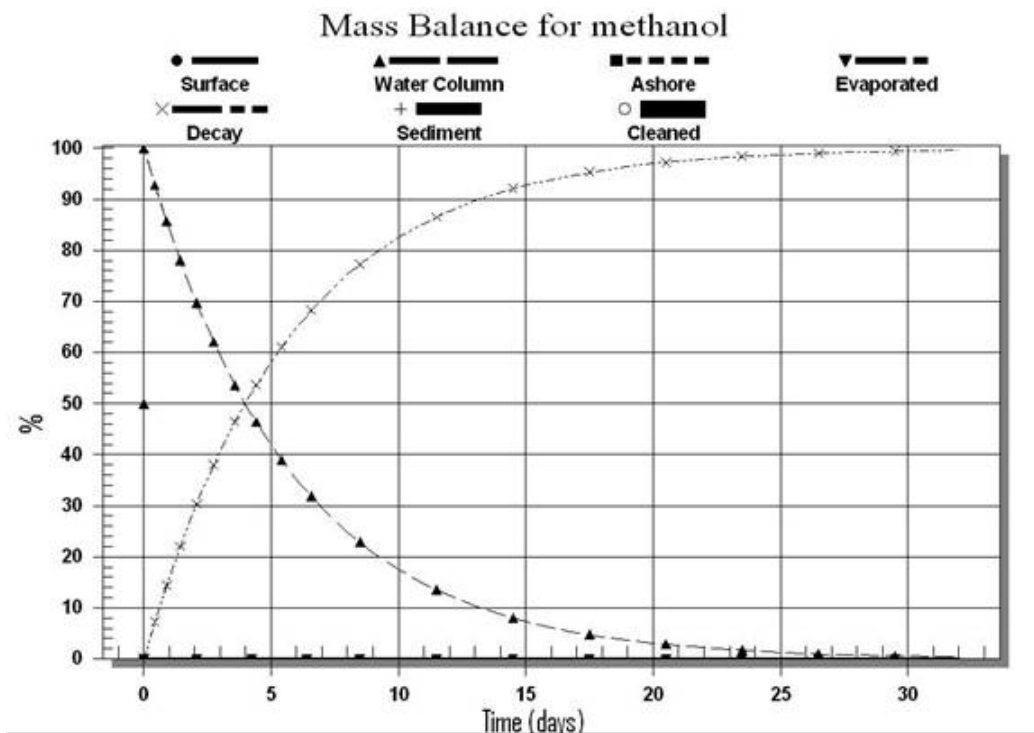
Figure 37.   Mass balance for methanol dropped in South San Diego Bay

Thus, the decayed methanol reaches 80% in only nine days, mainly due to the inert nature of methanol in combination with the shallow bathymetry of the southern part of the Bay. It is important to single out that in the first case (methanol spill over in the north), the dissolved concentration disappears after only 15 days, but in the second case (south), it needs 29 days.

The final conclusion is that the ecological catastrophe that can be caused with a relatively big amount of methanol spill over is very considerable, especially if the spill over is in the north. It can also be harmful to humans.

B.   BENZENE

1.   Pollutants Released at North San Diego Bay

Suppose that accidentally or on purpose there is a spill over of 10 tons of benzene, whish lasts five hours and happens at midnight on July 4, 1993, first in the same location as in the previous case in the northern part of San Diego Bay. Once more, the release depth is 1 m and the initial plum thickness is 0.5 m. In order to make the conditions more difficult for the propagation, assume again that there is no wind.

The model results are similar to the methanol scenario, at least as regards the propagation: In a little more than three hours, the benzene reaches San Diego port. In less than 12 hours, there is already a heavy impact outside the bay (Figure 38). Nevertheless, the southern part of the bay is contaminated much later. The Naval Station is not contaminated for the first five days (Figure 39) and in no time is there a heavy impact. By the time the benzene reaches the Naval Station (5 days), there is no dissolved concentration left. After eight days, there is no particle south of $\varphi = 32$ 39N and the benzene reaches the south end of the Bay only after 20 days, when its percentage in water column is less than 10%. Again, it is possible to conclude that in such a case, there is plenty of time to take protective measures for the southern part of the bay (Chula Vista area), where the results of such an incident would be minimal (Figure 40).

Furthermore, starting almost immediately and lasting for the entire period, a large amount of benzene (40%) evaporates. After five days only, 20% of the benzene is in the water column (Figure 41). However, for the port of San Diego, the effect is immediate and serious, as seen in Figure 42.
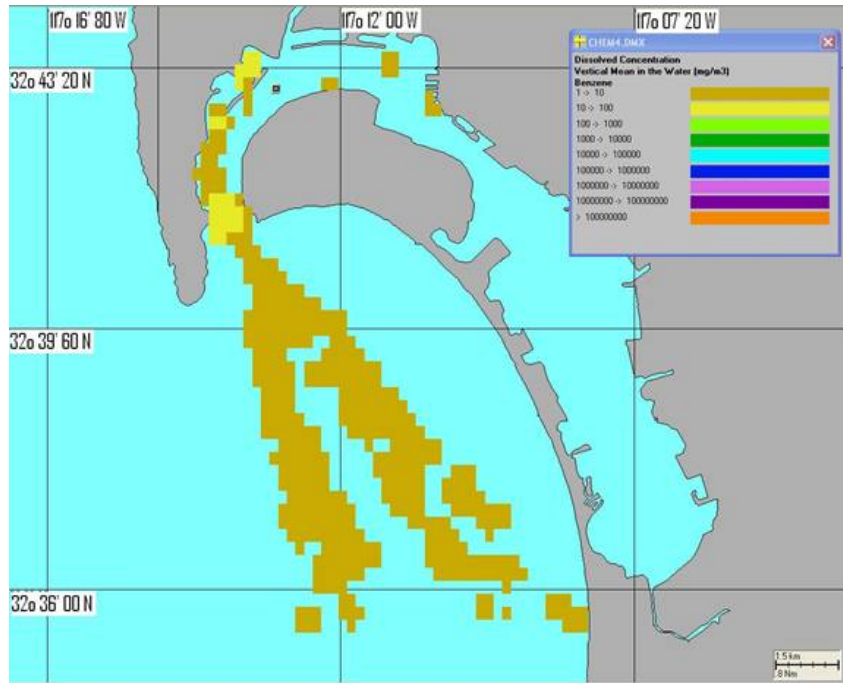
Figure 38.   Benzene dissolved concentration out of San Diego Bay in 12 hours.
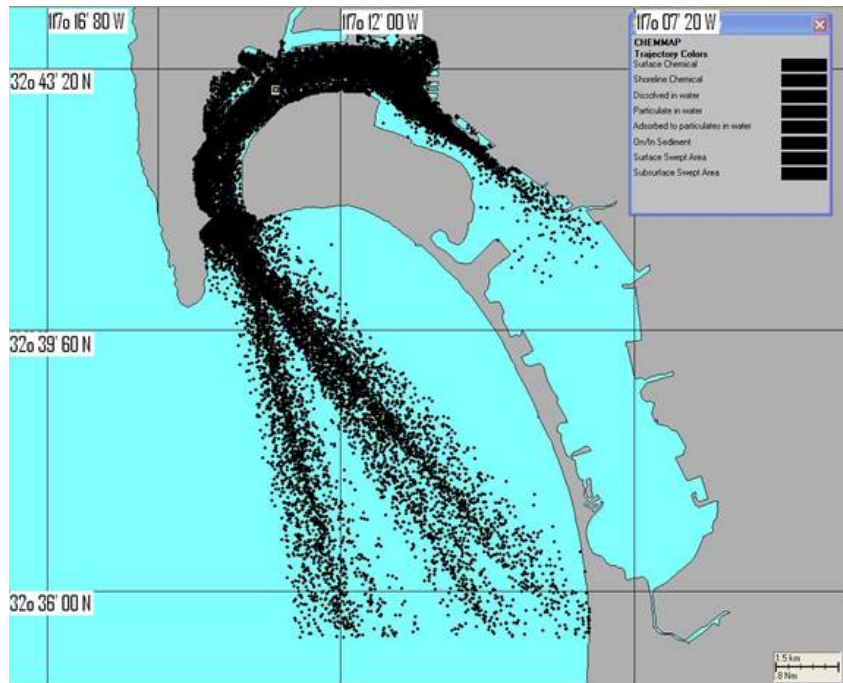

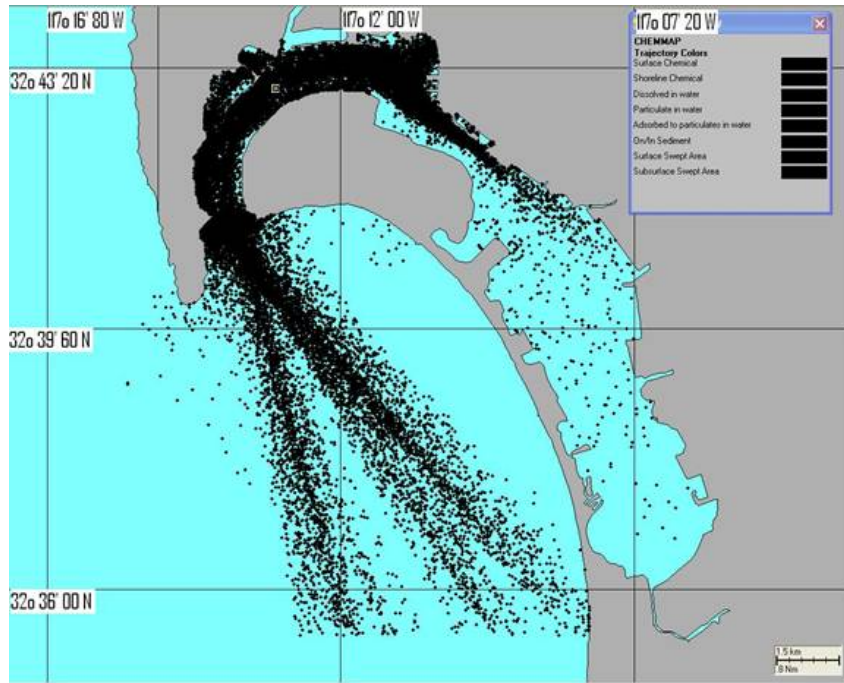Figure 39.   Benzene swept area after five days.

Figure 40.   Benzene swept area after 32 days.
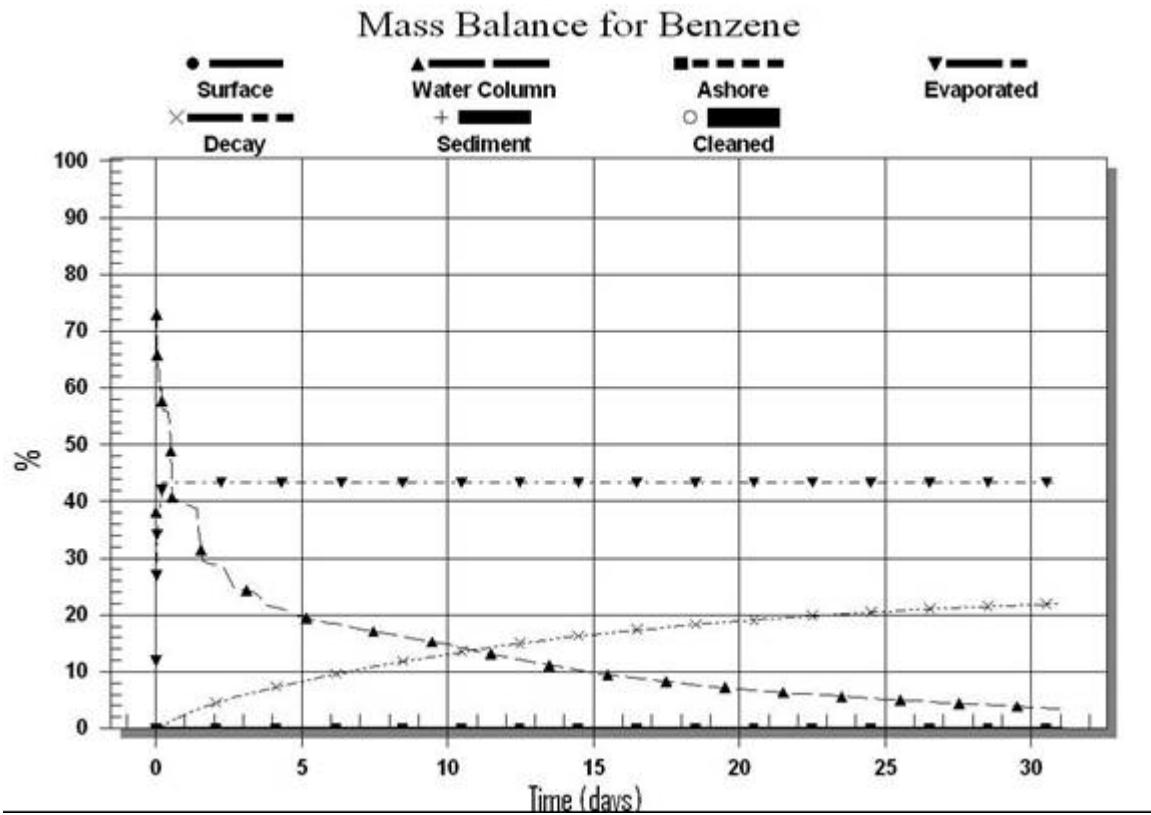

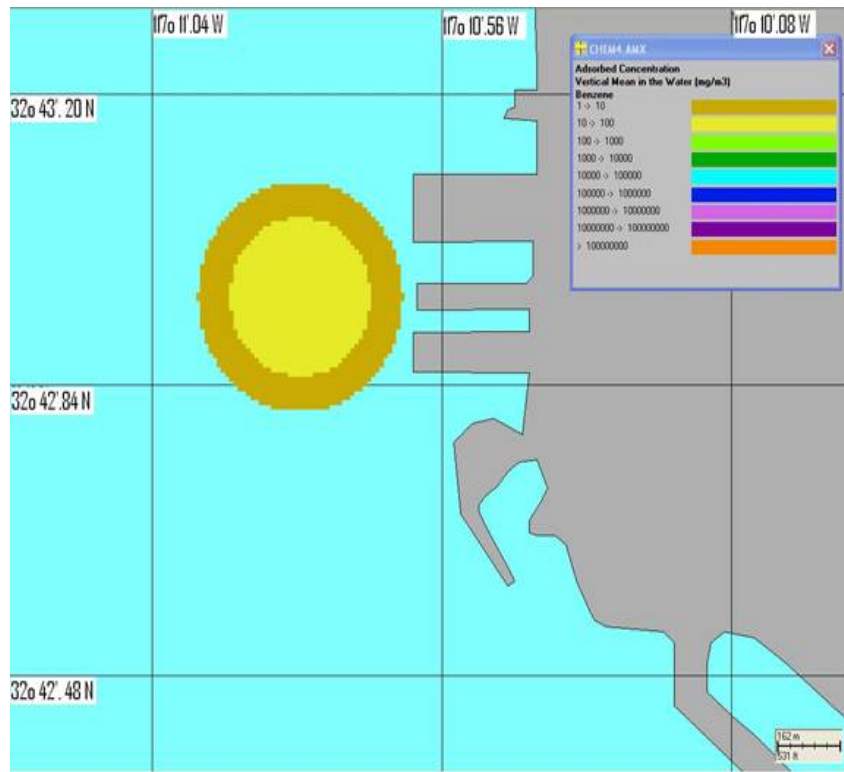Figure 41.   Mass balance for benzene dropped in North San Diego Bay.

Figure 42.   Absorbed benzene concentration after five hours in North San Diego Bay.

The decayed percentage never reaches more than 20%. Moreover, the end-state is the contamination not only of the San Diego Bay but also a considerable part of the sea outside the Bay. The scenario is repeated by increasing the amount of benzene and the previous results verified. The mass balance curves and the area contaminated remain the same.

2.   Pollutants Released at South San Diego Bay

Suppose that accidentally or on purpose there is a spill over of 10 tons of benzene, whish lasts five hours and happens at midnight on July 4, 1993, in the southern part of San Diego Bay, in a location closer to San Diego than in the respective methanol scenario (φ =32 39.34 N and λ =117 08.00W). The results are different, but again, similar to the methanol case. First of all, practically benzene particles do not reach San Diego. However, the Naval Station is reached within 12 hours (Figure 43) and completely contaminated in less than three days. It is important for protective measures to highlight

this fact because a chemical attack in the southern part of the Bay would affect the Naval Station, and in the northern part, would affect the city. Nevertheless, after 17 days, there is dissolved benzene at the city/port of San Diego (Figure 44). Figure 45 shows the end-state of benzene swept area.
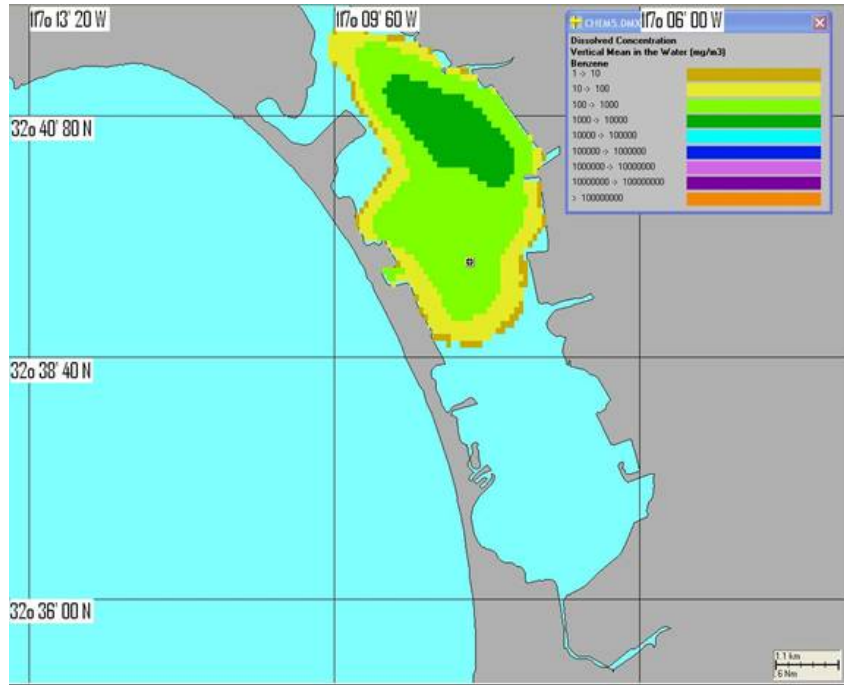

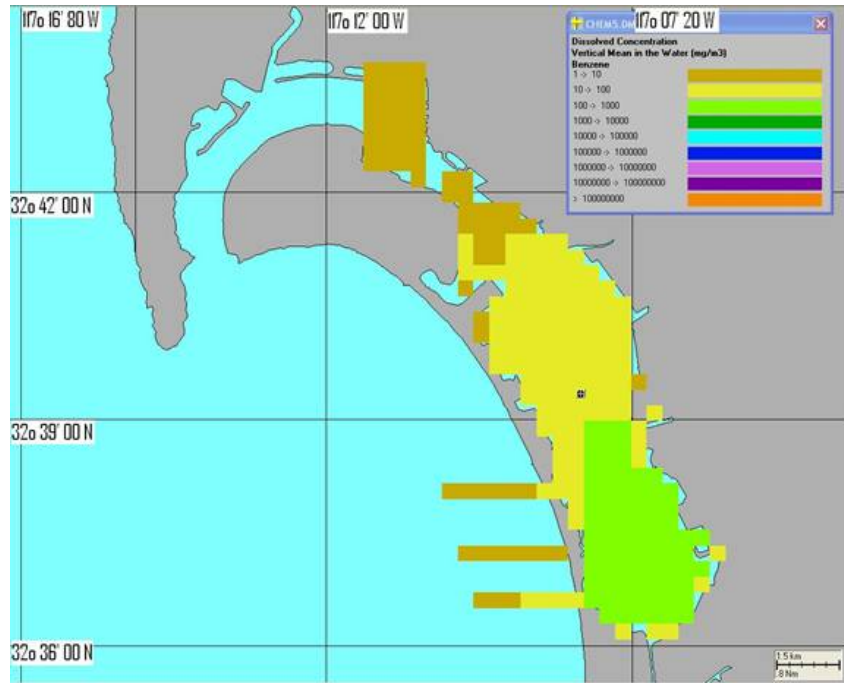Figure 43.   Benzene dissolved concentration at the San Diego Naval Station after 12 hours.

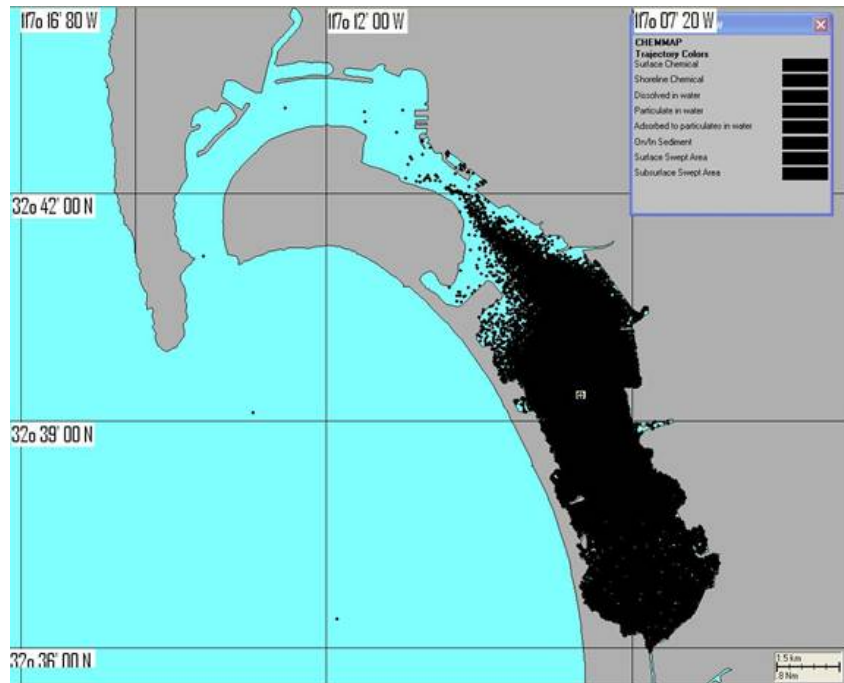Figure 44.   Benzene dissolved concentration after 17 days.

Figure 45.   Benzene swept area after 32 days.

As regards the mass balance curves, there is a similar but different result, as seen in Figure 46. Comparing Figures 41 and 46 shows that there is much more benzene in the water column (more than 30% after 10 days), the decayed benzene after a month exceeds 40% and only the rate of evaporation is the same.

The final conclusion is that the ecological catastrophe that can be caused with a relatively large amount of benzene spill over is very considerable and it can be harmful to humans and the eco-system.
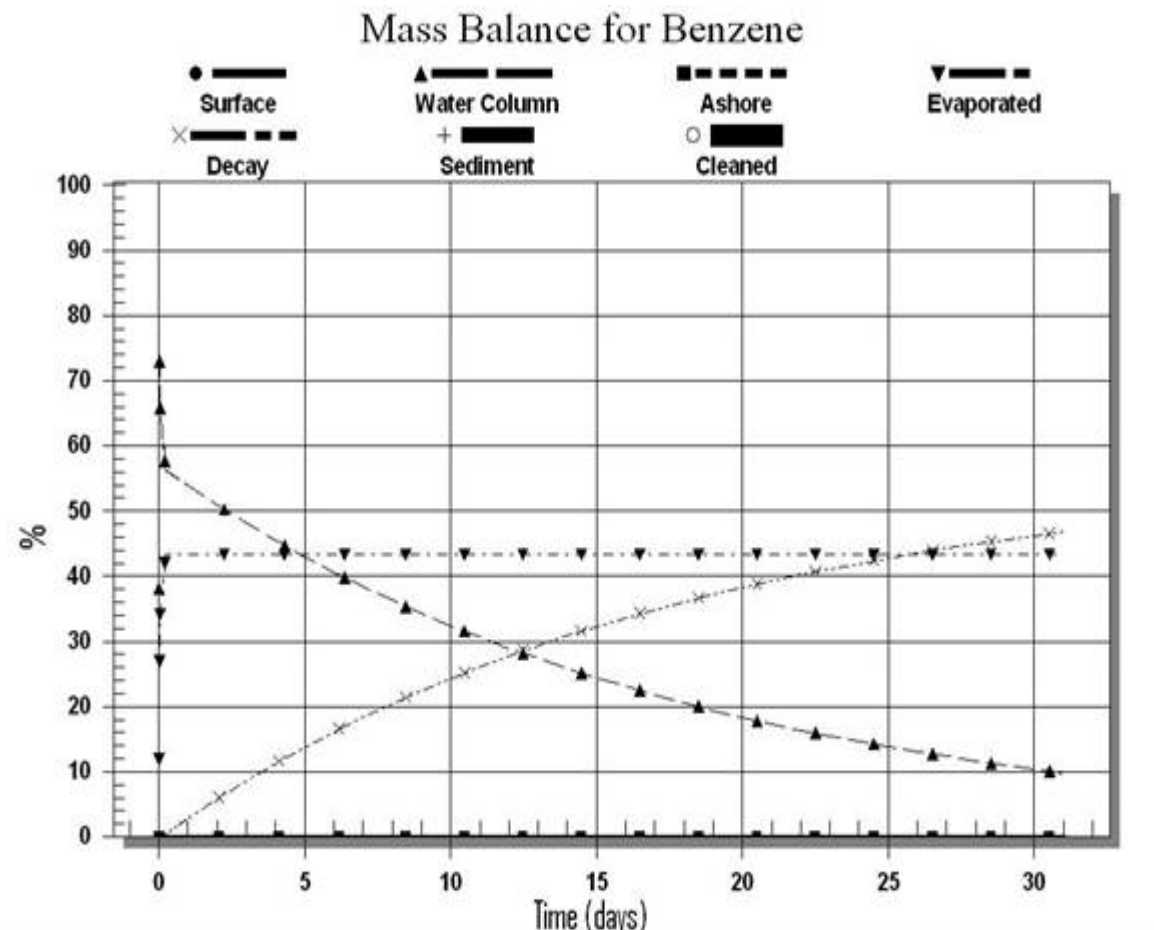
Figure 46.   Mass balance for benzene dropped in South San Diego Bay.

C.   AMMONIA

1.   Pollutants Released at North San Diego Bay

Suppose the sinking of a ship containing liquefied ammonia in the same two locations and time used in the previous scenario. This time in a depth of 3m there is

leakage of 200 tons of liquefied ammonia which is completed in 20 hours. This is more of an environmental threat than an immediate lethal threat to humans. Once again, there is no wind forcing.

The results are similar to both aforementioned scenarios as regards the propagation: In a little more than three hours, the ammonia reaches San Diego port (Figure 47) and in less than 12 hours, it is widespread outside of the bay (Figure 48). Nevertheless, the southern part of the Bay is contaminated much later. After five days, there is no particle south of $\varphi = 32\ 40N$ and the benzene reaches the southern end of the Bay only after 15 days (Figure 49). The Naval Station is contaminated in a period between 30 hours (Figure 50) and five days, in which the percentage of ammonia in the water column in between 45 and 80% (Figure 51). After 15 days, the decayed ammonia exceeds 50% and that left in the water column is a little more than 15%.

It is again possible to conclude that in such a case, there is plenty of time to take protective measures only for the southern part of the Bay (excluding the Naval Station), where the results of such an incident would be minimal. However, for both the city/port of San Diego and the Naval Station, the effect is immediate and serious. The end-state is the contamination of the entire San Diego Bay (Figure 52) as well as a considerable part of the sea outside the bay.
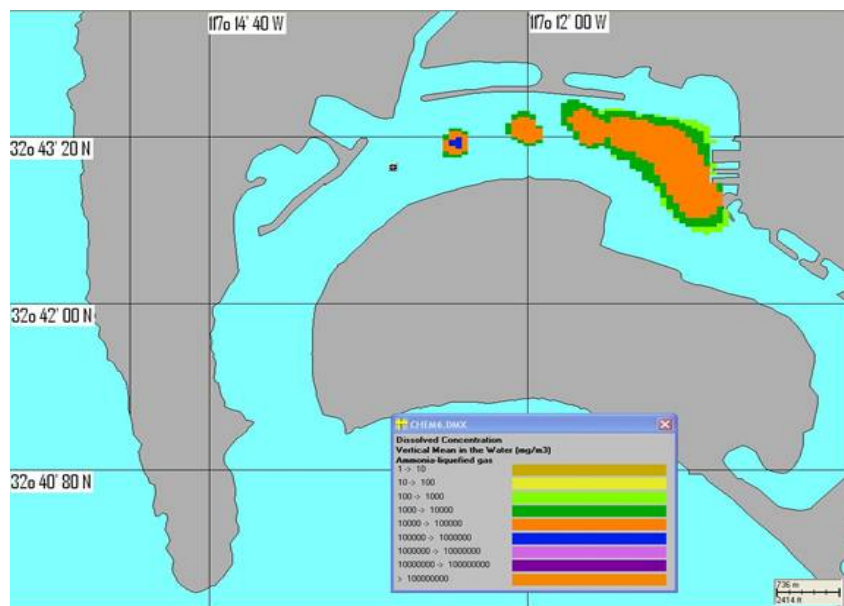

Figure 47.   Ammonia mean dissolved concentration after three hours.
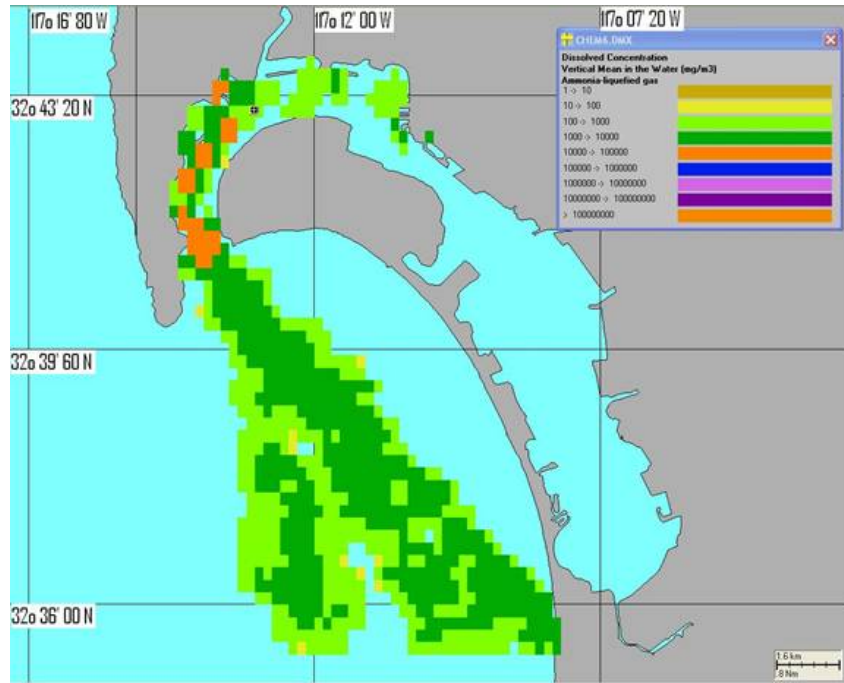
Figure 48.   Ammonia mean dissolved concentration after 12 hours.
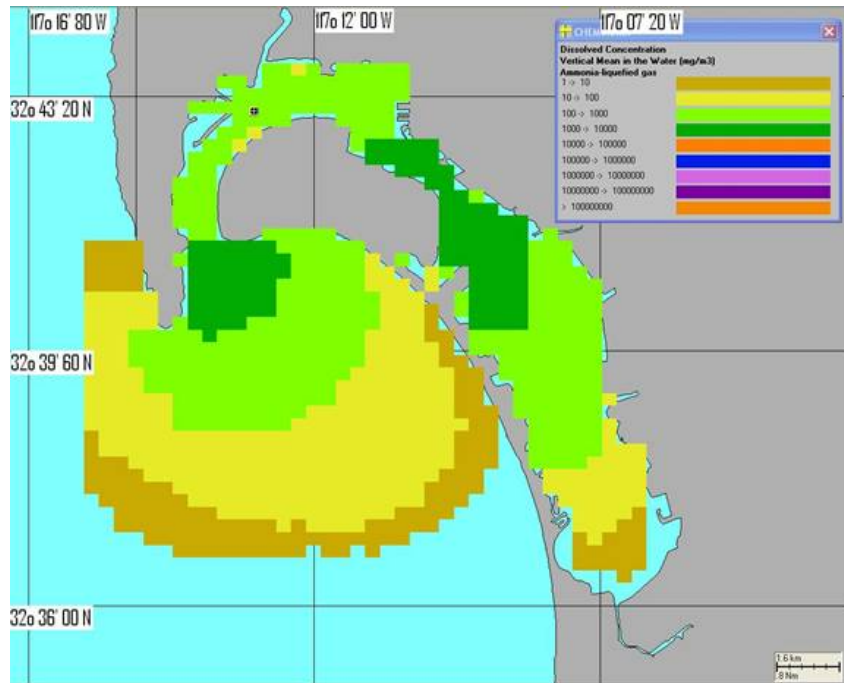

Figure 49.   Ammonia mean dissolved concentration after 15 days.
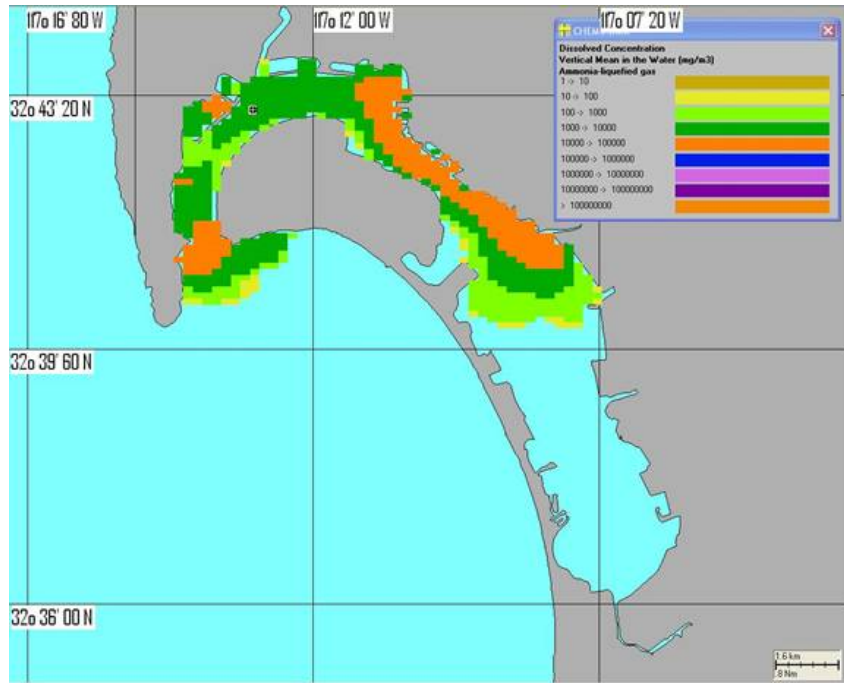
Figure 50.   Ammonia mean dissolved concentration after 30 hours.
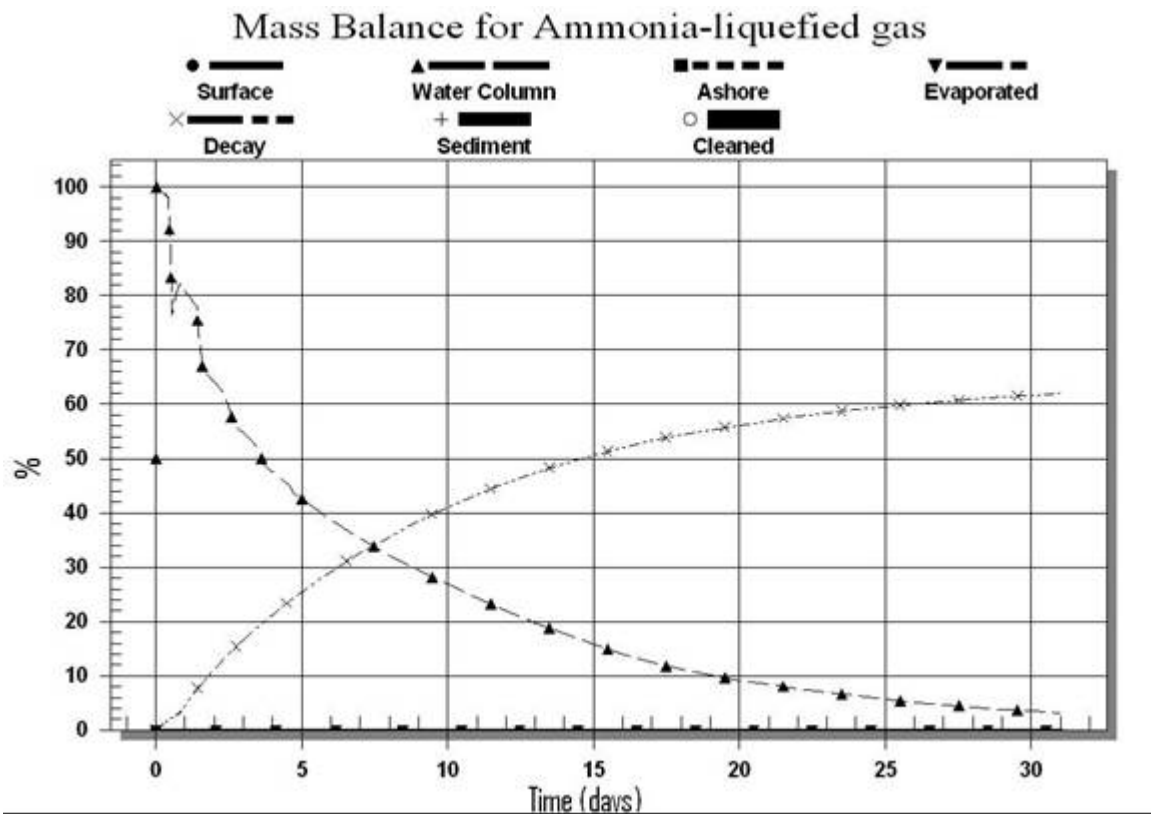

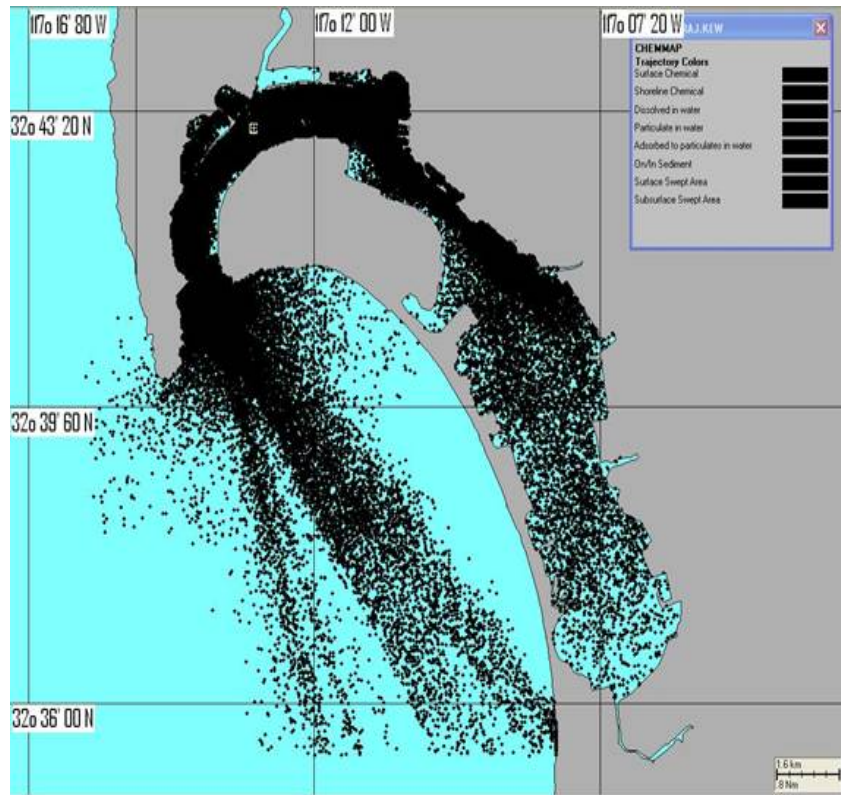Figure 51.   Mass balance for ammonia dropped in North San Diego Bay

Figure 52.   End-state as regards swept area for ammonia dropped in North San Diego Bay

2.   Pollutants Released at South San Diego Bay

Suppose the sinking of a ship containing liquefied ammonia in the southern part of the Bay, in the same location used in the methanol scenario (φ=32 39.00N and λ=117 07.92W). The results are different but again similar to the previous cases. First of all, practically benzene does not damage the port and city of San Diego (Figure 53). However, in 12 hours, it has reached the Naval Station (Figure 54) and in less than three days, it has a very heavy impact on it. It is important for protective measures to highlight this fact because a chemical attack in the southern part of the bay would have minimal effects on the city, which will be affected after 15 days (Figure 55) but are considerable at the Naval Station.

As regards the mass balance curves, there are similar but different results, as seen in Figure 56. By comparing Figures 38 and 39, notice that there is much more ammonia in the water column (more than 50% after seven days) and the decayed percentage in 25

days reaches 90%. The final conclusion is that the ecological catastrophe that can be caused with a relatively large amount of ammonia spill over is smaller than in the previous cases, yet considerable, for humans and the eco-system.
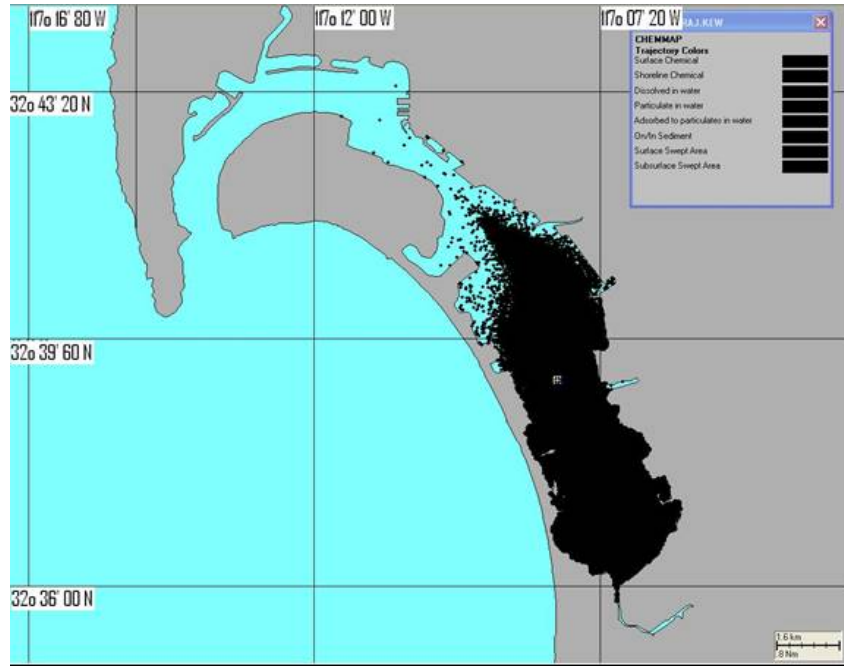

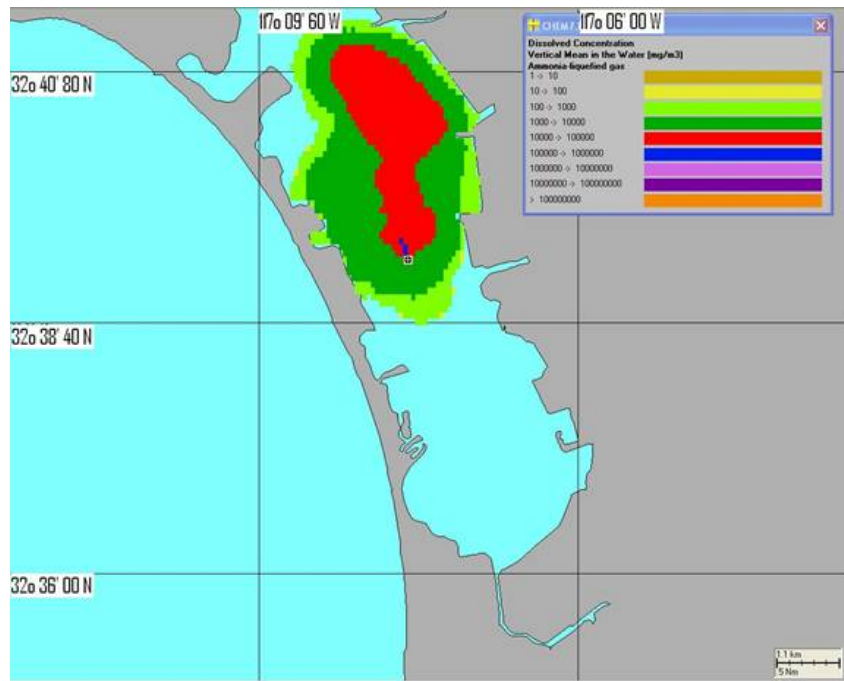Figure 53.   Total swept area for ammonia dropped in South San Diego Bay.

Figure 54.   Ammonia mean dissolved concentration after 12 hours.
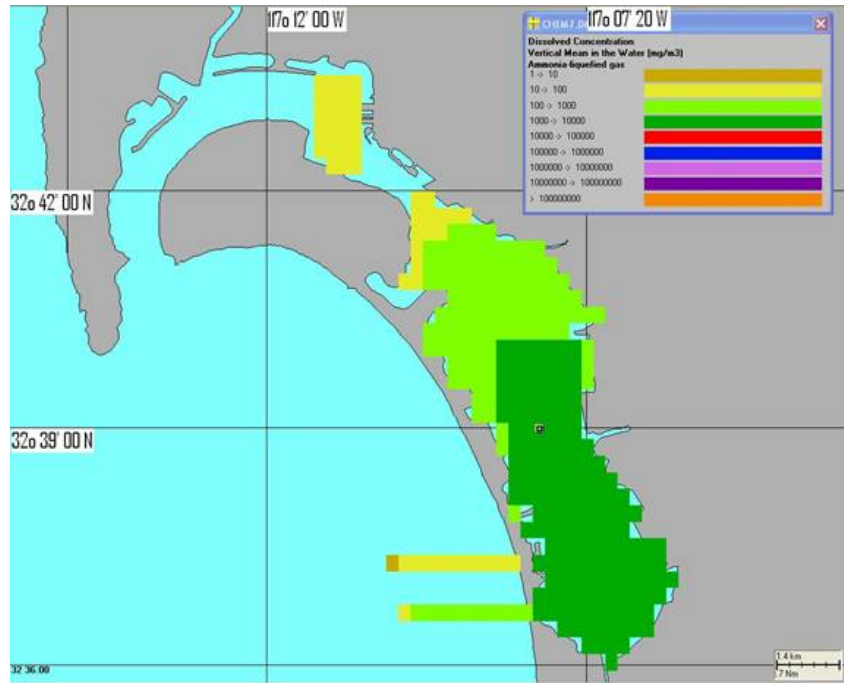
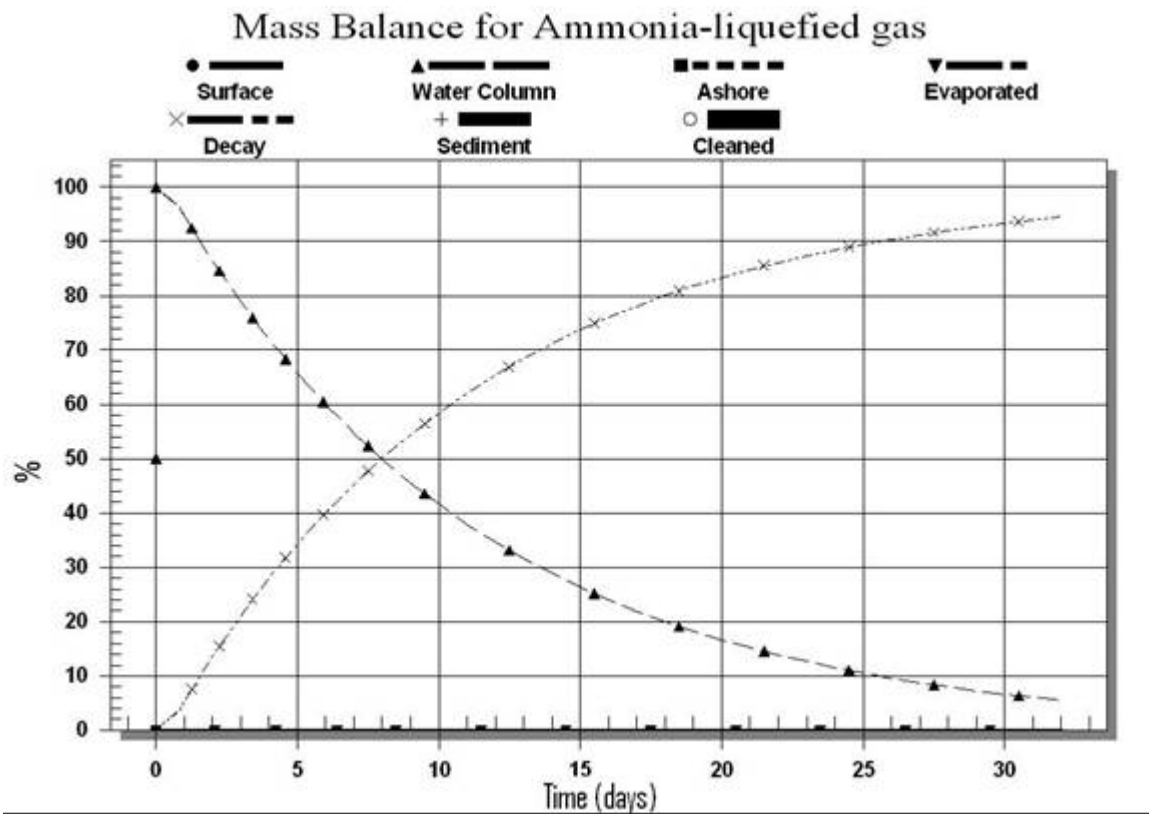Figure 55.   Ammonia mean dissolved concentration after 15 days.

Figure 56.   Mass balance for ammonia dropped in South San Diego Bay.

D.   CHLOROBENZENE

1.   Pollutants Released at North San Diego Bay

Suppose the sinking of a ship containing chlorobenzene, in the same two locations and time used in our previous scenarios. Again, in a depth of 3m, there is leakage of 200 tons, which is completed in 20 hours. Still, there is no wind forcing. The results are similar to all aforementioned scenarios as regards the propagation. In three hours, chlorobenzene reaches San Diego port (Figure 57) and in less than 12 hours, it is widespread outside of the bay (Figure 58). After 20 hours, there is no particulate concentration and after 30 hours, the Naval Station is contaminated (Figure 59). Nevertheless, the southern part of the bay is contaminated much later, in approximately 19 days (Figure 60), and finally note widespread chlorobenzene all over the bay (Figure 61).

Furthermore, after 42 hours, there is no sediment. There is very little decay and in no case exceeds 10%. What is more important is that chlorobenzene in the water column decreases from almost 90% to 45% after 32 days, which is a very impressive percentage of remaining chlorobenzene (Figure 62). The end-state is the contamination not only of the San Diego Bay but also a considerable part of the sea outside the bay.
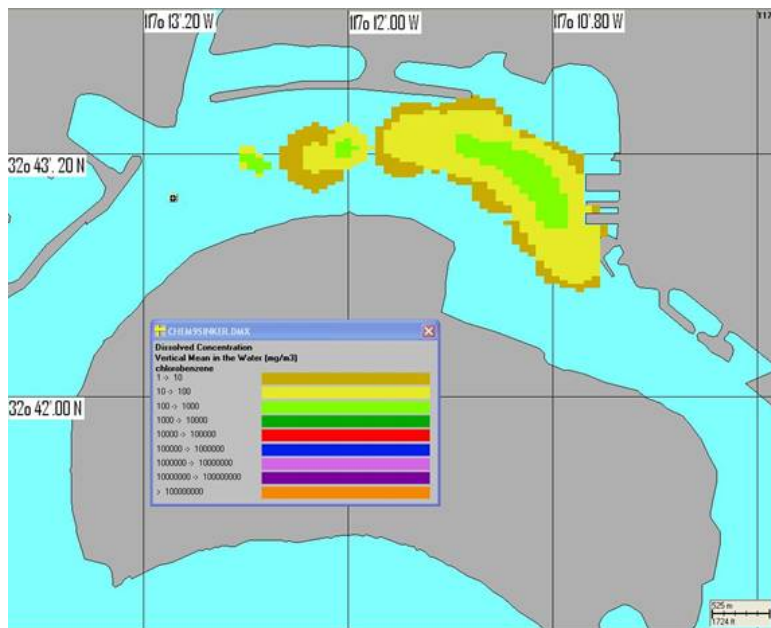

Figure 57.   Chlorobenzene mean dissolved concentration after three hours.
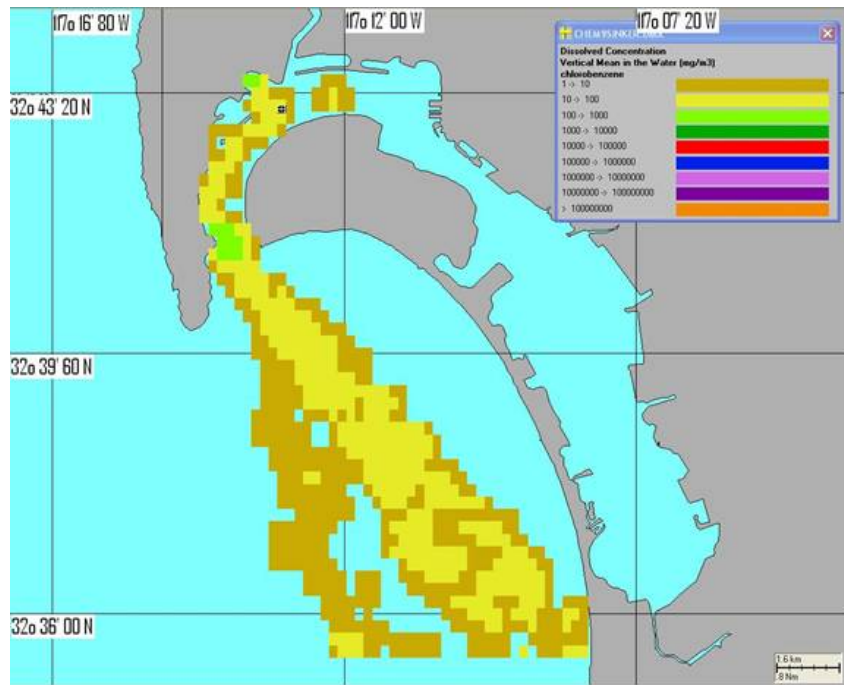
Figure 58.   Chlorobenzene mean dissolved concentration after 12 hours
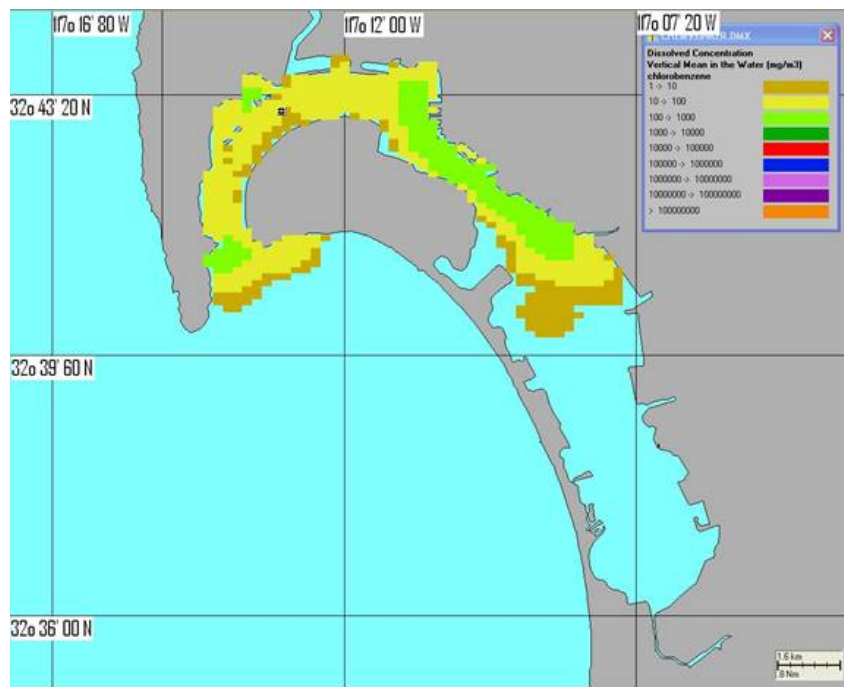

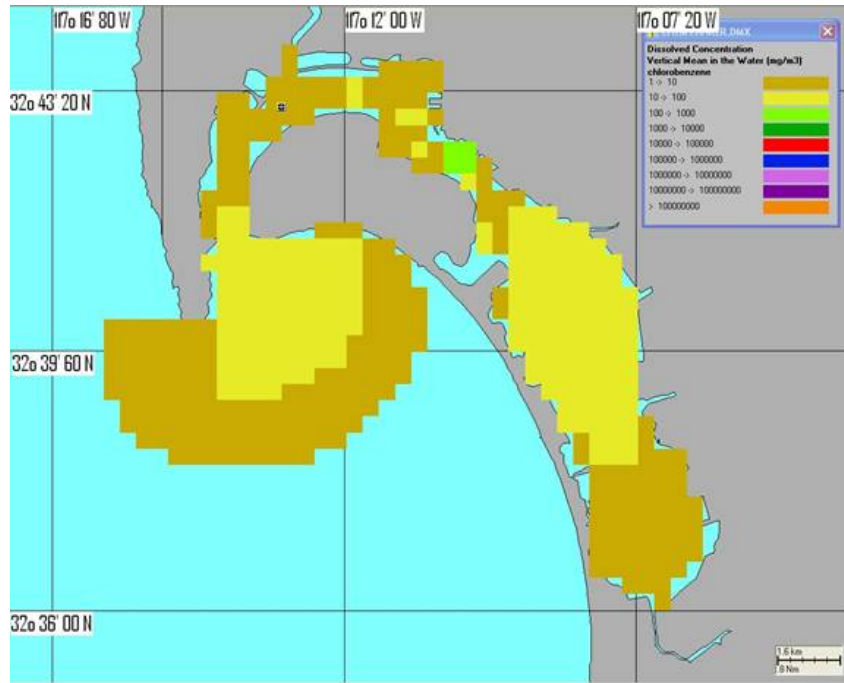Figure 59.   Chlorobenzene mean dissolved concentration after 30 hours

Figure 60.   Chlorobenzene mean dissolved concentration after 19 days
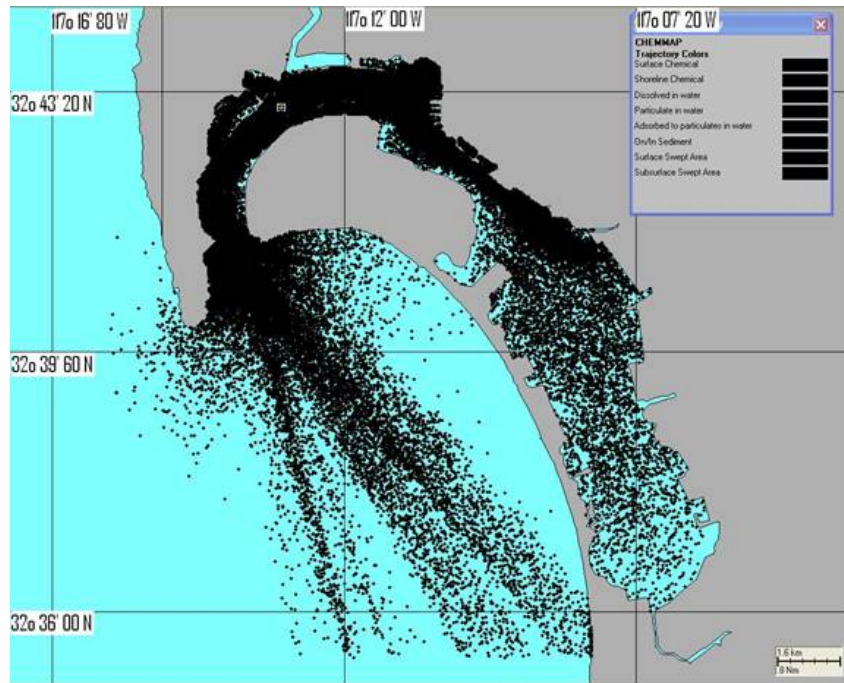

Figure 61.   Swept area of chlorobenzene dropped in North San Diego Bay after 32 days.
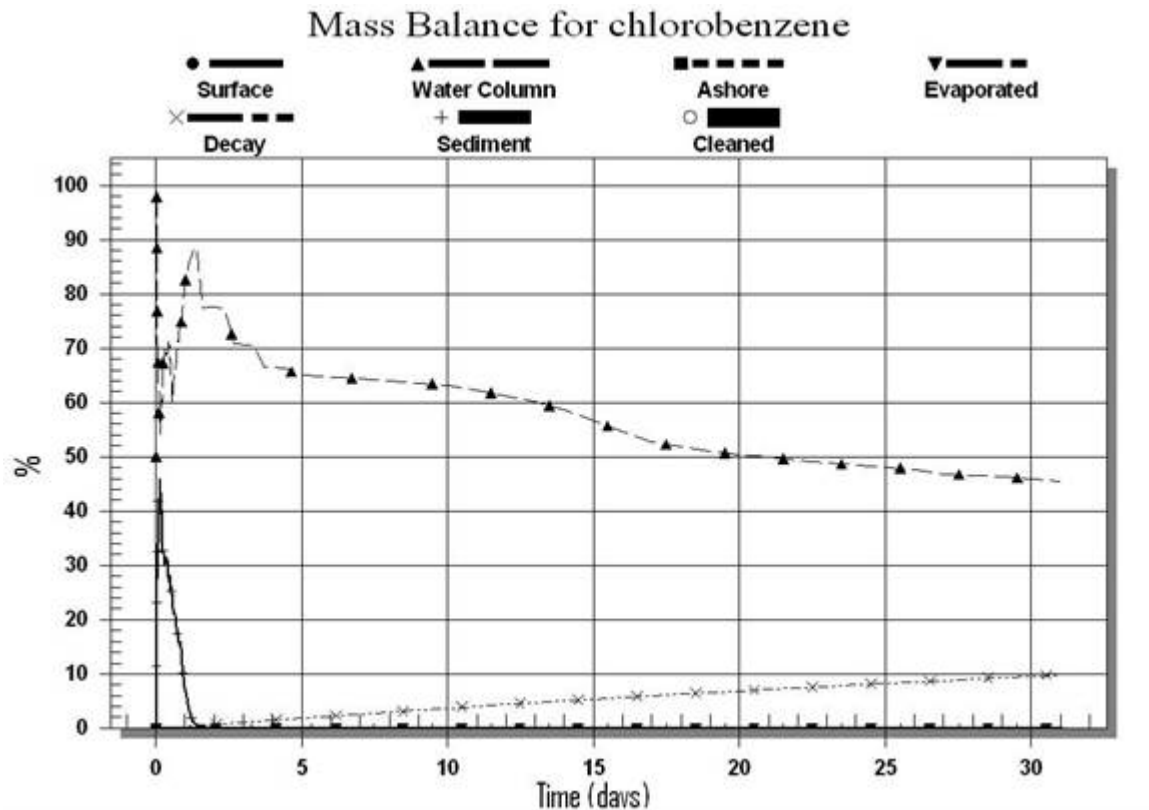
Figure 62.　　Mass balance for chlorobenzene dropped in North San Diego Bay.

2.　　Pollutants Released at South San Diego Bay

Suppose the sinking of a ship containing chlorobenzene in the southern part of the Bay, in the same location used in the previous scenarios (φ=32 39.00N and λ=117 07.92W), the results are very similar to the previous cases. First of all, practically benzene does not reach the port and city of San Diego (Figure 63). However, in 11 hours, it has reached the Naval Station (Figure 64).

As regards the mass balance curves, there is a similar but different result, as seen in Figure 65. Comparing Figures 62 and 65 shows that the results are the same concerning sediments and particulate concentrations. However, there is much more chlorobenzene in the water column (more than 80% after 32 days) and the decayed percentage reaches 15%. The final conclusion is that the sinker can cause a greater ecological catastrophe that a floater and in a carefully planned attack in the North San Diego Bay, the damage might be overwhelming.
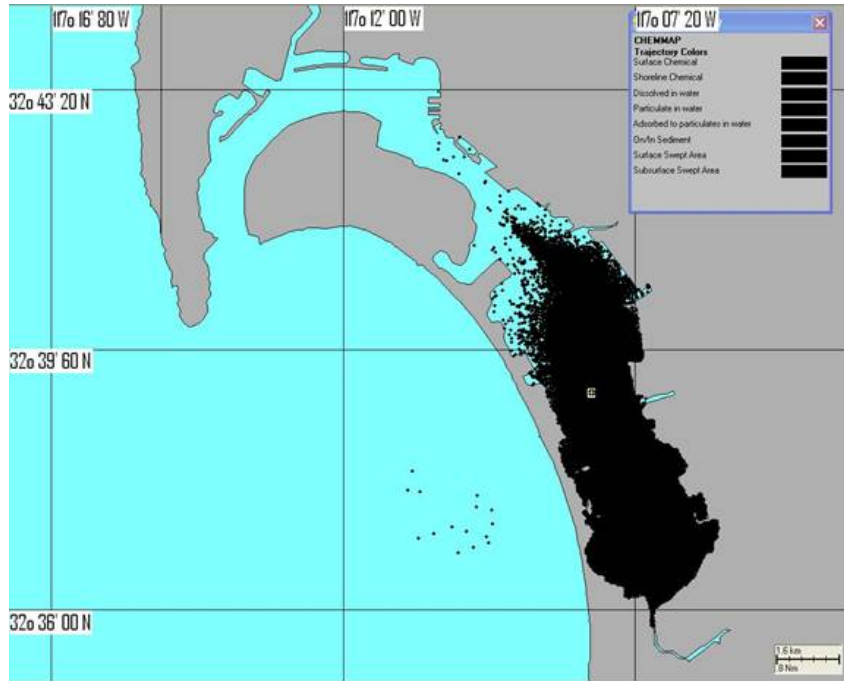
Figure 63.   Swept area of chlorobenzene dropped in South San Diego Bay.
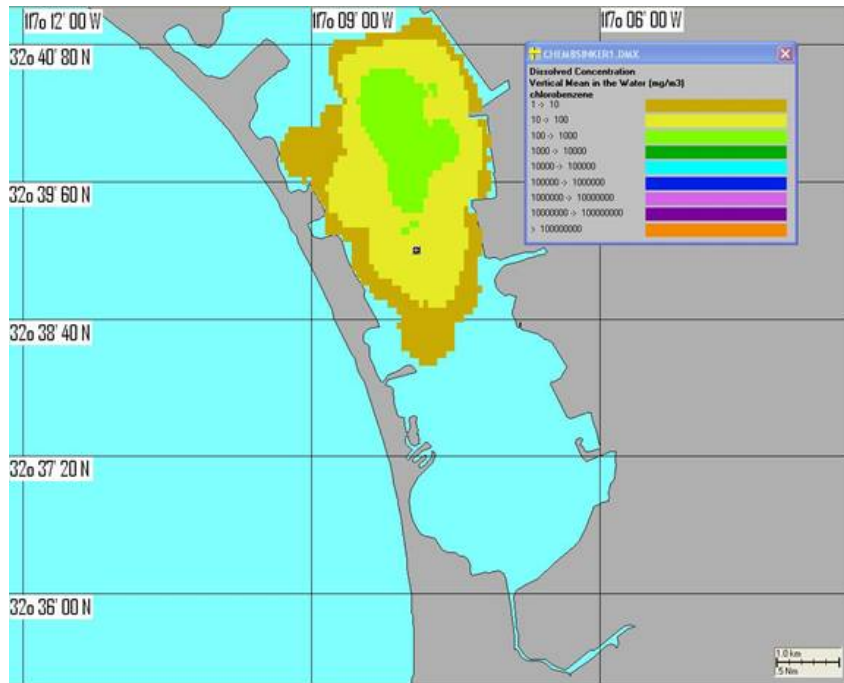

Figure 64.   Chlorobenzene reaches the Naval Station after 11 hours when dropped in
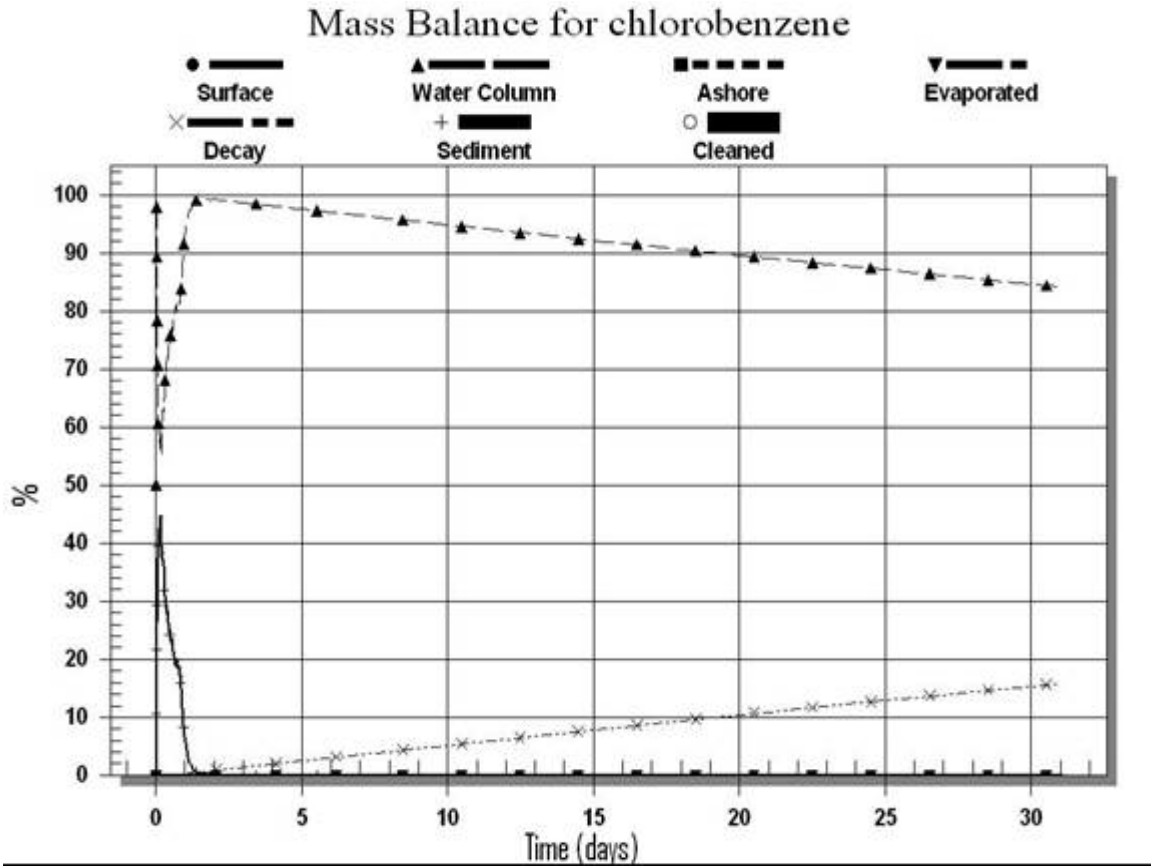South San Diego Bay

Figure 65.   Mass balance for chlorobenzene dropped in South San Diego Bay.

E.   TRICHLOROETHYLENE

1.   Pollutants Released at North San Diego Bay

Suppose the sinking of a ship containing trichloroethylene, in the same two locations and time used in the previous scenarios. Again, in a depth of 3m, there is leakage of 200 tons, which is completed in 20 hours. As in all previous scenarios, there is no wind forcing. The results are not surprisingly the same as regards the propagation. In three hours, trichloroethylene reaches San Diego port (Figure 66) and in 12 hours, it is widespread outside of the Bay. A small difference is that there is no particulate concentration and a very small percentage of sediments even after 32 days. The Naval Station is contaminated after 30 hours and the southern part of the Bay is contaminated in approximately 19 days. The swept area end-state is very similar to the respective case of chlorobenzene (Figure 67). Furthermore, the decay curve reaches 25% after 32 days. Trichloroethylene in the water column remains at a high level but not as high as

77

chlorobenzene in the previous scenario. It decreases from almost 90% to less than 30%. Nevertheless, the first 12 days, the percentage of the trichloroethylene in the water column is above 50% (Figure 68).
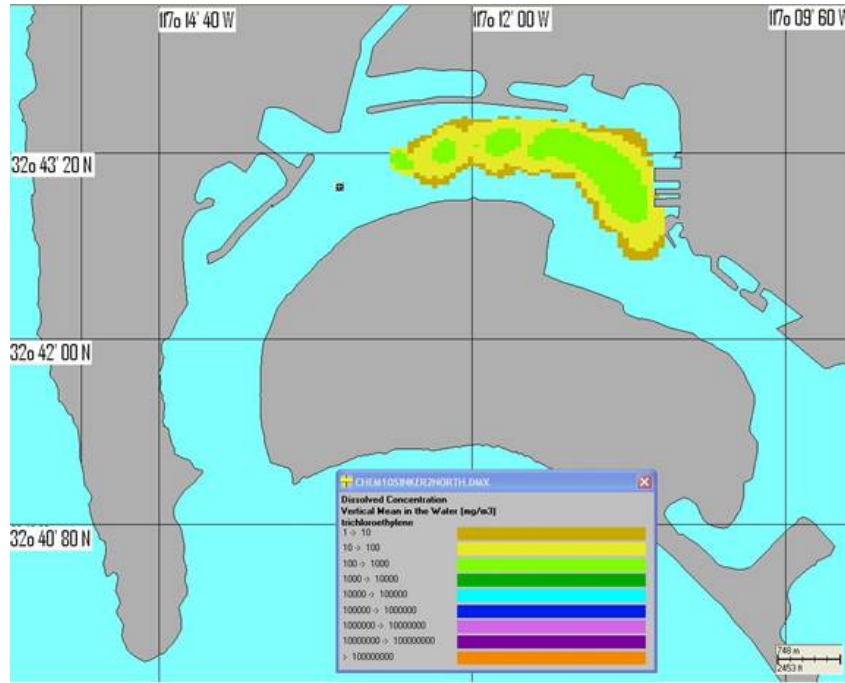

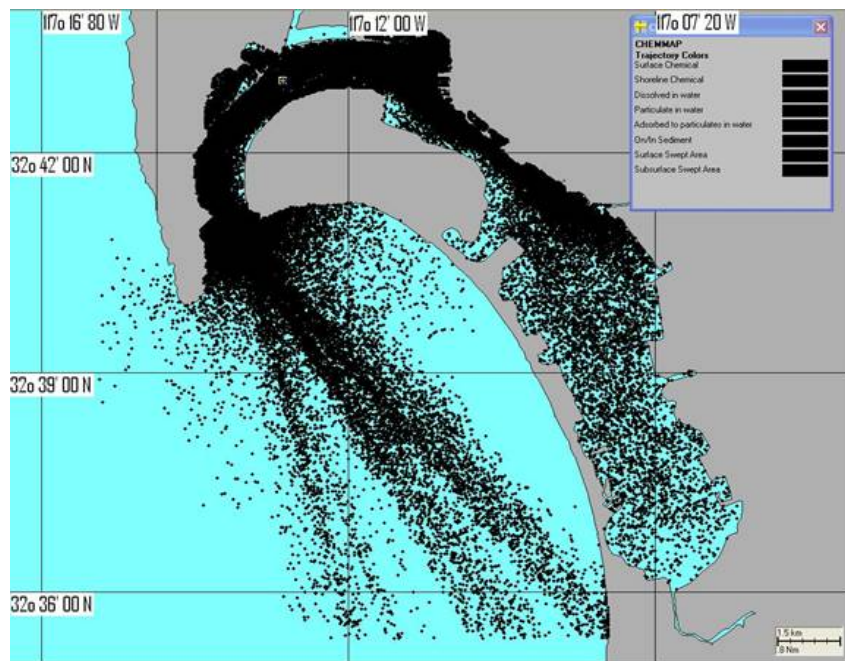Figure 66.   Trichloroethylene mean dissolved concentration after three hours.

Figure 67.   Swept area of trichloroethylene dropped in North San Diego Bay.
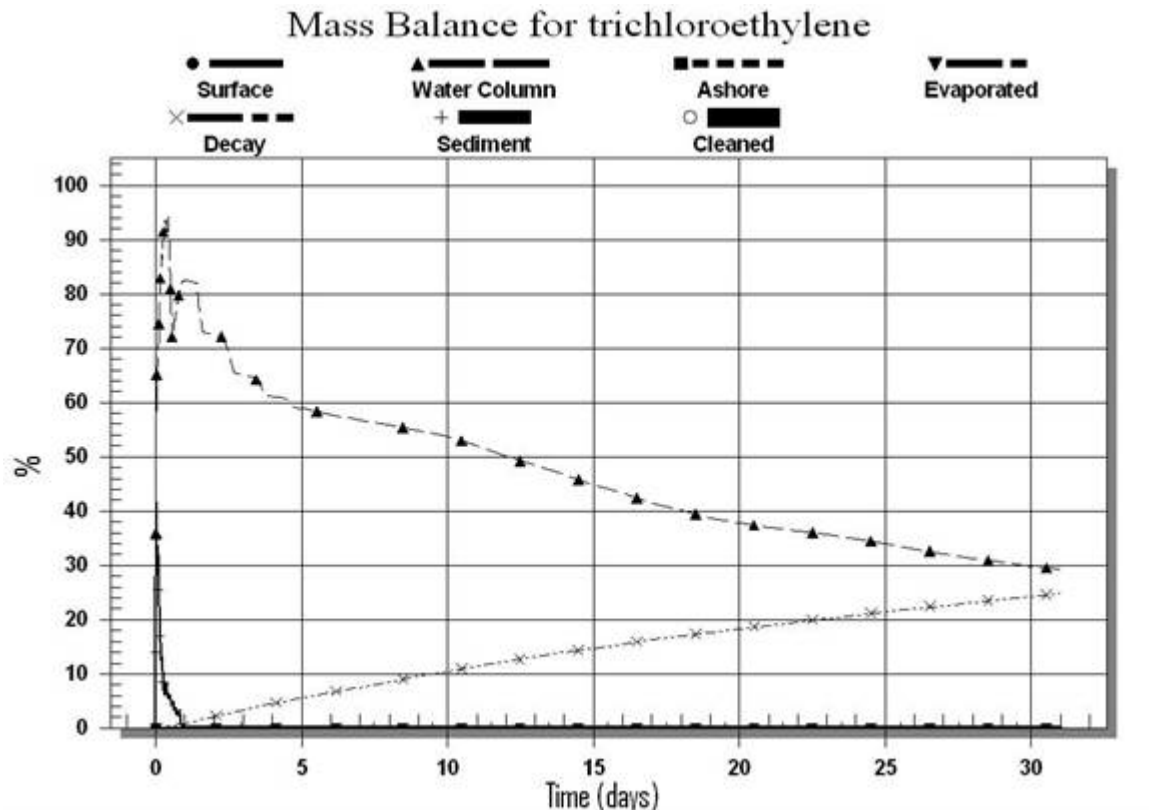
Figure 68.   Mass balance for trichloroethylene dropped in North San Diego Bay.

2.   Pollutants Released at South San Diego Bay

Suppose the sinking of a ship containing trichloroethylene in the southern part of the Bay, in the same location used in the previous scenarios (φ=32 39.00N and λ=117 07.92W), the results are very similar to the previous cases. Again, trichloroethylene does not reach the port and city of San Diego (Figure 69). However, in 11 hours, it has reached the Naval Station (Figure 70).

As regards the mass balance curves, there is a similar but different result, as seen in Figure 71. Comparing Figures 68 and 71 shows that the results are the same concerning sediments and particulate concentrations. However, there is much more trichloroethylene in the water column (almost 60% after 32 days) and the decayed percentage reaches 40%. The final conclusion is that the sinker can cause a greater ecological catastrophe than a floater but is much less significant in South San Diego Bay than in the northern part of the Bay.
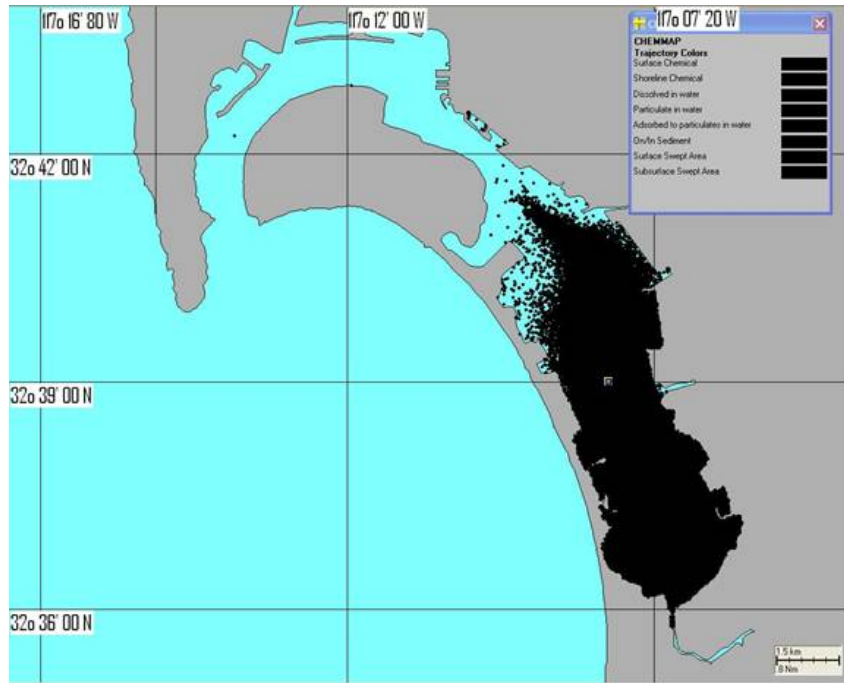
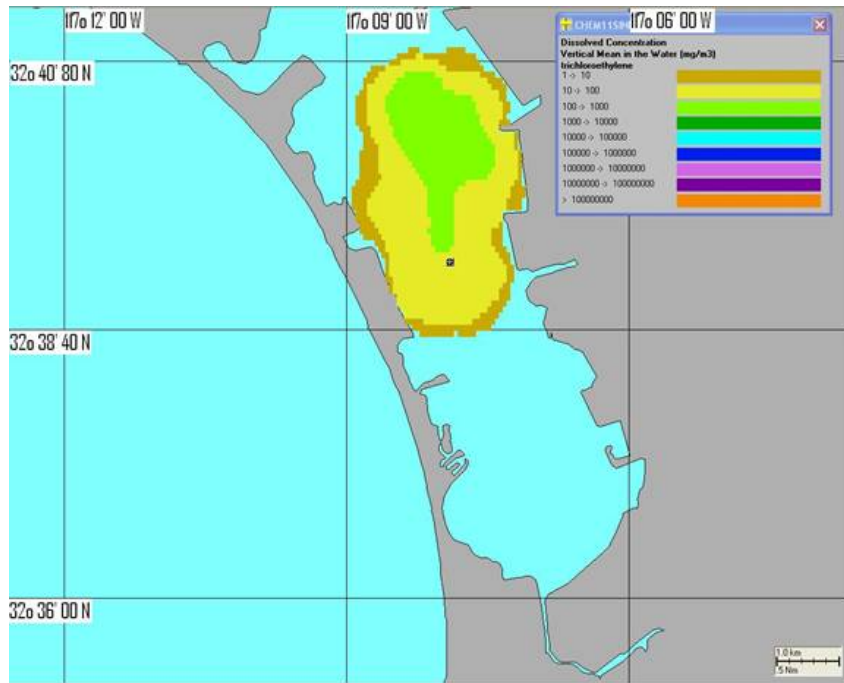Figure 69.   Swept area of trichloroethylene dropped in South San Diego Bay.

Figure 70.   Trichloroethylene reaches the Naval Station after 11 hours when dropped in South San Diego Bay.
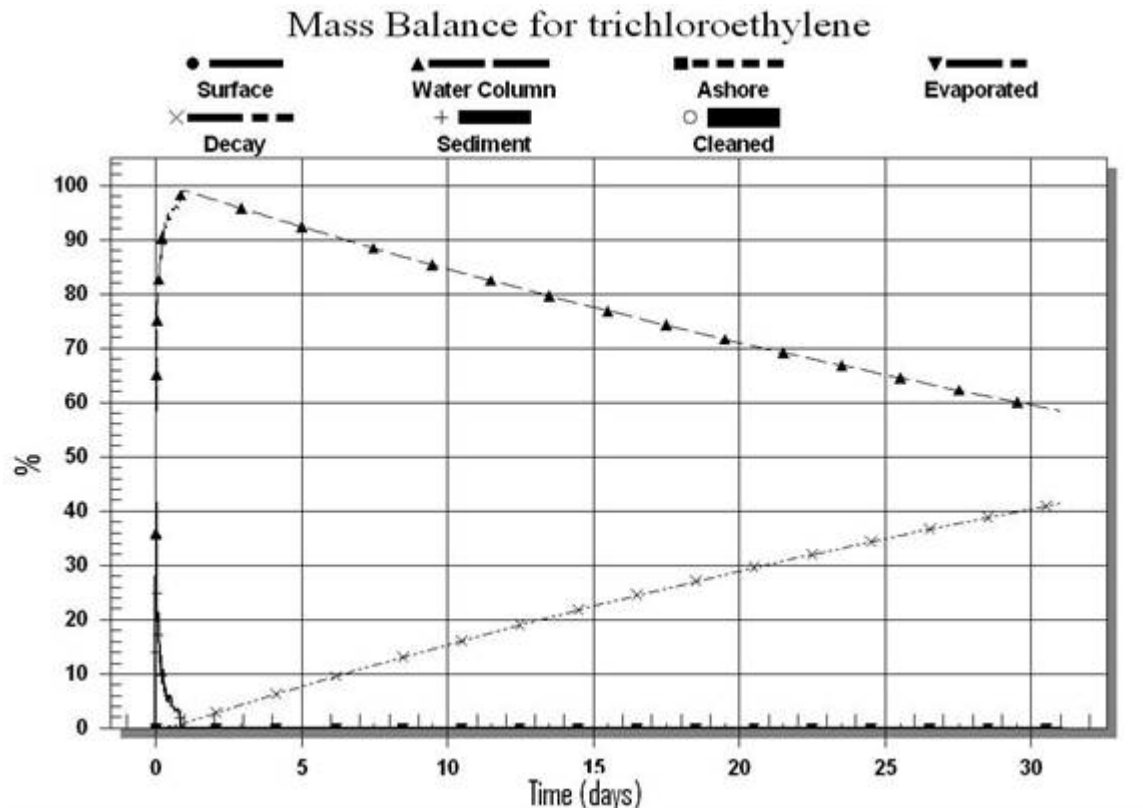
Figure 71.   Mass balance for trichloroethylene dropped in South San Diego Bay.

F.   NAPHTALENE

1.   Pollutants Released at North San Diego Bay

Suppose the sinking of a ship containing naphthalene, in the same two locations and time used in the previous scenarios. Again, in a depth of 3m, there is leakage of 200 tons, which is completed in 10 hours. Still, there is no wind forcing. Despite the much different qualities of this chemical, the results are identical to the aforementioned scenarios as regards the propagation. In three hours, naphthalene gas reaches San Diego port (Figure 72) and in less than 12 hours, it is widespread outside of the Bay. After 30 hours, the Naval Station is contaminated. The southern part of the Bay is contaminated much later, in approximately 20 days and finally, widespread naphthalene is observed all over the bay (Figure 73). As regards the mass balance curves, the final decay is a bit more than 30%. After the fourth day, the naphthalene in the water column is around 35%, and after 32 days, it is only 5%. After 11 days, both the decay and the water column percentage are at 23% (Figure 74). The most interesting difference is the existence of

81

important absorbed concentration. After 18 hours, there is much concentration in the port/city of San Diego (Figure 75) and after nine days, there is still some at the mouth of the bay (Figure 76).
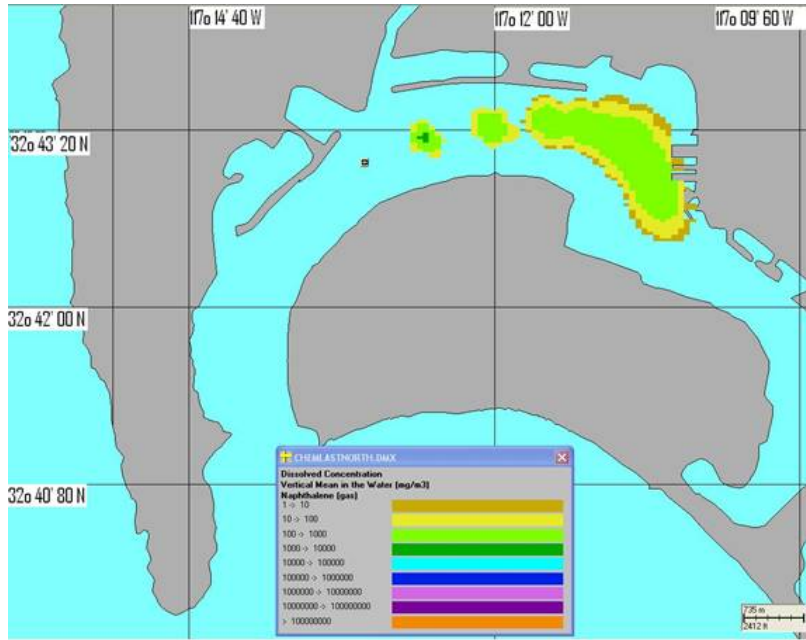

Figure 72.   Naphthalene mean dissolved concentration after three hours.
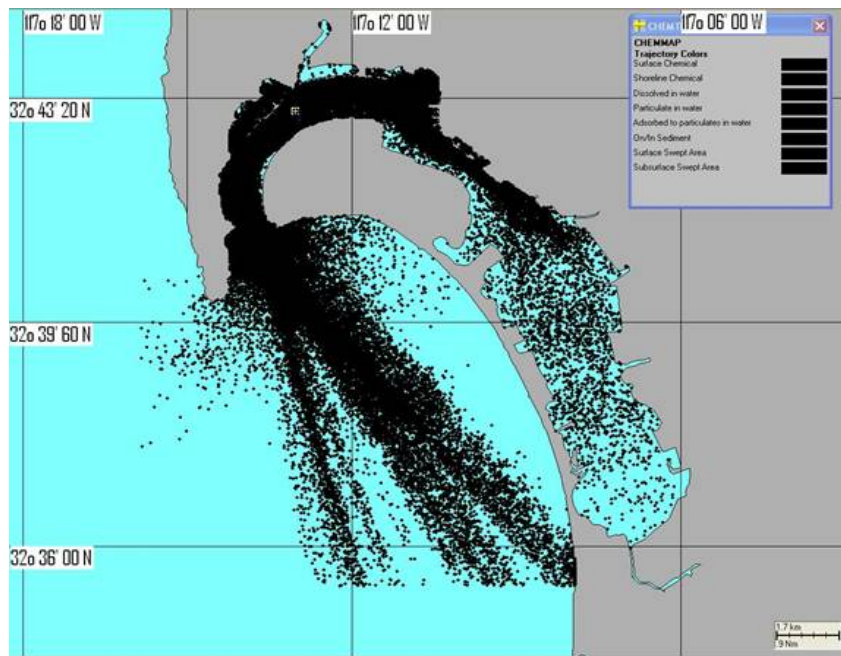

Figure 73.   Swept area after 32 hours of naphthalene dropped at North San Diego Bay.
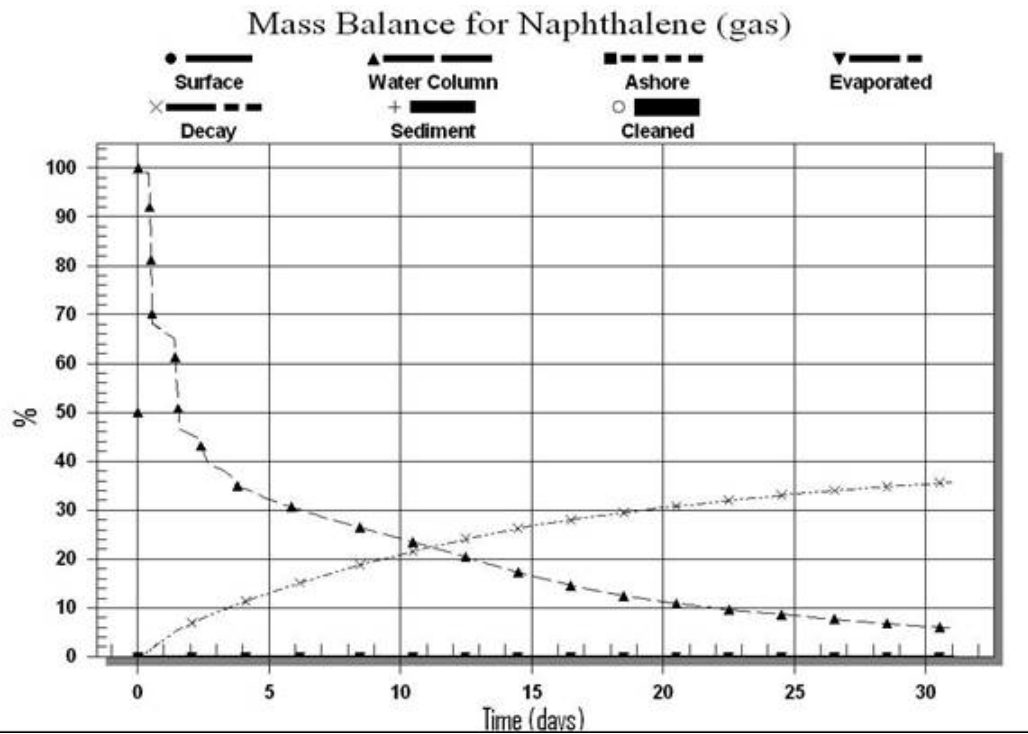
Figure 74.   Mass balance for naphthalene dropped in North San Diego Bay.

Figure 75.   Naphthalene mean absorbed concentration after 18 hours.

83
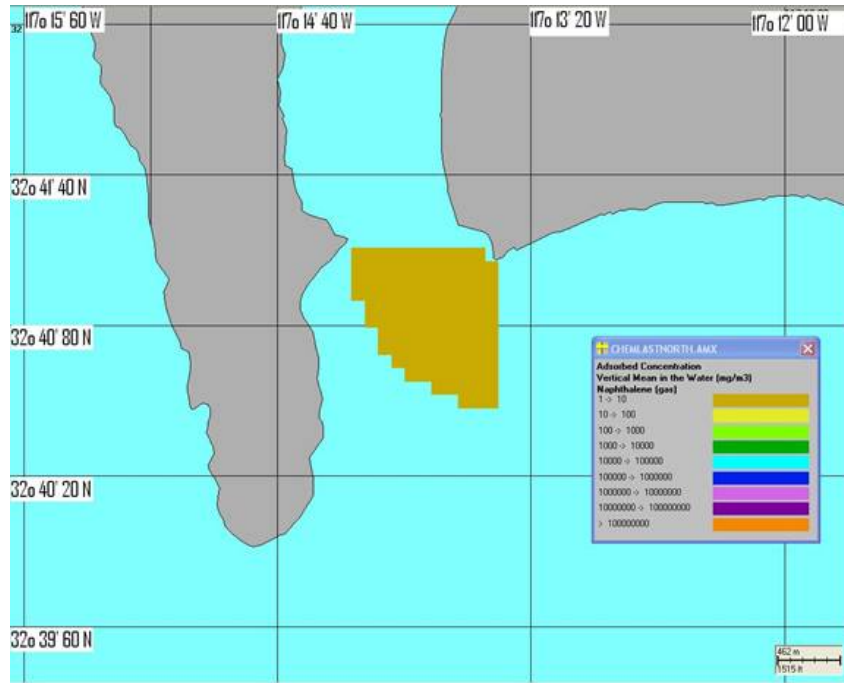
Figure 76.   Naphthalene mean absorbed concentration after nine days.

2.   Pollutants Released at South San Diego Bay

Suppose the sinking of a ship containing naphthalene in the southern part of the Bay, in the same location used in the previous scenarios (φ=32 39.00N and λ=117 07.92W), the results are very close to the previous cases. Naphthalene does not reach the port and city of San Diego (Figure 77). However, in 12 hours, it has reached the Naval Station, where there is also an important absorbed concentration (Figures 78 and 79). Moreover, absorbed concentration is still high after five days and six hours (Figure 80).

As regards the mass balance curves, there is a different result, as seen in Figure 81. The decay curve is exactly opposite to the water column one, and after 12 days, they are both at 50%. The end-state for the water column is a little less than 20% and the decayed naphthalene exceeds 80%. The final conclusion is that the semi to non-soluble naphthalene can cause a very large ecological catastrophe, probably more than any other sinker and definitely more than the floaters. Still, it is much less significant in South San Diego Bay than in the northern part of the bay.

Figure 77.   Swept area after 32 hours of naphthalene dropped at South San Diego Bay.
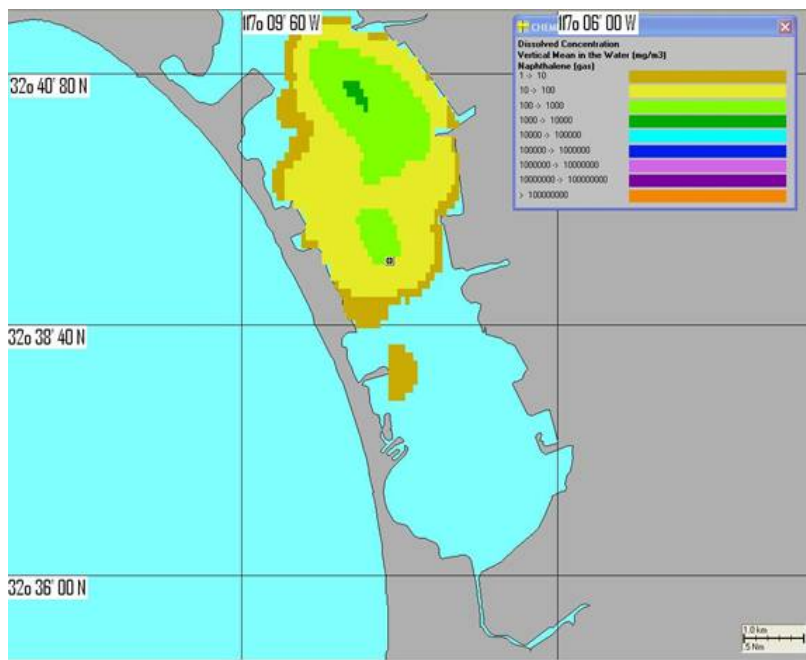
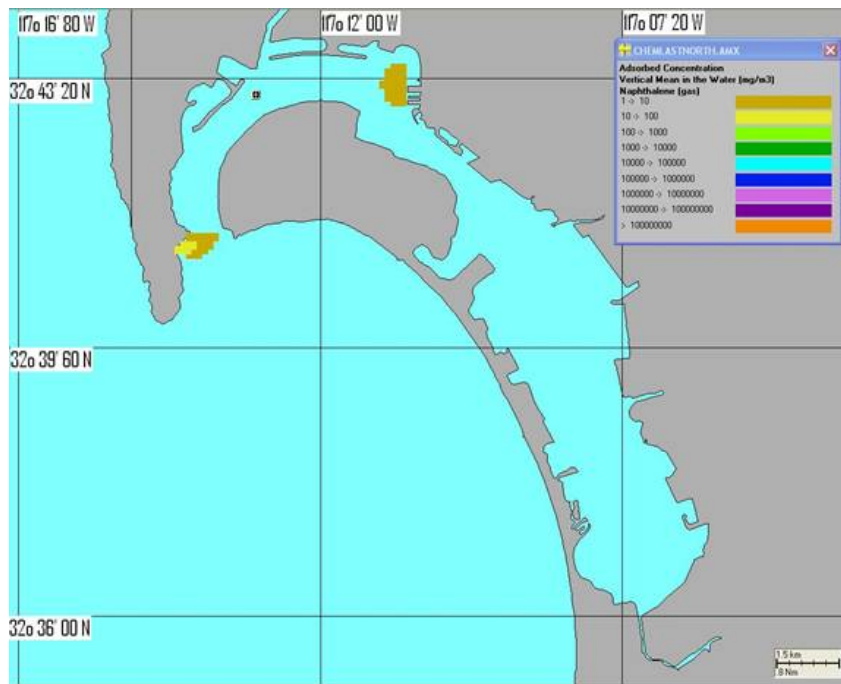Figure 78.   Naphthalene mean dissolved concentration after 12 hours.

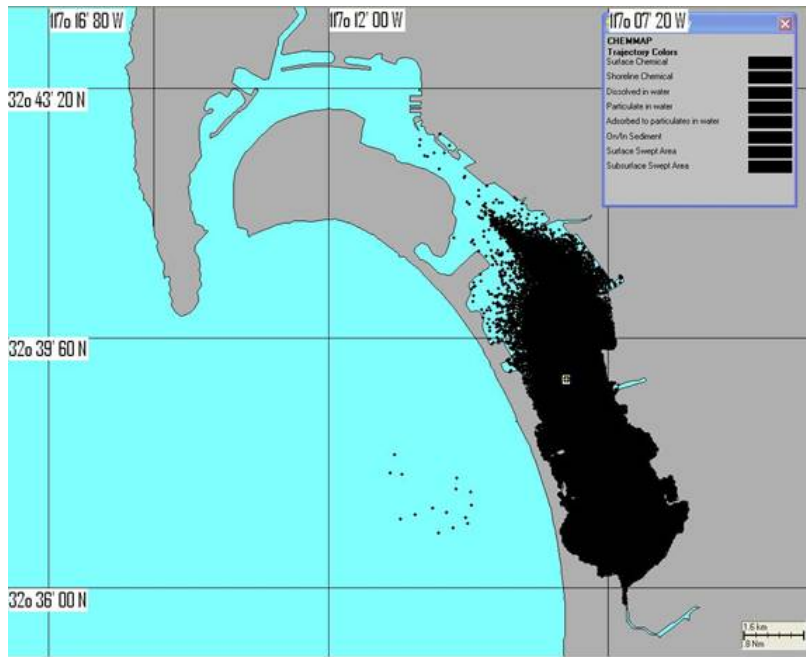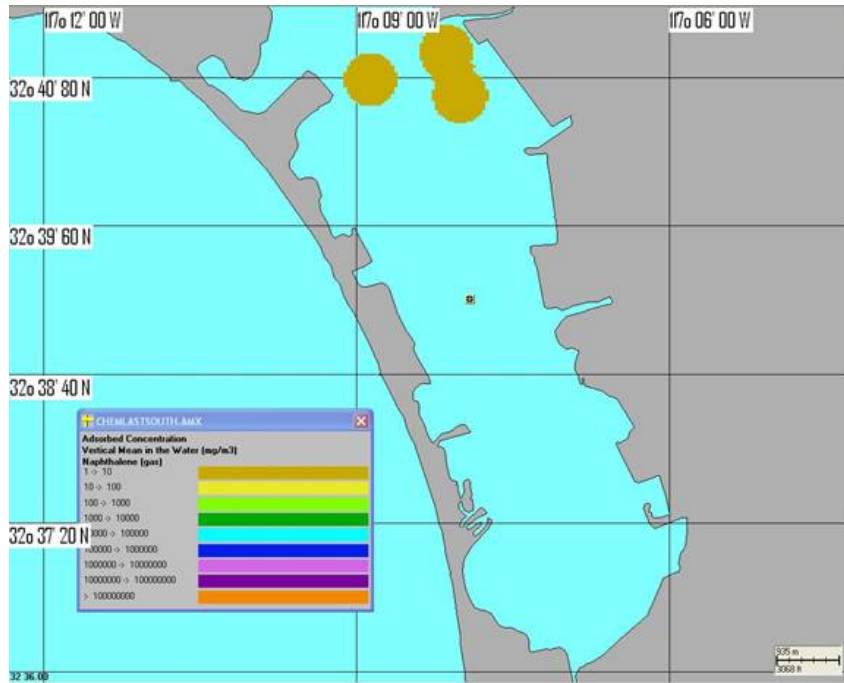Figure 79.   Naphthalene mean absorbed concentration after 12 hours.
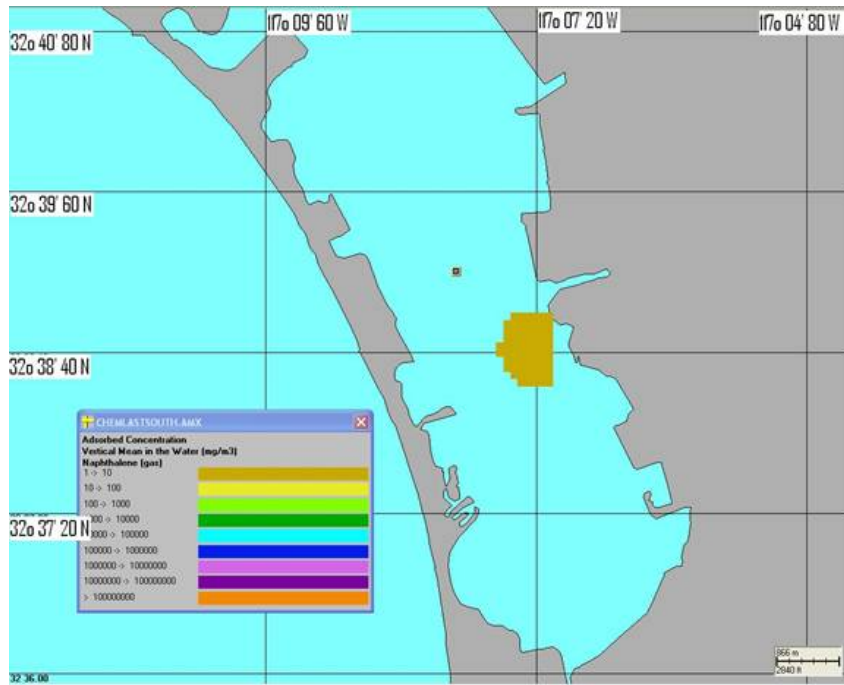
Figure 80.   Naphthalene mean absorbed concentration after 126 hours.

Mass Balance for Naphthalene (gas)

Legend: ● Surface ▲ Water Column ■ Ashore ▼ Evaporated
× Decay + Sediment ○ Cleaned
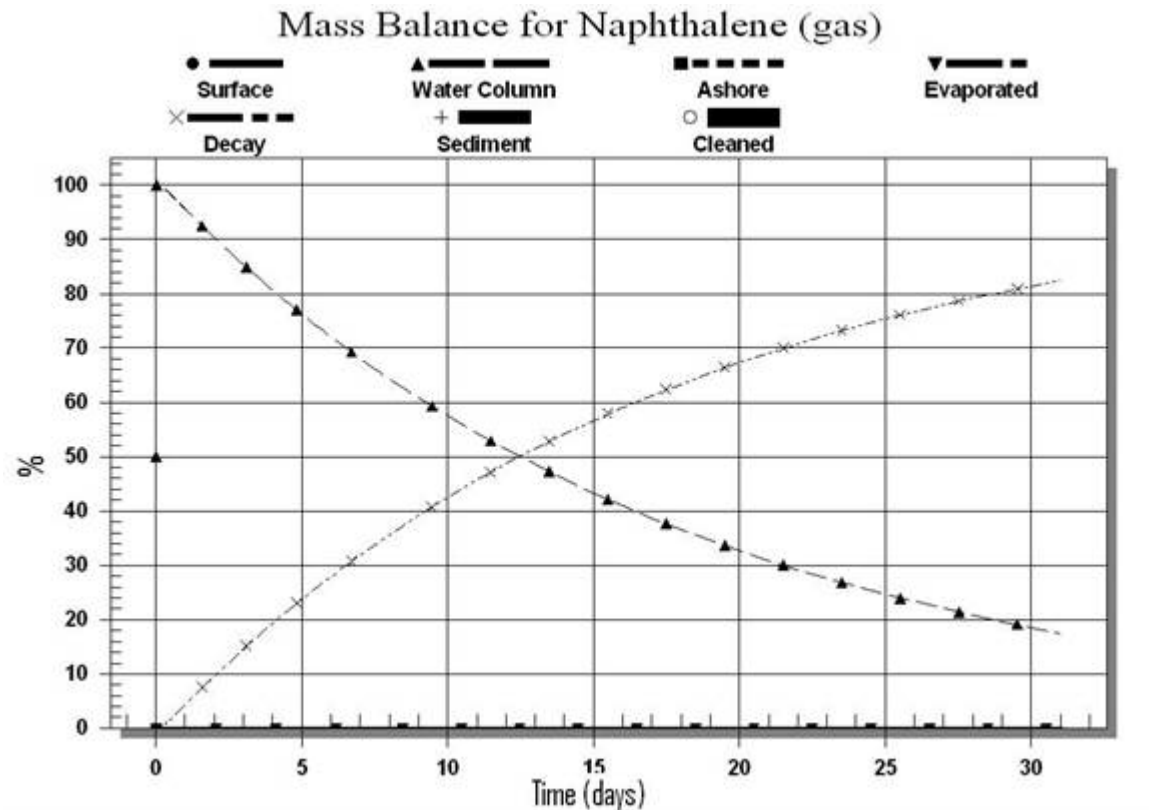
Figure 81.   Mass balance for naphthalene dropped in South San Diego Bay.

G.   OVERALL ASSESSMENT

An overall assessment is that San Diego Bay, being a semi-closed tidal basin, is a probable target for a terrorist chemical attack or a location where a chemical accident could cause severe problems. The sensitive eco-system would be impacted both inside and outside the Bay. If the chemical is a sinker, the results are more catastrophic than if it were a floater. Since the water exchange with the Pacific Ocean occurs only through a narrow entrance, the water would be contaminated for long time.

The propagation model shows that the northern part of the bay is more likely to be a target because it would affect the city and the Naval Station, and it would reach, even slightly, the South San Diego Bay and would spread outside the bay as well. Any attack or accident in the southern part (south of the Naval Station) would have minimal effects on the city and the shores of Coronado Island and none outside the bay. On the other hand, when the spill occurs in the southern part of the bay, a larger percentage of the chemical remains in the water column and for longer period of time.

In 3 hours: San Diego port/city

In 10 hours: Entire North SD Bay

In 12 hours: Outside SD Bay

In 16-30 hours: Naval Station

In 5 days: Heavy impact on Naval Station

In 20 Days: South end of the Bay

In 32 Days: The entire SD Bay

Table 14.   Results in North San Diego Bay

In 12 hours: Naval Station

In 15-17 days: Small part of absorbed or dissolved chemical in San Diego city/port

After 32 days: No effect to North San Diego Bay

Table 15.   Results in South San Diego Bay

Methanol: After 3 days, 45-50% in water column, after 20 days, less than 5% - rest decayed.

Benzene: 45% evaporates. After 2 days, 30-50% in water column, after 20 days 8-18% - rest decayed.

Ammonia: After 3 days, 50-75% in water column, after 20 days, 8-18% - rest decayed

Table 16.   Results for floaters in North San Diego Bay (first percentage) and South San Diego Bay (second percentage).

Chlorobenzene: After 5 days, 65 - 97% in water column, after 20 days, 50-90% - rest decayed.

Trichloroethylene: After 5 days, 60-93% in water column, after 20 days, 38-71% - rest decayed.

Naphthalene (gas/air dispersed): After 5 days, 33 - 78% in water column, after 20 days, 12-33% - rest decayed.

Table 17.   Results for sinkers in North San Diego Bay (first percentage) and South San Diego Bay (second percentage).

Taking into consideration that the database available does not contain highly acute toxic elements or any elements that consist of a chemical threat, it is necessary to highlight the vulnerability of the Bay in case of such an attack due to its oceanography/ topography and bathymetry.

Results concerning San Diego Bay can also be applied to studies in other semi-closed, barotropic, no-wind driven circulation basins.

THIS PAGE INTENTIONALLY LEFT BLANK

VIII. CONCLUSIONS - RECOMMENDATIONS

This study determined that a 2D depth-integrated model can satisfy certain Navy applications in coastal bays. In order to arrive to such a conclusion the thesis first showed that San Diego Bay is barotropic. Then, as regards the forcing mechanisms, it proved that the wind is not a significant factor. Hence, in a tidal semi-enclosed basin like San Diego a 2-D model can be used for time scales ranging from "instantaneous" (what a diver will feel in the water) to days (the drift of floating objects). However, we should notice that in the entrance of a semi-enclosed bay we should be more careful when applying a 2-D model (depending on the accuracy we wish to achieve), because both the influence of the wind and the system of the currents outside the bay cannot be ignored.

As regards the evaluation of the two models purchased by U.S. Naval Oceanographic Office, the conclusion is that they need improvement. The main consideration for applying them in littoral waters should be the smoothing of the bathymetry. On the one hand it is essential for the model to run properly and on the other hand might produce significant errors in very shallow areas (like the southern part of San Diego Bay).

Finally, the study shows the vulnerability of a semi-enclosed tidal basin in a possible chemical attack or accident, with the aforementioned particular results for San Diego Bay. In order to summarize these results, it should be repeated that in a case of a chemical attack or accident, first the sensitive eco-system would be severely damaged, no matter the nature of the event and the location. If the chemical were a sinker, the results would be more catastrophic than if it were a floater. Since the water exchange with the Pacific Ocean occurs only through a narrow entrance, the water would be contaminated for long time.

Two regimes of the chemical dispersion were found in this thesis. The first was the case of an attack/accident in the North San Diego Bay. In that case the entire bay would be contaminated. In 3 hours the chemical would reach San Diego port and city, in 12 hours the entire northern part of the bay would be affected and in 2-5 days the Naval

91

Station (located in the south part of the bay) would be contaminated as well. The rest of the Bay would be reached much later. The second regime was an attack/accident in the South San Diego Bay. In such case, the incident would have minimal effects on the city and the shores of Coronado Island (located in the north part of the bay) and none outside the Bay. On the other hand, when the spill occurs in the southern part of the Bay, a larger percentage of the chemical remains in the water column and for longer period of time, which makes it more "effective", which in a case of a chemical attack means lethal.

For the aforementioned reasons, the propagation model shows that the northern part of the bay is more likely to be a target because it would affect the city and the Naval Station, and it would reach, even slightly, the South San Diego Bay and would spread outside the bay as well. In general, results concerning San Diego Bay can also be applied to studies in other semi-closed, barotropic, no-wind driven circulation basins.

As regards recommendations for future research, it should be mentioned that the use of more accurate bathymetry and of a finer grid would give better results in a similar case. Moreover, the use of more recent ADCP measurements, during a longer period of time would further improve the results and verify the overall conclusions. It would be helpful if the ADCPs used in the future were located in a bigger distance from the shore.

A more detailed comparison of 3D vs. 2D model is encouraged, as well as its application for drift and for instantaneous current prediction. Last but not least, as regards chemical propagation, a classified research with data unavailable to foreigners about real chemical threats (e.g. anthrax) should be conducted.

LIST OF REFERENCES

Armstrong A. E., 2004. *Prediction of instantaneous currents in San Diego Bay for naval applications*. Master's Thesis in Meteorology and Oceanography, Naval Postgraduate School, Monterey, California, 56 pp.

Chadwick, D. B. and J. L. Largier, 1999a. *Tidal Exchange at the Bay-Ocean Boundary*. Journal of Geophysical Research, v. 104, no. C12, pp. 29,901-29,924.

Chadwick, D. B. and J. L. Largier, 1999b. *The Influence of Tidal Range on the Exchange Between San Diego Bay and the Ocean*. Journal of Geophysical Research, v. 104, no. C12, pp. 29, 885-29, 899.

Cheng R. T., V. T. Casulli and J. W. Gartner, 1983. *Tidal, Residual, Inter-tidal Mudflat (TRIM) Model and its Applications to San Francisco Bay, California*. Estuarine, Coastal and Shelf Science, 36:235-280.

Chu, P.C., S. H. Lu, and Y. C. Chen, 2001. *Evaluation of the Princeton Ocean Model using the South China Sea Monsoon Experiment (SCSMEX) Data*. Journal of Atmospheric and Oceanic Technology, 18, 1521-1539.

Defant A, 1961. *Physical Oceanography*, New York, Pergamon Press.

Delvigne, G. A. L., C. E. Sweeney, 1988. *Natural Dispersion of Oil*. Oil and Chemical Pollution, 4, pp. 281-310.

DiToro, D. M., C. S. Zarba, D. J. Hansen, W. J. Berry, R. C. Swartz, C. E. Cowan, S. P. Pavlou, H. E. Allen, N. A. Thomas, P. R. Paquin, 1991. *Annual Review: Technical Basis for Establishing Sediment Quality Criteria for Nonionic Organic Chemicals Using Equilibrium Partitioning*. Environmental Toxicology and Chemistry, 10, pp. 1541-1583.

Fagherazzi Sergio, Patricia L. Wiberg and Alan D. Howard, 2003. *Tidal Flow in a Small Basin*. Journal of Geophysical Research, v. 108, no. C3, pp. 16-1 to 16-10.

Fay, J. A., 1971. *Physical Processes in the Spread of Oil on a Water Surface*. Proceedings at Joint Conference and Control of Oil Spills, Washington, D.C., June 15-17, 1971.

Fischer H. B., E. J. List, R. C. Y. Koh, J. Imberger and N. H. Brooks, 1979. *Mixing in Inland and Coastal Waters*. Academic Press, p. 483, San Diego.

French, D., Reed, M., Jayko, K., Feng, S., Rines, H., Pavignano, S., Isaji, T., Puckett, S., Keller, A., French III, F. W., Gifford, D., McCue, J., Brown, G., MacDonald, E., Quirk, J., Natzke, S., Bishop, R., Welsh, M., Phillips, M., Ingram, B.S., 1996. *The CERCLA Type A Natural Resource Damage Assessment Model for Coastal and Marine Environments (NRDAM/CME).* Technical Documentation, Vol. I -VI, Final Report, submitted to the Office of Environmental Policy and Compliance, U.S. Dept. of the Interior, Washington, D.C., Contract No. 14-0001-91-C-11. April 1996.

Gambill, W. R., 1959. *How to calculate liquid viscosity without experimental data*. Chemical Engineering, p. 127.

Jackson J. A. and C. D. Winant, 1983. *Effect of a Kelp Forrest on Coastal Currents*. Continental Shelf Research, v. 2, no 1, pp. 75-80.

Lyman, C. J., W. F. Reehl, D. H. Rosenblatt, 1982. *Handbook of Chemical Property Estimation Methods*. McGraw-Hill Book Co., New York.

Mackay, D. and R. S. Matsugu, 1973. *Evaporation Rates of Liquid Hydrocarbon Spills on Land and Water.* The Canadian Journal of Chemical Engineering, Vol. 51, pp. 434-439.

Mackay, D., Shiu, W. Y., Ma, K. C., 1992a. *Monoaromatic Hydrocarbons, Chlorobenzenes, and PCBs.* Illustrated Handbook of Physical-Chemical Properties and Environmental Fate for Organic Chemicals, Vol. I. Lewis Publishers, Chelsea, Michigan, 668p.

Mackay, D., Shiu, W. Y., Ma, K. C., 1992b. *Polynuclear Aromatic Hydrocarbons, Polychlorinated Dioxins, and Dibenzofurans*. Illustrated Handbook of Physical-Chemical Properties and Environmental Fate for Organic Chemicals, Vol. II. Lewis Publishers, Chelsea, Michigan, 566p.

Mackay, D., Shiu, W. Y., Ma, K. C., 1992c. *Volatile Organic Chemicals*. Illustrated Handbook of Physical-Chemical Properties and Environmental Fate for Organic Chemicals, Vol. III. Lewis Publishers, Chelsea, Michigan, 885p.

Mackay, D., Shiu, W. Y., Ma, K. C., 1992d. *Oxygen, Nitrogen, and Sulfur Containing Compounds*. Illustrated Handbook of Physical-Chemical Properties and Environmental Fate for Organic Chemicals, Volume IV. Lewis Publishers, Chelsea, Michigan, 930p.

Madala, R. V. and S. A. Piaczek, 1977. *A Semi-Implicit Numerical Model for Baroclinic Oceans*. Journal of Computational Physics, 23, pp. 167-168.

McCay, F. D. P. and T. Isaji, 2002. *Evaluation of the Consequences of Chemical Spills Using Modeling: Chemicals Used in Deepwater Oil and Gas Operations*. International Marine Environmental Seminar 2001, Journal of Marine Systems, Special Issue 2002.

Peeling, T. J., 1975. *A Proximate Biological Survey of San Diego Bay, California*. Naval Undersea RD Center, San Diego, California, Technical Report No. TP389.

Pritchard, D. W., 1952. *Estuarine Hydrography*. Advances in Geophysics, Academic Press, pp. 342-280.

Spaulding M. L., D. L. Mendelsohn and C. J. Swanson, 1999. *WQMAP: An Integrated Three-Dimensional Hydrodynamic and Water Quality Model System for Estuarine and Coastal Applications*. Marine Technology Society Journal.

Swanson, J. C., and M. Ward, 2000. *Improving Coastal Model Prediction through Data Assimilation*. Proceedings of the 6th International Conference on Estuarine and Coastal Modeling, November 3-5, 1999, New Orleans, 10-11.

Wang, P. F., R. T. Cheng, K. Richter, E. S. Gross, D. Sutton, and J. W. Gartner, 1998. *Modeling Tidal Hydrodynamics of San Diego Bay, California*. Journal of the American Water Resources Association, 34 (5), 1123-1140.

Woodward-Clyde Consultants, 1996. *1995-1996 City of San Diego and Co-Permittee NPDES Stormwater Monitoring Program Report*.

Youssef, M. and M. L. Spaulding, 1993. *Drift Current Under the Action of Wind and Waves*. Proceedings of the 16th Arctic and Marine Oil Spill Program Technical Seminar, Calgary, Alberta, Canada, pp. 587-615.

THIS PAGE INTENTIONALLY LEFT BLANK

INITIAL DISTRIBUTION LIST

1.   Defense Technical Information Center
   Ft. Belvoir, Virginia

2.   Dudley Knox Library
   Naval Postgraduate School
   Monterey, California

3.   Mary L. Batteen
   Department of Oceanography
   Naval Postgraduate School
   Monterey, California

4.   Professor Peter C. Chu , Code OC/CU
   Department of Oceanography
   Naval Postgraduate School
   Monterey, California

5.   Dr. Steve D. Haeger
   Naval Oceanographic Office
   Stennis Space Center, Mississippi

6.   LCDR Kleanthis Kyriakidis
   HNGS, Athens, Greece